NATIONAL
ENRICHMENT
FACILITY

10 CFR 30.6
10 CFR 40.5
10 CFR 70.5

August 31, 2004

NEF#04-035

ATTN: Document Control Desk
Director
Office of Nuclear Material Safety and Safeguards
U.S. Nuclear Regulatory Commission
Washington, DC 20555-0001

Louisiana Energy Services, L. P.
National Enrichment Facility
NRC Docket No. 70-3103

Subject: Clarifying Information Related to External Hazards Analyses

References:

1. Letter NEF#03-003 dated December 12, 2003, from E. J. Ferland (Louisiana Energy Services, L. P.) to Directors, Office of Nuclear Material Safety and Safeguards and the Division of Facilities and Security (NRC) regarding "Applications for a Material License Under 10 CFR 70, Domestic licensing of special nuclear material, 10 CFR 40, Domestic licensing of source material, and 10 CFR 30, Rules of general applicability to domestic licensing of byproduct material, and for a Facility Clearance Under 10 CFR 95, Facility security clearance and safeguarding of national security information and restricted data"

2. Letter NEF#04-002 dated February 27, 2004, from R. M. Krich (Louisiana Energy Services, L. P.) to Director, Office of Nuclear Material Safety and Safeguards (NRC) regarding "Revision 1 to Applications for a Material License Under 10 CFR 70, "Domestic licensing of special nuclear material," 10 CFR 40, "Domestic licensing of source material," and 10 CFR 30, "Rules of general applicability to domestic licensing of byproduct material"

3. Letter NEF#04-029 dated July 30, 2004, from R. M. Krich (Louisiana Energy Services, L. P.) to Director, Office of Nuclear Material Safety and Safeguards (NRC) regarding "Revision to Applications for a Material License Under 10 CFR 70, "Domestic licensing of special nuclear material," 10 CFR 40, "Domestic licensing of source material," and 10 CFR 30, "Rules of general applicability to domestic licensing of byproduct material"

NMSS01

One Sun Plaza 100 Sun Lane NE, Suite 204 Albuquerque, NM 87109 [P] 505 944 0194 [F] 505 944 0198

By letter dated December 12, 2003 (Reference 1), E. J. Ferland of Louisiana Energy Services (LES), L. P., submitted to the NRC applications for the licenses necessary to authorize construction and operation of a gas centrifuge uranium enrichment facility. Revision 1 to these applications was submitted to the NRC by letter dated February 27, 2004 (Reference 2). A subsequent revision (i.e., revision 2) to these applications was submitted to the NRC by letter dated July 30, 2004 (Reference 3).

On May 27 and 28, 2004, NRC representatives conducted an in-office review of the National Enrichment Facility external hazards analyses documentation in the LES office in Hobbs, New Mexico. In subsequent conference calls between LES and NRC representatives, held on August 12 and 18, 2004, the NRC requested that clarifications be provided concerning these external hazards analyses. This information is included in Enclosure 1, "External Hazards Analyses Clarifications," and Enclosure 2, "Waste Control Specialists Fault Investigations."

If you have any questions or need additional information, please contact me at 630-657-2813.

Respectfully,

Daniel G. Green for

R. M. Krich
Vice President – Licensing, Safety, and Nuclear Engineering

Enclosures:
1. External Hazards Analyses Clarifications
2. Waste Control Specialists Fault Investigations

cc: T.C. Johnson, NRC Project Manager

ENCLOSURE 1

External Hazards Analyses Clarifications

External Hazards Analyses Clarifications

Seismology

1. Confirm that the faulting recently discovered at WCS site is not active.

LES Response

1. Consultants (Cook Joyce and Intera) to Waste Control Specialists (WCS) have completed the investigation of the fault recently identified at the WCS site. The fault investigations are described in Section 4.1.1.3 of the WCS consultant's report. NRC and Louisiana Energy Services (LES) representatives toured the fault site during the field portion of the fault investigation in May 2004.

   The conclusion of the fault investigation is that there are no geologic formations present in the fault excavation younger than Triassic age that are affected by faulting. Therefore, the faulting is not active. A copy of Section 4.1, "Faults," and associated Tables and Figures from the WCS consultant's report (i.e., Waste Control Specialists, Section VI, Geology Report, August 2004) is provided in Enclosure 2, "Waste Control Specialists Fault Investigations."

External Hazards Analyses Clarifications

Seismology (continued)

2. The PGA estimated at the National Enrichment Facility site from the 1992 magnitude 5.0 earthquake appears to be more than the PGA estimated from the seismic hazard calculations (refer to Figure 3.2-27).

LES Response

2. Information on the January 2, 1992 earthquake was obtained from published catalogs listed in Table 3.2-22 of the National Enrichment Facility (NEF) Safety Analysis Report (SAR). These catalogs list four epicentral locations for the 1992 earthquake. These epicentral locations are provided in Table 3.2-24 of the NEF SAR. Distances to the NEF site from the different epicentral locations range from 11 km to 19 km (6.8 mi to 11.8 mi). The average epicentral distance is 14 km (8.7 mi). Focal depth, which is only reported in the U.S. Geologic Survey (USGS) catalogs, is fixed at 5 km (3 mi) by the USGS for determination of the epicentral location coordinates. Examination of the attenuation models shown on Figure 3.2-27 of the NEF SAR for an earthquake of magnitude 5.0 at the average distance of 14 km (8.7 mi) show peak horizontal ground accelerations to be in the range of about 0.09g to 0.13g.

   It is noted that none of the obtained catalogs provide information on the maximum intensity observed for this event. Following the NRC/LES conference call on August 18, 2004, the USGS was contacted to determine if they possessed additional intensity information. The USGS provided LES with a list of localities in New Mexico and Texas and the reported maximum intensities at these locations. This list is provided in Table 1. Coordinates of localities were obtained from a national atlas. The maximum reported intensity for the January 1992 earthquake is V on the Modified Mercalli Intensity (MMI) scale.

External Hazards Analyses Clarifications

Table 1, Reported Intensities for January 1992 Earthquake

Locality	State	Longitude W		Latitude N		MMI
		degrees	minutes	degrees	minutes	
Seagraves	TX	102.0	34.1	32.0	56.5	V
Jal	NM	103.0	11.6	32.0	6.9	V
Lakewood	NM	104.0	22.6	32.0	37.9	V
Roswell	NM	104.0	31.6	33.0	23.7	V
Carlsbad	NM	104.0	14.0	32.0	25.0	IV
Hagerman	NM	104.0	19.8	33.0	6.6	IV
Hobbs	NM	103.0	7.9	32.0	42.0	IV
Lake Arthur	NM	104.0	21.9	33.0	0.1	IV
Loving	NM	104.0	5.5	32.0	17.1	IV
Andrews	TX	102.0	32.8	32.0	19.2	IV
Aspermont	TX	100.0	13.6	33.0	8.3	IV
Crane	TX	102.0	21.0	31.0	23.9	IV
Fort Davis	TX	103.0	53.7	30.0	35.3	IV
Gail	TX	101.0	26.8	32.0	46.2	IV
Kermit	TX	103.0	5.6	31.0	51.5	IV
Lamesa	TX	101.0	57.5	32.0	44.1	IV
Littlefield	TX	102.0	19.9	33.0	55.2	IV
Midland	TX	102.0	4.7	31.0	59.7	IV
Monahans	TX	102.0	53.5	31.0	35.7	IV
Odessa	TX	102.0	22.5	31.0	51.5	IV
Pecos	TX	103.0	29.6	31.0	25.6	IV
Seminole	TX	102.0	38.8	32.0	43.2	IV
Snyder	TX	100.0	54.7	32.0	43.6	IV
Stanton	TX	101.0	47.6	32.0	7.8	IV
Sterling City	TX	100.0	59.5	31.0	50.2	IV
Wilson	TX	101.0	43.6	33.0	19.0	IV
Wolforth	TX	102.0	0.9	33.0	30.3	IV
Ruidoso	NM	105.0	40.9	33.0	20.0	F
Abilene	TX	99.0	42.8	32.0	27.9	F

The distribution of intensity observations for the January 1992 earthquake is shown on Figure 1. No intensity reports were listed for Eunice, New Mexico, the nearest town to the NEF site. Local newspaper accounts describe the occurrence of an earthquake but did not report any significant impacts that could indicate a higher seismic intensity. Based on this information, a maximum intensity of V is attributed for the NEF site during the January 1992 earthquake.

External Hazards Analyses Clarifications

Peak accelerations associated with site intensity V effects are estimated using empirical correlations (Reiter, 1990; Earthquake Hazard Analysis, Issues and Insight, Columbia University Press).

Trifunac and Brady (Trifunac and Brady, 1975; On the Correlation of Seismic Intensity with Peaks of Recorded Strong Ground Motion, Bulletin of the Seismological Society of America, Vol. 65) provide:

$$\text{Log } A = 0.30 \text{ MMI} + 0.014 \qquad \text{[Equation 1]}$$

For MMI = V; A = 0.033g

Murphy and O'Brien (Murphy and O'Brien, 1977; The Correlation of Peak Ground Acceleration Amplitude with Seismic Intensity and Other Physical Parameter, Bulletin of the Seismological Society of America, Vol. 67) provide:

$$\text{Log } A = 0.17 \text{ MMI} + 0.07\, I_0 - 0.45 \log R + 0.83 \qquad \text{[Equation 2]}$$

Where I_0 is maximum epicentral intensity

For MMI = V at R = 14 km and I_0 = V; A = 0.033g

(Note: A is in cm/sec^2 units in Equations 1 and 2. Results were converted to g-units)

Each empirical approach produces a peak ground acceleration estimate of 0.033g. The standard error on this estimate is about a factor of 2 (Reiter, 1990). Based on the observed seismic intensities, it is likely that peak ground accelerations for the January 1992 event were well below 0.1g at the NEF site. As a result of the relatively low seismic intensities associated with the 1992 M=5 event, attenuation models selected for the probabilistic assessment are considered to be conservative predictors of regional peak ground accelerations.

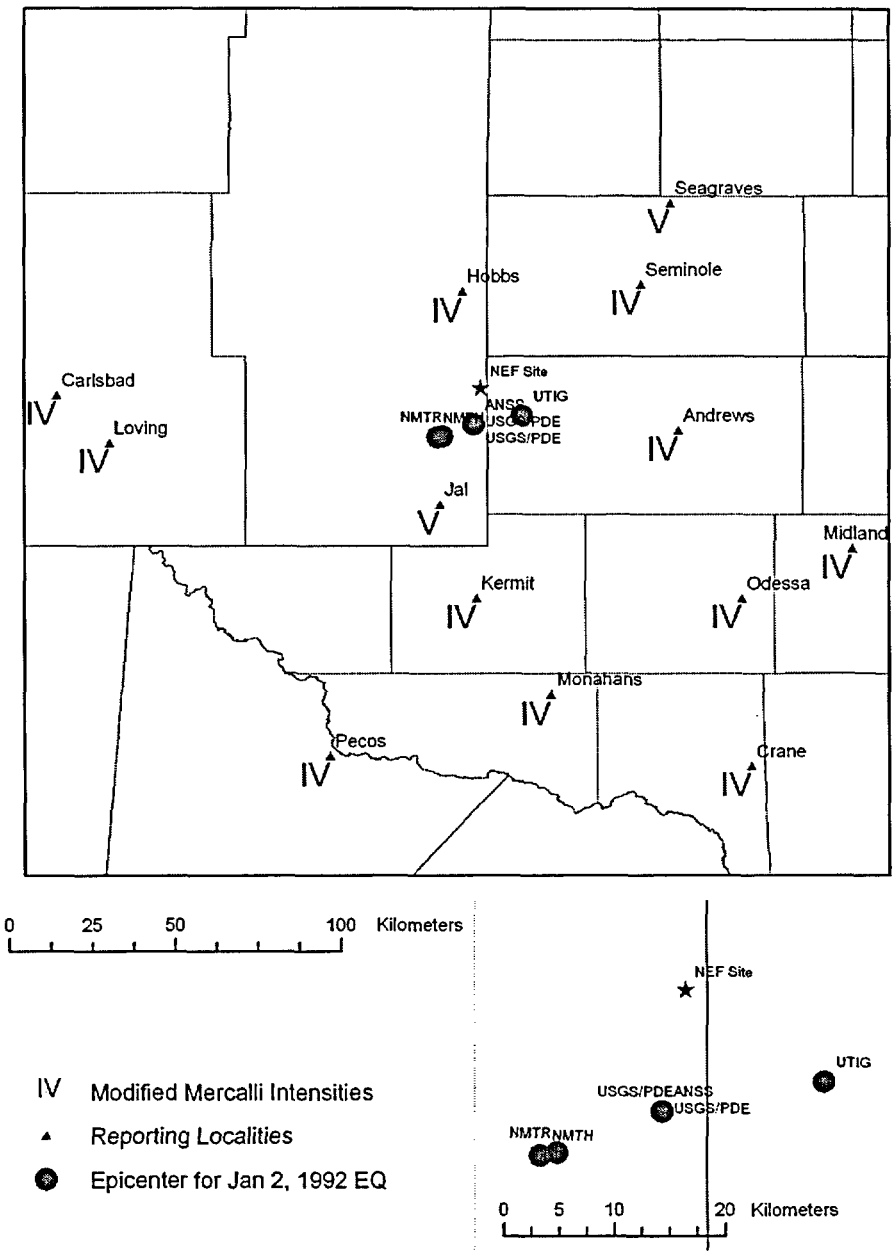

Figure 1

Intensity Observations for the January 1992 Earthquake

External Hazards Analyses Clarifications

Seismology (continued)

3. Section 3.2.6.4.1 states that the Nuttli, 1973 (WIPP attenuation model), Nuttli, 1986, and Toro, 1997 attenuation equations are used in the seismic hazard calculations. Results are only shown for the Toro, 1997 and Nuttli, 1973 attenuation models (refer to Table 3.2-29). Why aren't any results shown for the Nuttli, 1986, attenuation model (which is the most conservative model)?

LES Response

3. The Nuttli 1986 attenuation model was not used for the following reasons:

The Nuttli 1986 attenuation model (Nuttli, 1986; Nuttli-Newmark attenuation model, Letter to Dr. J.B. Savy (Lawrence Livermore National Laboratory) dated September 19, 1986) is a combination of an original Modified Mercalli Intensity (MMI) attenuation model coupled with Newmark and Hall response spectrum amplification factors (Newmark and Hall, 1978; Development of Criteria for Seismic Review of Selected Nuclear Power Plants, NUREG/CR-0098, U.S. Nuclear Regulatory Commission). The MMI attenuation component was developed using seismic intensity data observed for earthquakes in the North American mid-continent. The highest intensity at a particular locality likely was observed at a site/structure underlain by soil and resulted from a soil amplification effect. Nearby or adjacent sites/structures located on firm sites or bedrock sites typically reported lower seismic intensities. When maximum intensities are summarized for a specific municipality/locality this maximum value likely is attributed to soil amplification effects. MMI attenuation analyses performed on maximum site intensities thus are biased to effects observed at soil sites.

The response spectrum amplification component developed by Newmark and Hall (Newmark and Hall, 1978) relied on accelerograms recorded for California earthquakes, the majority of which were recorded for large events (M > 6.4) and recorded on deep alluvium sites. Resulting response spectra are thus representative of large magnitude events recorded at soil sites underlain by thick sequences of alluvium. Coupling of the Nuttli 1986 (MMI attenuation) and Newmark (spectral amplifications) elements into a single model produces a conservative ground motion estimate when compared to more recent models developed specifically for firm or hard bedrock site conditions.

The methodology used in the probabilistic seismic hazard assessment was to initially model bedrock ground motions and to apply soil amplification factors (National Earthquake Hazards Reduction Program (NEHRP) Soil Class C) to account for the geotechnical engineering description of the local soil column provided in the NEF Report of Preliminary Subsurface Exploration (MACTEC, 2003; Report of Preliminary Subsurface Exploration, Proposed National Enrichment Facility, Lea County, New Mexico, MACTEC Engineering and Consulting, Inc.). This report was previously submitted to the NRC in letter NEF#04-019 dated May 20, 2004. Design response spectra were then developed using the Newmark and Hall (Newmark and Hall, 1978) amplification factors applied to the amplified top-of-soil ground motion. Introduction of the Nuttli 1986 attenuation model (Nuttli, 1986) to estimate bedrock ground motion in this methodology, in our opinion,

would have overestimated the response spectra because of this model's bias toward soil sites and built-in soil amplification effects.

The Campbell attenuation model was not used for the following reasons:

The topic of suitability of the recent Campbell attenuation model (Campbell, 2003; Prediction of Strong Ground Motion Using the Hybrid Empirical Method and its Use in the Development of Ground Motion (Attenuation) Relations in Eastern North America, Bulletin of the Seismological Society of America, Vol. 93) was raised during the NRC/LES conference call on August 18, 2004. The Campbell attenuation model was not used, primarily because of its stated applicability to hard rock sites characterized by shear wave velocity of 2,800 m/sec (9,200 ft/sec) or greater. The NEF site is underlain by rock-like hard clay of the Chinle Formation. This foundation condition more likely fits a "firm" rock classification than a "hard" rock condition more typical of sites underlain by sound and un-weathered igneous/metamorphic bedrock. In addition, the Campbell attenuation model does not provide a peak ground acceleration attenuation model; rather it states "PGA was assumed to represent the value of PSA [peak spectral acceleration] at 0.01-sec period [i.e. 100 Hz.]." Historically, PGA was assumed to be near 33 Hz as an anchoring frequency for standard response spectra. Predictions by the Campbell attenuation model at frequencies of 50 Hz and 33 Hz are higher than for 100 Hz. No guidance is provided in the attenuation model documentation (Campbell, 2003) on anchor frequency (100 Hz, 50 Hz, 33 Hz) to be used for developing response spectra based on standard shapes.

Rationale for Selection of Attenuation Models

The probabilistic seismic hazard assessment was conducted using the Nuttli 1973 attenuation model (Nuttli, 1973; Design Earthquake for the Central United States, Miscellaneous Paper, S-73-1, U.S. Army Waterways Experiment Station) used in the Waste Isolation Pilot Project (WIPP) seismic hazard assessment. The Nuttli 1973 attenuation model was selected due to the precedent of its usage in the WIPP seismic hazard calculations and acceptance of seismic design criteria that resulted from the hazard assessment. This earlier Nuttli attenuation model differs from the later version, in that predictions are not coupled with the Newmark amplification factors. Nonetheless, being developed from a seismic intensity database, the Nuttli 1976 model is viewed to be a conservative predictor of bedrock ground motion. Sensitivity analyses were performed using the Toro et al. attenuation models (Toro et al, 1997; Model of Strong Ground Motions from Earthquakes in Central and Eastern North America - Best Estimates and Uncertainties, Seismological Research Letters, Vol. 68). The Toro et al. models are described to be applicable to the geologic conditions similar to those at the NEF site (refer to Figure 2, page 45 of Toro et al, 1997). Predictions of these models were compared to several other attenuation models published through 2003. These models were judged to make conservative predictions of seismic ground motion at firm bedrock. The response provided to Seismology Question 2 supports the assessment that attenuation models selected for the NEF seismic hazard assessment are conservative predictors of regional ground motion.

External Hazards Analyses Clarifications

Seismology (continued)

4. Was a background seismicity model used in the hazard calculations?

LES Response

4. A separate background seismicity zone was not applied in the seismic hazard assessment. A local background seismicity zone typically is used for cases when the site being studied is not located in any of the regional seismic source zones. In this hazard study, the NEF site is located within seismic source zones defined by approximate 161-km (100-mi) and 322-km (200-mi) radii from the site. Therefore, no additional background seismicity zone was used in the hazard calculations.

External Hazards Analyses Clarifications

Seismology (continued)

5. What weighting scheme was used to obtain the hazard result? How was the weighting scheme determined? Why isn't the most conservative hazard curve used instead (refer to Figure 3.2-29)? The most conservative hazard curve appears to correspond to a maximum magnitude of 6.5 (Mx 6.5) for the 1931 Valentine earthquake. The maximum magnitude estimated for the 1931 Valentine earthquake is between 6.0 and 6.4.

LES Response

5. Weights used to determine the hazard result are shown in the following tables.

The preferred seismicity model includes a Central Basin Platform seismic source embedded within a seismic source defined by a 161-km (100-mi) radius from the site. Alternative cases were developed by varying the maximum magnitude and earthquake recurrence models. The WIPP attenuation model was used in the four alternative cases, and total weight is 0.50.

Bk53B9W	Bk53BFW	B260B9W	B260BFW	W=WIPP (Nuttli, 1973) attenuation model
Mx=5.25	Mx=5.25	Mx=6.0	Mx=6.0	Maximum magnitude
0.125	0.125	0.125	0.125	Weight

Four other cases, also using the WIPP attenuation model, examined regional seismic sources of approximately 161-km (100-mi) and 322-km (200-mi) radii from the NEF site, without embedded seismic sources for the Central Basin Platform and the Rio Grande Rift. These homogeneous seismic source zonations are not preferred because of the distinct spatial pattern and higher earthquake frequency within these seismic sources. The combined weight for these four alternatives is 0.25.

B100B9W	B100BFW	B200B9W	B200BFW	W=WIPP (Nuttli, 1973) attenuation model
Mx=6.0	Mx=6.0	Mx=6.5	Mx=6.5	Maximum magnitude
0.0625	0.0625	0.0625	0.0625	Weight

External Hazards Analyses Clarifications

The final four cases are based on the preferred seismic zonation (i.e. that includes the Central Basin Platform), but with the Toro et al. attenuation model (Toro et al, 1997). The combined weight for these 4 alternatives is 0.25.

Bk53B9T	Bk53BFT	B260B9T	B260BFT	T=Toro (Toro et al, 1997) attenuation model
Mx=5.25	Mx=5.25	Mx=6.0	Mx=6.0	Maximum magnitude
0.0625	0.0625	0.0625	0.0625	Weight

The most conservative seismic hazard curve resulted from a seismic zonation scenario that inferred a homogeneous earthquake frequency within the 322-km (200-mi) radius of the NEF site. This hypothesis eliminates the association of the 1931 Valentine TX earthquake with faulting in the Rio Grande rift geologic province, and allows recurrence of events of magnitude 6.5 throughout the 322-km (200-mi) area. Quaternary faults, such as those mapped within the Rio Grande rift, are not mapped or inferred within 161 km (100 mi) from the NEF site, thus the homogeneous seismicity model is not preferred. Also, the WIPP hazard assessment defined seismic sources for the Basin and Range, and Rio Grande rift geologic provinces. Nonetheless, seismic hazard contributions from this conservative model are given a weight of 0.125 for computation of the final hazard result. This weight is the sum of the weights of the two cases with the maximum magnitude of 6.5 (i.e., cases B200B9W and B200BFW).

External Hazards Analyses Clarifications

Seismology (continued)

6. Is the shape of the uniform hazard spectra in Figures 3.2-31 and 3.2-32 a simplified version of the original uniform hazard spectra. Does it envelope the original uniform hazard spectra?

LES Response

6. The recommended horizontal and vertical design response spectra have a standard response spectrum shape based on Newmark and Hall amplification factors (Newmark and Hall, 1978). The spectrum is anchored at the 10^{-4} per year peak horizontal ground acceleration of 0.151g determined from the weighted final seismic hazard curve. Amplification factors were applied using NEHRP soil class C definition to account for the local soil column. The resulting spectrum is not a simplified version of the original uniform hazard spectra. The original spectra are for the bedrock surface. The bedrock ground motions are amplified to account for the soil column of approximate 12 m (40 ft) thickness, and the standard spectrum shape for 5% damping is applied at the ground surface.

External Hazards Analyses Clarifications

Tornado Generated Missiles

7. How were the impact velocities with the tornado-generated missiles determined? The "Assessment of Tornado, Tornado Missiles and High Wind Loads at NEF for ISA and Design Basis" report does not provide this information.

LES Response

7. The horizontal impact velocities at the NEF site were derived using the methods and results from an extensive study of tornado missiles conducted in 1999 by the NEF report author, J.R. McDonald (McDonald, 1999; Rational for Wind-borne Missile Criteria for DOE Facilities, UCRL-CR-135687 S/C B505188, Hazards Mitigation Center, Lawrence Livermore National Laboratory). Vertical missile velocities are 2/3 of the horizontal velocity.

   The 1999 study included computer simulation of trajectories for three classes of tornado missiles: timber plank, steel pipe, and automobile. The velocities for each missile class at NEF were derived using the 1999 study trajectory simulations and then scaling the results to meet the tornado wind speed design parameters specific to NEF.

   The NEF tornado missile velocity parameters are consistent with the design and evaluation criteria used for more than 40 U.S. Department of Energy (DOE) facilities at different sites around the country (DOE, 2002; Natural Phenomena Hazards Design and Evaluation Criteria for Department of Energy Facilities, DOE-STD 1020-2002, U.S. Department of Energy).

External Hazards Analyses Clarifications

Propane Explosion of Highway 234

8. Why were limited data (1997-2001) used in the highway propane explosion hazard risk assessment while more than twice the amount of data (1990-2001) were available?

LES Response

8. LES considers that the more recent data period 1997-2001 better represents current and future highway statistics. This is due, in general, to improvements in transportation equipment and roadway design and conditions.

External Hazards Analyses Clarifications

Natural Gas Pipeline

9. Why were limited data (1998-2001) used in determining natural gas pipeline rupture incidents per mile while more data (mid-1984-present for rupture incidents and 1987-2001 for telephone records) were available?

LES Response

9. Referring to Attachment 1 of the Natural Gas Pipeline Hazard Risk Determination Calculation (i.e., Framatome-ANP Document No. 32-2400572-02 which was previously submitted to the NRC in letter NEF#04-023 dated June 9, 2004), the summary of pipeline incidents for the years 1986 to 2002 indicates that the number of incidents for 1998, 1999, 2000 and 2001 is comparable to the number of incidents for the other years listed and representative of available pipeline incident data. As stated in the footnote on page 6 of the subject calculation, although transmission pipeline data were available for the year 2002, telephonic incident notifications were only available through the year 2001. Therefore, the 2002 data was not used in the calculation.

External Hazards Analyses Clarifications

Natural Gas Pipeline (continued)

10. Why was the limiting rupture length {3.1 cm [0.1 ft]} selected for the natural gas pipeline to exclude small rupture incidents from the hazard assessment?

LES Response

10. Based on past experience, LES assumed that ruptures less than 0.1 foot in length are unable to cause a plant hazard. However, as stated in Note 7 of Table 1 of the calculation, regardless of whether or not a rupture length was reported for an explosion incident, the explosion incident was included in the determination of R_{C1} (i.e., six of the seven explosions had no reported rupture length). Furthermore, the R_{C1} numerator of seven accounts for reported explosions associated with all incident types, not just ruptures (i.e., only two of the reported explosions are associated with rupture incidents). However, the denominator for R_{C1} was based only on rupture incidents greater than 0.1 foot, resulting in a conservative value for R_{C1}.

External Hazards Analyses Clarifications

Natural Gas Pipeline (continued)

11. Will the presence of the proposed National Enrichment Facility affect the explosion probability (R_{c1}, fraction of explosion) in the Natural Gas Pipeline Hazard Risk Determination report by Thomson?

LES Response

11. The presence of the proposed NEF will not affect the explosion probability, R_{c1}, fraction of explosion. The explosions in the data base that were used to develop R_{c1} resulted from a wide-range of ignition sources available at the time of the pipeline rupture event. These ignition sources could include sparks due to equipment impact on the pipeline or other nearby objects as well as ignition sources from nearby vehicles and fixed facilities. The NEF is not a unique ignition source and is considered representative of types of ignition sources that resulted in the explosions contained in the data base. Furthermore, pipeline explosions typically originate near the release point. The separation distance, between the pipeline and the NEF, makes the NEF an unlikely ignition source for a pipeline gas explosion. Therefore, the presence of the NEF will not affect the explosion probability given a pipeline rupture and subsequent gas release.

External Hazards Analyses Clarifications

Natural Gas Pipeline (continued)

12. Why was a wind speed of 1 m/s [3.3 ft/s] used in the ALOHA analysis in assessing natural gas pipeline hazards?

LES Response

12. The wind speed was based on NRC guidance. In particular, the NRC accepted value of the atmospheric dilution factor between the release and receptor points that is used in a chemical dispersion analysis, irrespective of the dispersion model, should be that value that is exceeded only 5% of the time (Section 3.3, Regulatory Guide 1.78, "Assumptions for Evaluating the Habitability of a Nuclear Power Plant Control Room During a Postulated Hazardous Chemical Release," Rev. 1, U.S. Nuclear Regulatory Commission, December 2001). From the NEF Environmental Report, Section 3.6.15, the joint frequency distribution of wind speed as a function of atmospheric stability class is in the range 0.4 to 1.3 m/sec for stability class F, which occurs 2.2% of the time. The value 1 m/sec is approximately at the mid-point of the joint frequency distribution range. This value satisfies the NRC guidance from Regulatory Guide 1.78.

External Hazards Analyses Clarifications

Natural Gas Pipeline (continued)

13. Why was a release duration of 1 hour used in the ALOHA analysis in assessing natural gas pipeline hazards? The 1-hour shut-off time was related to the carbon-dioxide pipeline. It is not clear whether or not this shut-off time is applicable to the natural gas pipeline.

LES Response

13. LES concluded that one hour represents a reasonable time to achieve shut off considering that there are shut offs at each end and in the middle of the 23-km (14-mi) pipeline as well as a check valve at the connection with the main service line located near Eunice and Highway 234. Based on discussion with the gas line operator (i.e., Sid Richardson Energy Services), one hour is considered a reasonable emergency response time for a potential gas line rupture. A two hour response time would be more appropriate if a rupture were to occur overnight. However, according to the pipeline operator, considering that the pipeline is under low pressure (i.e., less than 50 pounds per square inch), it is unlikely to rupture. Rather, a small leak of ¼ inch to 1 inch is more likely, which might result in a small ground surface hole. A guillotine pipeline break, as assumed in the calculation, is only likely if the pipe were to be ripped by equipment. Considering the unlikelihood of digging in the middle of the night and that the State of New Mexico requires that the pipeline owner be notified prior to digging, the one hour shut-off time assumed in the ALOHA analysis is appropriate to the gas pipeline for the hazard assessment. In addition, in the event of a rupture, steady state concentration is reached in less than one hour. As a result, the shut-off time of two hours (i.e., the response time if the rupture occurs at night), does not affect the explosion probability determined in the analysis.

External Hazards Analyses Clarifications

Carbon-Dioxide Pipeline

14. Why is the segment of the carbon-dioxide pipeline south of the National Enrichment Facility, co-located (approximately) with the natural gas pipeline, not a safety concern for the Technical Services Building. This carbon-dioxide pipeline has a high pressure. The pipeline pressure is 13,445 kPa [1,950 psi] according to the Safety Analysis and 14,470 KPa [2,100 psi] based on a telephone conversation record with the pipeline operator (Appendix 5 of the Natural Gas Pipeline Hazard Risk Determination report by Thomson).

LES Response

14. Based on discussion with the carbon-dioxide (CO_2) pipeline operator (Trinity Gas), a minimum separation distance of 25 to 30 feet is required between parallel running pipelines for corrosion purposes and safety concerns (i.e., digging). Clearance requirements also apply where pipelines cross one another. Furthermore, since the pipeline carries liquid CO_2 rather than a potentially explosive gas, it will not explode. Rupture of the high pressure CO_2 pipeline will not adversely impact the gas pipeline due to separation requirements. Therefore, the relocation of the CO_2 line in the vicinity of the natural gas pipeline south of the National Enrichment Facility is not a safety concern for the Technical Services Building or any other portion of the NEF. The 134.4 bar (1,950 psi) pipeline pressure provided in NEF SAR Section 3.2.2.4, Industrial Areas, is representative of the normal operating pressure of the CO_2 pipeline. Based on discussions with the pipeline operator, the maximum operating pressure of the pipeline is 144.8 bar (2,100 psi).

External Hazards Analyses Clarifications

Carbon-Dioxide Pipeline (continued)

15. Will the presence of the carbon-dioxide pipeline affect the hazard probability of the natural gas pipeline? A segment of the carbon-dioxide pipeline will be located where the natural gas pipeline is.

LES Response

15. As described in the response to Carbon-Dioxide Pipeline Question 14, a minimum separation distance is required between parallel running pipelines. Considering that there will be sufficient separation between the two pipelines, if the CO_2 line were to fail, the natural gas line will not be adversely impacted. Therefore, the presence of the carbon-dioxide pipeline will not affect the hazard probability of the gas pipeline.

External Hazards Analyses Clarifications

Onsite Natural Gas Pipeline

16. Why is the hazard related to the explosion of the onsite natural gas pipeline in the Central Utility Building the bounding case while the potential rupture and subsequent explosion of the section of the onsite gas pipeline outside of the Central Utility Building is not? The natural gas pipeline out the property is determined to be credible. Given the close proximity of the onsite natural gas pipeline to safety-significant structures such as the Technical Services Building and Separations Building Module, the onsite gas pipeline should be a credible safety concern as well. Only in this case, the probability of explosion-induced thermal hazards may not be readily dismissed as that of the natural gas pipeline.

LES Response

16. The present level of design for the natural gas supply for on-site use is a 10-cm (4-in) diameter, low pressure (10 psig) pipeline. The pipeline will be routed outside to the Central Utilities Buildings (CUB) and not under any building. The pipeline, in addition, will have an excess flow valve at the connection to the entrance of the NEF site. If a breach occurs on the NEF site, the excess flow valve will automatically shut the flow of gas off.

    Given the small diameter of the on-site pipeline, low pressure of the pipeline, pipeline routing that results in it not passing under any buildings and the excess flow valve, hazards to the NEF from an outside release of gas downstream of the excess flow valve is not considered to be credible. Hazards associated with releases upstream of the excess flow valve are already addressed by the Natural Gas Pipeline Hazard Risk Determination Calculation (i.e., Framatome-ANP Document No. 32-2400572-02 which was previously submitted to the NRC in letter NEF#04-023 dated June 9, 2004). The bounding event of a leak inside the CUB was selected as bounding since it provides a mechanism for gas build-up from a small leak inside the CUB.

External Hazards Analyses Clarifications

Aircraft Crash Hazards

17. Why are the random holding patterns at the Eunice and Lea County/Jal Airports excluded from further consideration as a potential hazard? The justification provided in the Aircraft Hazard Risk Determination report stated because both airports meet the first proximity criterion (distance and number of operations of the airport) outlined in NUREG-0800, the issue of holding patterns should not be relevant to either airport. This justification does not appear to be adequate. The proximity criteria have three aspects and the third proximity criteria deals specifically with holding patterns. We believe all three proximity criteria need to be satisfied to avoid further analysis of aircraft crash hazards. Satisfying one criterion is not sufficient justification to dismiss other criteria.

LES Response

17. There are no specific holding patterns in these airports. LES based this conclusion on two sources of information. First, the U.S. Federal Aviation Authority (FAA) supplied no information on holding patterns for these airports. Holding pattern information was supplied for other airports by the FAA. Second, a conversation with the airport manager at the Eunice airport also confirmed that there is no instrumental procedure into the airport, nor is there any holding pattern. In addition, the number of annual operations into the Eunice airport has been shown to be extremely small compared to the NUREG-0800 limit (480 versus 225,000). LES, therefore, judged that this airport does not pose any aircraft crash hazard to the proposed facility.

    For Lea County/JAL airports, since they are more than 32 km (20 mi) away from the site, and landing procedure is not usually initiated until the aircraft is within 32 km (20 mi), there is no need to evaluate the impact of holding patterns. LES based this conclusion of the fact that no holding pattern data was supplied by the FAA and the fact that even if there were, at times, planes put into a holding pattern, the pattern would not bring the planes near the NEF site due to the separation distances between the NEF site and these airports.

External Hazards Analyses Clarifications

Overpressure Design Basis

18. Why was the design basis overpressure {6.9 kPa [1 psi]} for safety-significant structures not included in Section 3.3.2, Structural Design Criteria, of the Safety Analysis Report? In assessing potential hazards of propane truck accidents and a nearby gas pipeline explosion, an assumption that safety-significant structures of the proposed National Enrichment Facility would be designed to withstand a 6.9 kPa [1 psi] overpressure was used.

LES Response

18. The consideration of pressure loads due to postulated pipeline explosions has been included in revision 2 of the Safety Analysis Report, Section 3.3.2.2.8.2.D, "Gas Pipeline Hazards." A future revision to the SAR will also address the potential hazards of propane truck accidents.

ENCLOSURE 2

Waste Control Specialists Fault Investigations

SECTION VI

GEOLOGY REPORT

AUGUST 2004

Prepared for:

WASTE CONTROL SPECIALISTS LLC
ANDREWS, TEXAS

Prepared by:

Cook-Joyce, Inc.
812 West Eleventh
Austin, Texas 78701

&

Intera, Inc.
9111A Research Boulevard
Austin, Texas 78758

4.0 ACTIVE AND INACTIVE GEOLOGIC PROCESSES

This section addresses active geologic processes in the vicinity of the facility. In discussing the "active" geologic processes, the "inactive" processes are discussed as well. Active geologic processes include flooding and submergence, faulting, seismicity, land surface subsidence, and the potential for surface erosion. Flooding is addressed by locating the facility out of a 100-year floodplain and submergence applies only to coastal zones. Faults, seismicity, land surface subsidence, and surface erosion are discussed in the following sections.

4.1 FAULTS

This section provides an analysis of faults in the vicinity of the facility at the regional and local scales. Various regulatory requirements for land disposal activities, as well as storage and processing of wastes, require delineation of all faults within the area of the facility, together with demonstrations for any such faults that:

(i) fault displacement has not occurred within Holocene time, or if fault displacement has occurred within Holocene time, that no such faults pass within 200 feet of the portion of the surface facility where treatment, storage, or disposal of wastes will be conducted;

(ii) it will not result in structural instability of the surface facility or provide for groundwater movement to the extent that there is endangerment to human health or the environment; and

(iii) disposal units will not be located near a capable fault that could cause a maximum credible earthquake larger than that which the unit could reasonably be expected to withstand.

The WCS site is situated over the north central portion of a prominent Paleozoic structural feature known as the Central Basin Platform. Significant faults are known in the deep subsurface as interpreted from petroleum exploration activities. The faults are expressed in Paleozoic rocks at depths of thousands of feet. The deep faults lose their expression as

significant stratigraphic offsets after early Permian (Wolfcampian) time. All of the major faulting in the vicinity of the Central Basin Platform occurred in response to tectonic forces active before the global plate tectonic reorganization that created the North American continent. (Bally et al., 1989). The Paleozoic faults exhibit low natural microseismicity as a result of passive response to relatively low levels of tectonic stress in the trailing edge of the westward-drifting North American plate. The closest area of active regional tectonic stress and active faulting offsetting Quaternary or younger geologic deposits is the Rio Grande Rift that forms the eastern boundary of the Basin and Range Province. The Rio Grande Rift is over 200 miles west of the WCS area. There is no surface evidence of faulting within 3000 feet the WCS permitted area.

4.1.1 Regional Tectonic Setting and Faults

The WCS facility is located within the Permian Basin region of west Texas. The Permian Basin derives its name from the fact that it is underlain by extensive deposits of Permian sediments.

4.1.1.1 *Tectonic Setting*

The WCS site is situated over the north-central portion of a prominent structural feature known as the Central Basin Platform (Figure 6.4-1). The Central Basin Platform is a deep-seated horst-like structure that extends northwest to southeast from southeastern New Mexico to eastern Pecos County, Texas. The Central Basin Platform is flanked by two prominent structural depressions known as the Delaware Basin to the southwest and the Midland Basin to the northeast, and by the Val Verde Basin to the south.

From the Cambrian to late Mississippian, west Texas and southeast New Mexico experienced only mild structural deformation that produced broad regional arches and shallow depressions (Wright, 1979). The Central Basin Platform served intermittently as a slightly positive feature during the early Paleozoic (Galley, 1958). During the Mississippian and Pennsylvanian, the Central Basin Platform uplifted using ancient lines of weakness (Hills, 1985), and the Delaware, Midland, and Val Verde Basins began to form as separate basins.

Late Mississippian tectonic events uplifted and folded the platform and were followed by more intense late Pennsylvanian and early Permian deformation that compressed and faulted the

area (Hills, 1963). Highly deformed local structures formed ranges of mountains oriented generally parallel to the main axis of the platform (Wright, 1979).

This period of intense, late Paleozoic deformation was followed by a long period of gradual subsidence and erosion that stripped the Central Basin Platform and other structures to near base-level (Wright, 1979). The expanding sea gradually encroached over broad eroded surfaces and truncated edges of previously deposited sedimentary strata. New layers of arkose, sand, chert pebble conglomerate and shale deposits accumulated as erosional products along the edges and on the flanks of both regional and local structures. Throughout the remainder of the Permian, the Permian Basin slowly filled with several thousand feet of evaporites, carbonates, and shales (Figure 6.4-2).

From the end of the Permian until late Cretaceous, there was relatively little tectonic activity except for periods of slight regional uplifting and downwarping. During the early Triassic, the region was slowly uplifted and slightly eroded. These conditions continued until the late Triassic, when gentle downwarping formed a large land-locked basin in which terrigenous deposits of the Dockum Group accumulated in alluvial flood plains and as deltaic and lacustrine deposits (McGowen, et al., 1979). In Jurassic time, the area was again subject to erosion.

During Cretaceous time, a large part of the western interior of North America was submerged, and the west Texas/southeastern New Mexico region was part of a large continental shelf sea in which a thick sequence of Cretaceous rocks was deposited. The Cretaceous sequence of sediments comprised a basal clastic unit (the Trinity, Antlers or Paluxy sands) and overlying shallow marine carbonates.

Uplift and southward– and eastward-retreating Cretaceous seas were coincident with the Laramide Orogeny, which formed the Cordilleran Range west of the Permian Basin. The Laramide Orogeny uplifted the region to essentially its present position, supplying sediments for the late Tertiary Ogallala Formation. The major episode of Laramide folding and faulting occurred in the late Paleocene. There have been no major tectonic events jn North America since the Laramide Orogeny, except for a period of minor volcanism during the late Tertiary in northeastern New Mexico and in the Trans-Pecos area. Hills (1985) suggests that slight Tertiary movement along Precambrian lines of weakness may have opened joint channels

which allowed the circulation of groundwater into Permian evaporite layers. The near-surface regional structural controls may be locally modified by differential subsidence related to groundwater dissolution of Permian salt deposits (Gustavson, 1980).

4.1.1.2 *Faults*

Two types of faulting were associated with early Permian deformation. Most of the faults were long, high-angle reverse faults with several hundred feet of vertical displacement that often involved the Precambrian basement rocks (Hills, 1985). The traces of these faults are shown on the Precambrian structure map provided in Figure 6.4-3. The second type of faulting is found along the western margin of the Central Basin Platform where long strike-slip faults, with displacements of tens of miles, are found (Hills, 1985; Bebout and Meador, 1985) (Figure 6.4-4).

The large structural features of the Permian Basin are reflected only indirectly in the Mesozoic and Cenozoic rocks, as there has been virtually no tectonic movement within the basin since the Permian (Nicholson and Clebsch, 1961). The east-west and north-south regional cross-sections provided in Figures 6.4-5 and 6.4-6 illustrate this relationship. Figure 6.4-5 shows the draping of the Permian and Triassic sediments over the Central Basin Platform structure, located approximately 7000 feet beneath the present land surface. The faults that uplifted the platform do not appear to displace the younger Permian sediments. The northernmost fault on Figure 6.4-6, located at the Matador Uplift, terminates in lower Wolfcampian sediments.

A further comparison of the structure of the Devonian Woodford Formation to the structure of the younger Upper Guadalupe Whitehorse Group (Permian) (Figures 6.4-7 and 6.4-8) indicates that the faults in the Devonian section do not continue upward into the overlying Permian Guadalupe Whitehorse Group. The regional geologic and tectonic information does not indicate the presence of significant post-Permian faulting within the regional study area, although minor post-Permian faulting in the WCS area is discussed below. In addition, the local information does not indicate Holocene displacement of faults within 3000 feet of the proposed WCS landfill site. The site-specific structural setting is discussed below.

Two regional stratigraphic cross sections constructed in the vicinity of the WCS site using oil and gas well logs are shown as Plates 6.2-2 and 6.2-3. The locations of the cross sections are

shown in Figure 6.2-1. These cross sections depict the major stratigraphic units that occur within about 2000 feet below ground surface in the vicinity of the site. The stratigraphic units depicted on Plates 6.2-2 and 6.2-3 include the upper OAG unit of a few tens of feet in thickness, the underlying Triassic red beds of the Dockum Group with a thickness of 1,000 to 1,500 feet, the underlying Permian Dewey Lake Formation red beds, and the Permian evaporites of the Rustler and Salado Formations. These cross sections do not indicate the presence of significant faulting in the upper 2,000 feet of sediments within 3 to 4 miles of the WCS site. The base of the underground source of drinking water (USDW) is the bottom of the Santa Rosa Formation at about 1,400 feet below ground surface in the vicinity of the WCS facility. The Santa Rosa Formation is the lowermost formation of the Triassic Dockum Group.

4.1.1.3 *Post-Permian/Pre-Cretaceous Fault Investigation*

Faulting in a sandstone in the upper portion of the Triassic red beds of the RCRA landfill was anecdotally identified at a WCS project meeting February 11, 2004. Subsequently, photos taken in 1996 of an apparent southward-dipping reverse fault were located (Figure 6.4-9). Since regulatory criteria address the age of faults and the age of any geologic units affected or displaced by faulting, a geologic investigation of the fault was undertaken. The southeast wall of the RCRA landfill was extended about 200 feet to the southeast in May and June 2004, yielding about 60 feet of vertical geologic exposure along a length of about 400 feet. Two benches with subvertical walls were exposed.

The upper wall was approximately 25 feet high, extending about 6 feet into the Triassic red beds of the Dockum Group. The upper wall exposed caprock caliche developed on Cretaceous Antlers Formation sand and gravel, underlain by non-calichified Antlers sands and gravels, in turn underlain by the red bed clays of the Triassic Dockum Group. The upper 3 to 4 feet of the red beds have been altered from red to gray. Along the relatively sharp contact between the altered gray clay and unaltered red clay were numerous small faults with offsets ranging from a few inches to a few feet.

The lower wall was excavated an additional 30 to 35 feet into the red beds exposing a 10- to 15-foot thick sandstone layer in the upper part of the wall. The sandstone exhibited two opposing reverse faults with offsets of about 20 feet on the southward-dipping southern fault and about 3

feet on the northward-dipping northern fault (Figure 6.4-10). The southern reverse fault in the Triassic sandstone bed is the southeastern extension of the southward-dipping reverse fault in the 1996 photographs.

Geologic mapping

Geologic mapping of the upper and lower walls was completed by two field mapping teams, supervised by a senior coordinating geologist. Elevation baselines were surveyed onto both the upper and lower walls, and the walls were subdivided into five-foot square townships and ranges. Detailed geologic mapping was conducted on parts of the upper and lower walls using moveable five-foot square grids, subdivided into 25 one-foot square sections. The mapping focused on geologic contacts and distinguishable geologic features, including faults, joints, slickensides, bedding planes, partings, channels, alteration and weathering zones. The mapped geologic sections are provided in Figure 6.4-11.

The upper wall was mapped in considerably more detail than the lower wall in order to determine the youngest geologic units affected by faulting. The southern end of the upper wall, where the largest faults and offsets were observed, was mapped in the greatest detail. Parts of the upper wall were mapped by field sketching and photographic interpretation. The two faults in the lower wall were mapped in detail using the 5-foot grids, while the remainder of the lower wall was documented using photo mosaics.

Observations - Lower wall

The geologic materials exposed on the lower wall are part of the Triassic Dockum Group, specifically the Cooper Canyon Formation (Lehman, 1994b). The red beds are characteristically red and purple claystones, with interbedded discontinuous siltstone and sandstone units. As indicated above, a fine grained sandstone layer about 10 to 15 feet thick occurred in the upper third of the lower wall. The claystones were relatively plastic on excavation, drying within a week to a stiff, blocky structure.

The red beds exhibited nominally orthogonal, subvertical jointing with well-developed joints at about 0.5 to 1 foot spacing. Lower hemisphere stereonet projections of the poles to the

subvertical joints show a maximum concentration at about 320° (north 40° west) with a secondary concentration at about 40° (north 40° east) (Figure 6.4-12). The subvertical joints are an expression of the orthogonal regional jointing system.

The concentration of subvertical joint directions at about 320° is partially due to bias induced by the orientation of the northeast-striking wall. If a similar length northwest-striking wall were available for measurement of subvertical joints, it is likely that the secondary concentration at about 40° would be more pronounced and the orthogonal pattern of the regional jointing system would be more obvious on the stereonet plot. There was only about 50 feet of northwest-striking wall exposed beneath the sandstone at the north end of the excavation, yielding a limited opportunity to eliminate the bias of the longer northeast-striking exposure of about 400 feet. The subvertical joints were often coated or partially coated with dark brown to purplish-black weathering products, likely manganese oxide. Slickensides on the subvertical joints were not observed.

Relatively large, continuous and 'wavy' lower-angle joints at about 30° to 60° from horizontal were also present, without an apparent well-developed spacing or repetition, as in the subvertical joints. The lower angle joints exhibited continuity over 10 to 15 feet of exposure on the lower wall, and slickensides were numerous and well developed on the wavy joints. The strike of the irregular, wavy joint planes show a maximum at about 300° (Figure 6.4-13), however the strikes of the irregular joint planes appear to be quite well distributed about the stereonet.

The sandstone exposed in the upper third of the lower wall was 10 to 15 feet in thickness. The sandstone exhibited two opposing reverse faults about 200 feet apart with apparent dips of the order of 30° to 40°. The southern reverse fault is the southeastern extension of the southward-dipping reverse fault in the 1996 photographs. The reverse fault in the southern end of the wall was south-dipping with a south-hanging-wall-up offset of about 20 feet. The reverse fault in the northern part of the wall was north-dipping with a north-hanging-wall-up offset of about 3 feet. The poles of the measured fault planes show a strike of the fault planes of about 277° to 280° (north 83° west to north 80° west) (Figure 6.4-14). Slickensides were measured on both the south and north fault planes, indicating dip slip with a compressional stress azimuth of about 15°

(north 15° east) (Figure 6.4-15). The sandstone was lower in the section on the northern third of the wall. The change in altitude may be related to possible fold development in the red beds in the vicinity of the reverse faults, or it may be depositionally-related in that the poorly developed bedding appeared to remain subhorizontal for much of the exposure.

Observations - Upper Wall

The geologic materials exposed on the upper wall include the upper 3 to 10 feet of Triassic red beds, overlain by Cretaceous Antlers Formation sands and gravels. The upper 10 to 15 feet of the Antlers Formation has been highly calichified and has developed into the characteristic caprock caliche of the Southern High Plains. The joint system in the red beds in the upper wall provided fewer subvertical joints to measure due to the limited exposure of only the upper few feet of the red beds over most of the upper wall. Of the comparatively limited number of measured subvertical joints, the strike maximum occurred at about 290° to 295° (Figure 6.4-16). The upper wall irregular, lower-angle, wavy joints with well-developed slickensides plotted similar to the lower wall irregular, low-angle, wavy joints, with a strike maximum at about 330° but also with a well distributed pole pattern throughout the stereonet (Figure 6.4-17).

There are numerous fault planes in the red beds on the upper wall. The faults in the red beds on the upper wall are very apparent, since the offsets occurred after the development of a grayish-colored altered layer approximately 3 to 4 feet thick at the top of the red beds. The sharp lower contact of the altered layer shows the offsets very well.

The faults in the red bed on the upper wall are virtually all reverse faults, with both south and north apparent dips on the fault planes. The offsets on the reverse faults range from inches to as much as several feet. The largest fault in the red beds on the upper wall, with an offset of about 4 feet, is in the southern third of the exposed wall. This fault is an upward continuation of the southern hanging-wall-up reverse fault in the sandstone on the lower wall, which shows an offset of about 20 feet. The fault appears to die out quickly in the vertical direction. The stress which caused the brittle failure and 20 feet of offset of the sandstone on the lower wall appears to be accommodated throughout the remainder of the red bed claystone/clay in the upper wall by a number of smaller faults and perhaps plastic deformation in the clays.

The faults in the red beds on the upper wall show a pattern of anastamozing slip surfaces, with many of the south- and north-dipping slip planes appearing to pair up and join into a primary slip plane with smaller dendritic slip surfaces splaying off the primary plane. The fault planes on the upper wall dip at about 30° to 40° to the northeast and southwest. Strikes of the fault planes on the upper wall show a maximum at about 284° (north 76° west) (Figure 6.4-18). Slickensides on the fault planes show dip-slip movement, with slickenside azimuths between about 340° and 30° (north 20° west and north 30° east) (Figure 6.4-19), consistent with the 15° apparent compressional stress azimuth of the faults on the lower wall.

During late Jurassic or early Cretaceous time, it appears that the upper part of the red beds was subjected to geochemically reducing conditions that altered the red bed clays from red to gray. The thickness of the altered layer is very uniform along the upper wall, which suggests that the alteration occurred while the top of the red beds were at some relatively uniform elevation, prior to faulting or folding. The reducing conditions and vertical downward advance of the alteration front suggest that the area may have been a submerged bog or shoreline with relatively stagnant, marshy conditions.

The alteration occurs to a very uniform depth marked by a sharp vertically delimited alteration front of about ¼ to ½ inch where the color of the red beds changes from gray to red. The sharp alteration front is most likely a diffusion front within the relatively impermeable clays. The uniform depth of penetration suggests matrix-dominated transport of a diffusion front, since the alteration front does not extend significantly further downward adjacent to the joints or fractures. The joints, though preferred fluid paths and perhaps marginally more transmissive than the unfractured matrix, apparently did not allow any significant additional downward penetration of alteration fluids. The joints were essentially non-transmissive to alteration fluids, likely due to the presence of swelling montmorillonite clays (Glass et al., 1973) and joint closure.

Liesegang banding between joints is very well developed within the altered layer. The liesegang banding parallels and mimics the joint surfaces in three dimensions. Alteration clearly occurred post-jointing, most likely as successive diffusion fronts moved inward from the joints from all directions under saturated conditions. The altered layer may have developed under

successive, perhaps seasonal, wetting and drying conditions, with liesegang banding developing between joints as the joints swelled closed on passage of the wetting fronts.

At the top of the gray altered layer was a readily apparent parting that was present over approximately 80 to 90% of the exposed wall. The parting appears to be an erosional/depositional surface of either late Jurassic or early Cretaceous age based on the presence of some Cretaceous-aged gravels mixed into the upper portion of the zone above the parting. Above the parting are both reworked altered red beds (reworked and redeposited clays of the altered layer) as well as a second zone of alteration in the southern part of the wall where the reworked clays of the gray altered layer have apparently been further altered to a mixture of silt- to sand-sized crystalline carbonates and sulfates.

Above the reworked or reworked and altered clays are the Cretaceous-aged Antlers Formation sands and gravels. The lower part of the Antlers Formation contains numerous clasts and angular blocks of altered upper red beds or reworked altered red beds. The Antlers Formation exhibits a depositional pattern characteristic of braided streams, with a sequence of younger channels cross-cutting older channels and smaller channels a few tens of feet in width embedded within larger channel deposits. The Antlers Formation sands and gravels range from well-sorted fine to medium grained sands to poorly sorted sands and gravels with occasional cobble-sized particles. The lower few feet of the Antlers Formation is poorly to partially cemented sands and gravels apparently unaffected by the calichification process which is readily apparent in the upper parts of the section. Some of the finer sands higher in the section exposed on the upper wall appear well cemented, although the cementing may be due in part to the development of the caprock caliche.

The relationship between faulting in the Triassic red beds and the overlying Cretaceous Antlers Formation was carefully evaluated to determine if any displacement of the younger Cretaceous deposits had occurred. The Triassic red beds are separated from the overlying Cretaceous Antlers Formation sands and gravels by the distinct and mappable parting at the top of the gray altered layer of red beds. None of the observed fault planes or slip surfaces in the Triassic red beds in the extensively mapped section cross or offset the parting. In addition, the bedding in the Antlers Formation is continuous where observable and not calichified, and in particular,

there are no Triassic/Cretaceous contact offsets or bedding offsets in the Cretaceous Antlers Formation above the area in the Triassic red beds where the largest displacements occur nor is there any apparent folding of the Antlers Formation in this area. Therefore, there are no indications that the Cretaceous-aged Antlers Formation was affected by the faulting in the Triassic red beds. There are clearly no geologic Formations present in the excavation younger than Triassic that are affected by faulting and there are no regulatory issues related to faulting at the WCS site. Additionally, there are no issues with respect to potential migration pathways resulting from the faulting at the WCS site. The uppermost faulting occurred completely within the Triassic red beds; which have great capacity for healing and closing fault planes and joints to fluid migration as indicated by the limited penetration of the alteration front in the red beds.

4.1.1.4 *Red Bed Ridge Development*

Faulting of any significance in the vicinity of the WCS site or the Central Basin Platform is generally considered to be Permian or earlier (Nicholson and Clebsch, 1961). Galley (1958, p.439-441) indicates that although "events associated with Laramide and several Tertiary orogenies have broken, destroyed, submerged, or obscured various segments of Paleozoic structures at the southwest edge of the Permian Basin", "Elsewhere the Paleozoic strata lie at almost the same attitudes they had attained at the end of Ochoa time, having been affected subsequently only by regional tilting and local folding or faulting of small vertical displacement." These statements indicate that the Central Basin Platform area has not been significantly disturbed by tectonic events since late Permian (Ochoa) time.

The post-Permian/pre-Cretaceous tilting, folding and faulting discussed in the previous section may have contributed to the development of the red bed ridge by creating a relatively local topographic high uplifted by the minor compressional faulting/folding of the red beds. The local geology discussed in Section 5.3 indicates that the first continuous red bed sandstone, which occurs at an approximate depth of about 225 feet below ground surface, has a south/southwestward dip of about 80 feet per mile. The south/southwestward dipping bedding may represent the southwestern limb of an anticline or monocline with the red bed ridge as the fold axis. The red bed ridge area may have been an inter-drainage topographic high since the compressional event.

The Cretaceous seas began to retreat at the start of the Laramide Orogeny which uplifted the area. From late Paleocene to the end of the Pliocene the area was subjected to erosion, removing most of the Cretaceous deposits. Late Tertiary Ogallala and Gatuna Formations were deposited in stream channels between inter-drainage highs. Apparently neither the Ogallala nor the Gatuna Formations were deposited over the ridge in the WCS vicinity, suggesting that relatively resistant Cretaceous limestones over the Antlers Formation may have effectively capped the red bed ridge, maintaining the ridge as a mesa or inter-drainage high. The red bed ridge remains a local topographic high today, between Monument Draw Texas which drains to the Colorado River, and Monument Draw New Mexico which drains to the Pecos River.

4.1.2 Seismicity

The WCS facility lies in a region with crustal properties that indicate minimum risk due to faulting and seismicity. Crustal thickness is the most reliable predictor of seismic activity and faulting in intracratonic regions (EPRI, 1993). Crustal thickness in the vicinity of the WCS facility is approximately 30 miles (50 km), one of the three thickest crustal regions in North America (Mooney and Braile, 1989). In comparison, the crustal thickness of the Rio Grand Rift is as little as 7.5 miles (12 km) in places. Further, the seismic velocity of the crust in the Southern Great Plains implies that the crust is unusually intact and continuous in this region (EPRI, 1989).

The Central Basin Platform is an area of moderate, low intensity seismic activity based on data obtained from the National Geophysical Data Center of the National Oceanic and Atmospheric Administration (NOAA, 1992 as reported in Terra Dynamics, 1993) and the U.S. Geological Survey (USGS) Earthquake Data Base available from the National Earthquake Information Center (http://neic.usgs.gov/). Table 6.4-1 provides the historical seismic activity within 250 kilometers of the WCS facility (32.433°N, 103.05°W). Table 6.4-1 includes the data through 1992 from the NOAA data base, which was submitted in the original RCRA permit application, updated with information through 2003 from the national seismic data base operated by the USGS. The computer search for all recorded seismic activity within a 250 km (155 mile) radius of the proposed WCS landfill site provided a list of 188 seismic events (188 total with 68 suspected duplicates by Terra Dynamics (1993)) during the period from 1931 to 2003. Seismic activity for New Mexico and bordering areas, which includes Andrews County, is shown on

Figure 6.4-20. With respect to seismicity in the WCS area, Sanford et al. (2002) indicate that a large fraction of activity in southeastern New Mexico and adjacent areas of west Texas is induced by oil and gas production, secondary recovery, or waste injection.

Figure 6.4-21 illustrates the largest earthquakes (moment magnitudes >3) from the same data set used to develop Figure 6.4-20. The largest earthquake in the vicinity of the WCS facility, referred to as the Rattlesnake Canyon earthquake with a magnitude of 5, occurred in 1992. The Rattlesnake Canyon earthquake was located by the seismograph stations monitored by the New Mexico Institute of Mining and Technology at latitude 32°17.80N and longitude 103°10.33W (Sanford et al., 1993), which is approximately 11 miles southwest of the facility. The USGS located the Rattlesnake Canyon earthquake at latitude 32°20.16N and longitude 103°06.06W, about 7 miles southwest of the WCS facility; however, Sanford et al. (1993) indicate that due to the uncertainty in the location reported by the USGS, the location reported by Sanford et al. (1993) is more accurate. The location of the Rattlesnake Canyon earthquake was approximately three miles east of the Paleozoic west platform fault (Figure 6.4-4). The Rattlesnake Canyon earthquake was interpreted by Sanford et al. (1993) as a reverse fault, with movement consistent with the approximately east–west maximum horizontal stress orientation reported by Zoback and Zoback (1991) and Zoback et al. (1991).

The seismic hazard at a particular geographic position is due to ground motion or shaking. Seismic hazard is based on historical seismic activity and frequently presented as Peak Ground Acceleration (PGA) maps. The maps present the probability of the PGA due to earthquakes exceeding a particular value of acceleration (expressed as a fraction or percent of gravitational acceleration) over a particular time period. A PGA of greater than about 0.2 g is considered the acceleration level at which considerable damage can begin to occur to weakly built structures (Sanford et al., 2002). Figure 6.4-22 is a seismic hazard map of the western United States prepared by the USGS (http://geohazards.cr.usgs.gov/eq/, October 2002 revision). The map indicates that at the 90% probability level over a 50-year time period, the PGA of the southeastern New Mexico/Andrews County area would not exceed approximately 0.03 to 0.04 g (site specific search yields 0.0322 g). Figure 6.4-23 is a similar seismic hazard map of the western United States, which indicates that at the 98% probability level over a 50-year time period, the PGA of the southeastern New Mexico/Andrews County area would not exceed

approximately 0.14 to 0.16 g (site specific search yields 0.1535 g). Golder Associates (1998) calculated the PGA at the WCS site for the Rattlesnake Canyon earthquake in the range of 0.06 to 0.07 g, which is well below the PGA of 0.2 g where considerable damage can begin to occur to weakly built structures (Sanford et al., 2002). Golder Associates (1998) indicate that these low estimated accelerations are "generally considered to be insignificant to well designed and constructed engineered structures or facilities."

4.1.3 Lineaments

Lineaments are relatively straight physiographic features typically identified by a review of surficial geologic maps, surface topography maps, LANDSAT images, and aerial photographs, including high altitude aerial photographs. Based on Landsat imagery, Finley and Gustavson (1981) identified more than 4600 lineaments throughout the Texas Panhandle, ranging in length from 1.2 miles up to 25 miles (Figure 6.4-24). Finley and Gustavson (1981) noted that the Landsat-identified lineaments fell into six categories: 1) stream segments, or short stream reaches commonly connecting at sharp angular junctions, 2) drainage lines, or linear valley trends independent of the orientation of stream segments within the trend, 3) scarps, or prominent topographic breaks, 4) playa alignments, 5) geologic contacts, or contacts between surficial materials with different reflectivities, and 6) tonal anomalies, or linear features that are not clearly a member of any of the previous categories and may be composites of previous categories.

Finley and Gustavson (1981) conclude that the development of physiographically-expressed lineaments is controlled or at least influenced by geologic structure. They further interpret that since few surface faults are mapped in the study area (91,500 square miles of the Texas Panhandle, including the Southern High Plains and most of Andrews County), joints rather than widespread faults are the likely geologic structural control on lineament development. Joints are fractures or partings in rocks along which movement has been negligible or absent (Dennis, 1972). The development of joints is an indication of the brittle behavior of rock, and is most evident in the Triassic and Permian sandstones within the area of the Southern High Plains. The poorly consolidated sediments of the Ogallala Formation do not exhibit well-developed

jointing patterns. The Caprock caliche often exhibits an irregular, nearly orthogonal jointing pattern (Finley and Gustavson, 1981).

Finley and Gustavson (1981) suggest that minor or poorly developed jointing in the Pleistocene and Holocene deposits overlying the Caprock caliche may have offered preferred infiltration focus that could foster playa development at the intersection of joint sets, and that an area of increased joint density may localize playa-lake depressions.

Several mechanisms can account for the relationship between physiographically-expressed surface lineaments and susbsurface jointing. Joints form preferential planes that can be exploited by surficial and subsurface weathering processes. Joints offer paths of weakness and less resistance to erosional processes, allowing the development of surface drainage systems and linear stream segments in preferred orientations. Consequently, drainage systems in the Southern High Plains are often classified as lineaments, since their linear orientation is controlled by the joint systems that they exploit (Finley and Gustavson, 1981). Joints can be propagated upward into geologically younger sediments by many processes, including residual tectonic stresses (Price, 1966), crustal extension due to post-glacial rebound (Grisak and Cherry, 1975), shrinkage and differential compaction related to wetting and drying of clay-rich sediments, and differential compaction and dissolution of underlying materials (Finley and Gustavson, 1981). In the Southern High Plains, the orientation of joints and their associated surface lineations is controlled primarily by historical tectonic and structural trends (Finley and Gustavson, 1981). As shown in Figure 6.4-24, the dominant orientation for surface lineations in the Southern High Plains is northwest to southeast, with a secondary orientation of northeast to southwest.

At the regional scale mapped by Finley and Gustavson (1981), Figure 6.4-24 shows a multicomponent northwest-southeast lineament approximately 3 to 4 miles in total length about 10 miles north of the WCS facility in Gaines County. The lineament is located in the approximate vicinity of Monument Draw, Texas (note: there are two Monument Draws in the WCS vicinity: one in Texas which starts between Hobbs and Eunice in New Mexico and heads eastward as a tributary to Mustang Creek in Texas; and one which starts west of Monument, New Mexico, continuing southeasterly and turning south around Eunice about 5 miles west of

the Texas/New Mexico border). A second lineament at the regional scale identified by Finley and Gustavson (1981) lies in Andrews County, about 14 miles east of the WCS facility. This lineament appears to be the continuation of Monument Draw, Texas. The lineament map of Finley and Gustavson does not indicate the presence of Landsat-identified lineaments at the WCS facility.

Also at the regional scale, Bolden (1984) suggests that there are several regional-scale lineaments 200 to 330 miles in length in Trans-Pecos Texas and the Texas Panhandle oriented between 298° and 306°. The nearest of these to the WCS facility is a shorter offshoot line oriented approximately 345°, extending through Ward and Winkler counties in Texas into Lea County in New Mexico. The offshoot line appears to be defined by Monument Draw, New Mexico and its southern extension to the Pecos River through Winkler and Ward Counties, Texas.

At the local scale, lineaments were identified by Terra Dynamics in the vicinity of the WCS site based on an analysis of NASA color-infrared aerial photographs (Terra Dynamics, 1993). Terra Dynamics indicated the lineaments were related to linear drainage features and ground surface color tone anomalies. The lineaments were shown as straight lines on the color infrared imagery used by Terra Dynamics (Terra Dynamics, 1993, Figure VI.A.12). Terra Dynamics identified 5 northwest trending lineaments. The southernmost of these lineaments extended through the WCS facility. Terra Dynamics also identified two north trending lineaments between the WCS site and Eunice. The lineament through the WCS site was described as an anomaly in the ground surface color tone on the color-infrared

Figure 6.4-25 is a 1983 color infrared photograph of the WCS area from the National High Altitude Program (note: the 1982 photograph included in the Terra Dynamics Geology report is not available from the EROS data center) and Figure 6.4-26 is a 1986 color infrared photograph of the same area at a slightly different scale. Four of the five northwest and north trending lineaments near the WCS site identified by Terra Dynamics are shown on Figure 6.4-26. The northernmost northwest-trending lineament identified by Terra Dynamics is off the photo approximately 8 miles to the north of the WCS site.

Golder Associates also conducted an analysis of the lineaments in the vicinity of the WCS facility and provided a summary of their evaluation in a draft document to WCS dated January 4, 1999. Lineaments identified by Terra Dynamics and Golder Associates are discussed below.

The southernmost northwest-trending lineament through the WCS facility, identified by Terra Dynamics, is represented by aligned zones of enhanced vegetation, shallow depressions and darker ground tones trending about 300° to 310°. The aligned depressions are most evident where the Caprock caliche is at or very near the surface. The tonal contrast in the center of the photo is where the Caprock caliche is either at ground surface or covered by only a thin veneer of windblown sand. The largest of the depressions, which may be considered a small playa about 15 acres in size, is located about one-half mile northeast of the existing landfill. The alignment of the playas at the WCS site likely results from their development at the intersection of joints, with the primary jointing direction trending 300° to 310°.

Part of the surface expression of the 300° to 310° lineament is a bench in the topography between Windmill Hill and the existing landfill. The bench alignment is coincident with the regional 300° to 320° alignment of lineaments in the Southern High Plains (Finley and Gustavson, 1981) that likely represents one of the primary jointing directions in the Southern High Plains. The bench overlies and is aligned with the red bed ridge and is topographically expressed for about 6000 feet with a relief of about 20 feet. The bench is on the southwest slope of the drainage divide between the Pecos River and the Colorado River. The bench has developed as an erosional feature along the preferred jointing direction in the Southern High Plains. The bench projects to Baker Spring, to a notch in the topography about one-half mile northwest of Baker Spring, and parallels Mescalero Ridge, part of the Caprock escarpment about 15 miles northwest of the WCS site.

Two smaller lineaments oriented about 45° were identified by Golder Associates to the west and east of the permitted area. The westernmost 45° lineament, which is about 4000 feet in length, is a surface draw that empties into a depression at Baker Spring, New Mexico. The 45° lineament east of the permitted area is less developed. It extends through the ranch house area for a total length of about 4,500 to 5,000 feet, developing into a shallow draw southwest of the ranch house area. The north-trending lineaments identified by Terra Dynamics about 3 miles

west of the WCS site in Lea County, New Mexico, may be related to tonal contrasts in the vicinity of Monument Draw, New Mexico.

The lineaments in the vicinity of the WCS facility do not have any geologic or geomorphic characteristics typical of active faults. There are no topographic shifts along the lineament, or any apparent offsets in local drainage, or any interruptions in the gradient of erosional terraces above Baker Spring (assuming Baker Spring comprises part of the lineament). The lineament in the vicinity of the WCS facility is considered to be an erosional feature.

4.2 LAND SURFACE SUBSIDENCE

This section addresses the potential for land surface subsidence due to ongoing geologic processes and human activities in the vicinity of the WCS facility. Subsidence can be defined as the sudden sinking or gradual downward settling of the earth's surface with little or no horizontal movement. Subsidence may be caused by natural geologic processes such as solution or compaction or by human activities such as subsurface mining or pumping of oil or groundwater.

4.2.1 Land Surface Subsidence due to Geologic Processes

No subsidence features related to geologic processes have been identified within the permitted area or the immediate vicinity of the site. The nearest active subsidence features to the WCS facility are the San Simon Swale, the San Simon Sink, the Wink Sinks, and a sink northwest of Jal, New Mexico (Figure 6.4-27). The San Simon Swale and the San Simon Sink are located approximately 20 miles west-southwest of the WCS facility in Lea County, New Mexico. The San Simon Swale is a large (100 mi^2), northwest- to southeast-trending, elongate depression that overlies and is parallel to the inner margin of the Permian Capitan Reef (Figure 6.4-27). The San Simon Sink is located within the southern end of the San Simon Swale and covers an area of 0.5 mi^2. The sink is approximately 130 feet deep and is filled with 400 feet of alluvium deposited on top of Triassic red beds (Baumgardner et al., 1982). Subsidence was last recorded at the San Simon Sink approximately 50 years ago.

7.0 REFERENCES

Ashworth, J.B., 1990, Evaluation of Ground-Water Resources in parts of Loving, Pecos, Reeves, Ward, and Winkler Counties, Texas: Texas Water Development Board Report 317, 51 p.

Baker, C.L., 1915, Geology and Underground Waters of the Northern Llano Estacado: Austin, University of Texas Bulletin 57, 93 p.

Bally, A.W., C.R. Scotese, and M.I. Ross, 1989, North America; Plate-Tectonic Setting and Tectonic Elements *in* The Geology of North America-An Overview: Volume A, Decade of North American Geology, p. 1-15, Geological Society of America, Boulder, Colorado.

Barnes, V.E., 1976, Geologic Atlas of Texas, Hobbs Sheet: The University of Texas at Austin, Bureau of Economic Geology, Scale 1:250,000.

Baumgardner, R.W., Jr., 1980, Suspended Sediment Concentration and Stream Discharge Relationships for the Prairie Dog Town Fork of the Red River: An Approach to Determine Erosion Rates, *in* Geology and Geohydrology of the Palo Duro Basin, Texas Panhandle, A Report on the Progress of Nuclear Waste Isolation Feasibility Studies (1979): The University of Texas at Austin, Bureau of Economic Geology Circular 80-7, p. 63-66.

Baumgardner, R.W., Jr., A.D. Hoadley, and A.G Goldstein, 1982, Formation of the Wink Sink, a Salt Dissolution and Collapse Feature, Winkler County, Texas, The University of Texas at Austin, Bureau of Economic Geology Report of Investigations No. 114, 38 p.

Bebout, D.G., and K.J. Meador, 1985, Regional Cross Sections – Central Basin Platform, West Texas: The University of Texas at Austin, Bureau of Economic Geology, 4 p., 11 plates.

Blandford, T.N., D.J. Blazer, K.C. Calhoun, A.R. Dutton, T. Naing, R.C. Reedy, and B.R. Scanlin, 2003, Groundwater Availability of the Southern Ogallala Aquifer in Texas and New Mexico Numerical Simulations through 2050: Texas Water Development Board Draft Report, 160 p.

Bolden, G.P., 1984, Wrench Faulting in Selected Areas of the Permian Basin, *in* Transactions, Southwest Section American Association of Petroleum Geologists, Publication No. SWS 84-78: West Texas Geological Society, Midland, TX, p. 131-140.

Bodvarsson, G.S., J.T. Birkholzer, S. Finsterle, H.H. Liu, J. Rutqvist and Y.S. Wu, 2003, "The use of TOUGH2/ITOUGH2 in support of the Yucca Mountain Project: successes and limitations," Proc., TOUGH Symposium 2003, Lawrence Berkeley national Laboratory, Berkeley, CA, May 12-14.

Bodvarsson, G.S. and Y. Tsang (editors), 1999, Special Issue on Flow and Transport at Yucca Mountain, J. Contaminant Hydrology, vol. 38.Bradley, R.G., and S. Kalaswad, 2003, The Groundwater Resources of the Dockum Aquifer in Texas: Texas Water Development Board Report 359, 73 p.

Brooks, R. H., and C. T. Corey, 1964. Hydraulic Properties of Porous Media. Hydrology Paper 3, Colorado State University, Fort Collins, Colorado, 27p.

Brune, G., 1981, Springs of Texas: Branch-Smith, Inc., Fort Worth, TX, 566 p.

Chem-Nuclear Systems, L.L.C., 2001. Waste Control Specialists Major Ion Study Report, BEDL-01-021, Chem-Nuclear Systems, L.L.C., Environmental and Dosimetry Laboratory, Barnwell, South Carolina. 14p.

Comer, J.B., 1991, Stratigraphic Analysis of the Upper Devonian Woodford Formation, Permian Basin, West Texas and Southeastern New Mexico: The University of Texas at Austin, Bureau of Economic Geology Report of Investigations No. 201, 63 p.

Conner, N.R., H.W. Hyde, and H.R. Stoner, 1974, Soil Survey of Andrews County, Texas: U.S. Department of Agriculture, Soil Conservation Service, 45 p.

Cronin, J.G., 1969, Groundwater in the Ogallala Formation in the Southern High Plains of Texas and New Mexico: U.S. Geological Survey Hydrological Investigations HA-330, 9 p.

CRWMS M&O, 1998, Total System Performance Assessment Viability Analysis Technical bases Document, Chapter 2, Unsaturated Zone Hydrology Model, TRW, Yucca Mountain Project, Las Vegas, NV.

Davis, S.D., W.D. Pennington, and S.M. Carlson, 1989, A Compendium of Earthquake Activity in Texas: The University of Texas at Austin, Bureau of Economic Geology Geological Circular 89-3, 27 p.

Dennis, J.G., 1972, Structural Geology: John Wiley and Sons, Inc., New York, NY, 532 p.

Dumble, E.T., 1888, Geological Survey of Texas, Second Report of Progress, January 1892: Texas Geological and Mineralogical Survey, Department of Agriculture, Insurance, Statistics, and History, 91 p.

Dunne, T., and L.B. Leopold, 1978, Water in Environmental Planning: W.H. Freeman and Company, San Francisco, 817 p.

Dutton, S.P., R.J. Finley, W.E. Galloway, T.C. Gustavson, C.R. Handford, and M.W. Presley, 1979, Geology and Geohydrology of the Palo Duro Basin, Texas Panhandle, A Report on the

Progress of Nuclear Waste Isolation Feasibility Studies (1978): The University of Texas at Austin, Bureau of Economic Geology Geological Circular No. 79-1, 99 p.

Dutton, A.R., 1995, Groundwater Isotopic Evidence for Paleorecharge in U.S. High Plains Aquifers: Quaternary Research 43, p. 221-231.

Dutton, A.R., and W.W. Simpkins, 1986, Hydrogeochemistry and Water Resources of the Triassic Lower Dockum Group in the Texas Panhandle and Eastern New Mexico: University of Texas at Austin, Bureau of Economic Geology Report of Investigations No. 161, 51 p.

Electric Power Research Institute (EPRI), 1993, EPRI Technical Report-1022293, Guidelines for Determining Design Basis Ground Motions, 3412 Hillview Avenue, Palo Alto, California

Evans, G.L., and G.E. Meade, 1945, Quaternary of the Texas High Plains: University of Texas, Austin, Bureau of Economic Geology Publication 4401, p. 485-507.

Ewing, T.E., 1991, The Tectonic Framework of Texas, Text to Accompany "The Tectonic Map of Texas": The University of Texas at Austin, Bureau of Economic Geology, 36 p.

Fallin, J.A., 1989, Hydrogeology of Lower Cretaceous Strata under the Southern High Plains of Texas and New Mexico: Texas Water Development Report No. 314, 39 p.

Finley, R.J., 1979, Climate of the Texas Panhandle and its Influence on Erosion, *in* Geology and Geohydrology of the Palo Duro Basin, Texas Panhandle, A Report on the Progress of Nuclear Waste Isolation Feasibility Studies (1978): The University of Texas at Austin, Bureau of Economic Geology Geological Circular No. 79-1, p. 65-68.

Finley, R.J., 1981, A 10-year Storm: Its Effects and Relationship to Age-Dated Alluvial Stratigraphy, Randall, County, Texas Panhandle, *in* Geology and Geohydrology of the Palo Duro Basin, Texas Panhandle, A Report on the Progress of Nuclear Waste Isolation Feasibility Studies (1980): The University of Texas at Austin, Bureau of Economic Geology Geological Circular No. 81-3, p. 138-143.

Finley, R.J., and Baumgardner, R.W., Jr., 1981, Sedimentology and Basin Morphometry of the Little Red River Basin: Insights into Retreat of the Eastern Caprock Escarpment, Texas Panhandle, *in* Geology and Geohydrology of the Palo Duro Basin, Texas Panhandle, A Report on the Progress of Nuclear Waste Isolation Feasibility Studies (1980): The University of Texas at Austin, Bureau of Economic Geology Geological Circular No. 81-3, p. 148-151.

Finley, R.J., and T.C. Gustavson, 1980, Climatic Controls on Erosion in the Rolling Plains and along the Caprock Escarpment of the Texas Panhandle: The University of Texas at Austin, Bureau of Economic Geology Geological Circular 80-11, 50 p.

Finley, R.J., and T.C. Gustavson, 1981, Lineament Analysis Based on Landsat Imagery, Texas Panhandle: The University of Texas at Austin, Bureau of Economic Geology Geological Circular 81-5, Plate 1, 37 p.

Freeze, R.A., and J.A. Cherry, 1979, Groundwater, Prentice-Hall, Inc., Englewood Cliffs, N.J., 604 p.

Galley, J.E., 1958, Oil and Geology in the Permian Basin of Texas and New Mexico, *in* Habitat of Oil: American Association of Petroleum Geologists, p. 395-446.

Galloway, W.E., T.E. Ewing, C.M. Garret, N. Tyler, and D.G. Bebout, 1983, Atlas of Major Texas Oil Reservoirs: The University of Texas at Austin, Bureau of Economic Geology, p. 90..

Glass, H.D., John C. Fry, and A. Byron Leonard, 1973, Clay Minerals in East-Central New Mexico: New Mexico Bureau of Mines and Mineral Resources, Circular 139, 14 p.

Golder Associates, 1998, Earthquake Location and Effects at the WCS Site with Respect to the January 2, 1992 Rattlesnake Canyon Earthquake, New Mexico: Letter Report to MT & Associates, December 18, 1998, 6 p.

Grisak, G.E., and J.A. Cherry, 1975, Hydrologic Characteristics and Response of Fractured Till and Clay Confining a Shallow Aquifer: Canadian Geotechnical Journal Volume 12, No. 1, p. 23-43.

Gustavson, T.C., 1980, Faulting and Salt Dissolution, *in* Geology and Geohydrology of the Palo Duro Basin, Texas Panhandle, A Report on the Progress of Nuclear Waste Isolation Feasibility Studies (1979): The University of Texas at Austin, Bureau of Economic Geology Circular 80-7, p. 83-87.

Gustavson, T.C., 1996, Fluvial and Eolian Depositional Systems, Paleosols, and Paleoclimate of the Upper Cenozoic Ogallala and Blackwater Draw Formations, Southern High Plains, Texas and New Mexico: University of Texas at Austin, Bureau of Economic Geology Report of Investigations No. 239, 62 p.

Gustavson, T.C., and R.J. Finley, 1985, Late Cenozoic Geomorphic Evolution of the Texas Panhandle and Northeastern New Mexico: The University of Texas at Austin, Bureau of Economic Geology Report of Investigations No. 148, 42 p.

Gustavson, T.C., and W.W. Simpkins, 1989, Geomorphic Processes and Rates of Retreat Affecting the Caprock Escarpment, Texas Panhandle: The University of Texas at Austin, Bureau of Economic Geology Report of Investigations No. 180, 49 p.

Gustavson, T.C., R.J. Finley, and R.W. Baumgardner, Jr., 1980, Preliminary Rates of Slope Retreat and Salt Dissolution along the Eastern Caprock Escarpment of the Southern High

Plains and in the Canadian River Valley, *in* Geology and Geohydrology of the Palo Duro Basin, Texas Panhandle, A Report on the Progress of Nuclear Waste Isolation Feasibility Studies (1979): The University of Texas at Austin, Bureau of Economic Geology Circular 80-7, p. 76-82.

Gustavson, T.C., R.J. Finley, and R.W. Baumgardner, Jr., 1981, Retreat of the Caprock Escarpment and Denudation of the Rolling Plains in the Texas Panhandle: Bulletin of the Association of Engineering Geologists, Vol. XVIII, No. 4, p. 413-422.

Gustavson, T.C., V.T. Holliday, and S.D. Hovorka, 1995, Origin and Development of Playa Basins, Sources of Recharge to the Ogallala Aquifer, Southern High Plains, Texas and New Mexico: The University of Texas at Austin, Bureau of Economic Geology Report of Investigations No. 229, 44 p.

Gustavson, T.C., R. W. Baumgardner, Jr., S.C. Caran, V.T. Holliday, H.H. Mehnert, J.M. O'Neill, and C.C. Reeves, Jr., 1991, Quaternary Geology of the Southern Great Plains and an Adjacent Segment of the Rolling Plains, *in* Quaternary Nonglacial Geology: Conterminous U.S., The Geology of North America Volume K-2, Decade of North American Geology, p. 477-501.

Hawley, J.A., 1993, The Ogallala and Gatuna Formations in the Southeastern New Mexico Region, A Progress Report: New Mexico Geological Society Guidebook, 44th Field Conference, p. 261-269.

Hills, J.M., 1963, Late Paleozoic Tectonics and Mountain Ranges, Western Texas to Southern Colorado, American Association of Petroleum Geologists Bulletin, vol. 47, p. 1709-1724.

Hills, J.M., 1985, Structural Evolution of the Permian Basin of West Texas and New Mexico, *in* Structure and Tectonics of Trans-Pecos Texas: West Texas Geological Society, Field Conference Publication 85-81, p. 89-99.

Hobbs News-Sun, 1998, Newspaper Article, Jal has a Big Hole, September 13, 1998.

Holliday, V.T., 1989, The Blackwater Draw Formation (Quaternary), A 1.4-plus m.y. Record of Eolian Sedimentation and Soil Formation on the Southern High Plains: Geological Society of America Bulletin 101, p. 1598-1607.

Holliday, V.T., 1990, Sedimentation, Soil Stratigraphy, and Age of the Blackwater Draw Formation, *in* Geologic Framework and Regional Hydrology: Upper Cenozoic Blackwater Draw and Ogallala Formations, Great Plans, ed. T.C. Gustavson: Bureau of Economic Geology, p. 10-22.

Holliday, V.T., 1995, Stratigraphy and Paleoenvironments of Late Quaternary Valley Fills on the Southern High Plains: Geological Society of America Memoir No. 186, 136 p.

Holliday, V.T., S.D. Hovorka, and T.C. Gustavson, 1996, Lithostratigraphy and Geochronology of Fills in Small Playa Basins on the Southern High Plains, United States: Geological Society of America Bulletin 108(8), p. 953-965.

Jones, I.C., 2001, Cenozoic Pecos Alluvium Aquifer, *in* Aquifers of West Texas: Texas Water Development Board Report 356, ed. R.E. Mace, W.F. Mullican III, and E.S. Angle, p. 120-134.

Kelley, V.C., 1980, Gatuna Formation (Late Cenozoic), Pecos Valley, New Mexico and Trans-Pecos Texas: New Mexico Geological Society Guidebook, 31st Field Conference, p. 213-217.

Lehman, T.M, 1994a, The Saga of the Dockum Group and the Case of the Texas/New Mexico Boundary Fault: New Mexico Bureau of Mines and Mineral Resources, Bulletin 150, p. 37-51.

Lehman, T.M, 1994b, Save the Dockum Group!: West Texas Geological Society Bulletin 34(4), p. 5-10.

Levey, R.A., 1976, Characteristics of Coarse-Grained Point Bars, Upper Congaree River, South Carolina, *in* Hayes, M.O., and Kana, T.W., editors, Terrigenous Clastic Depositional Environments: Coastal Research Division, Department of Geology, University of South Carolina, Technical Report No. 11-CRD, p. 11-38 to 11-51.

Liu, H.H. and C.F. Ahlers, 2003, Calibrated Properties Model, MDL-NBS-HS-000003, BSC, Yucca Mountain Project, Las Vegas, NV.

Liu, H.H., C. Doughty and G.S. Bodvarsson, 1998, "An active fracture model for unsaturated flow and transport in fractured rock," Water Resources Research, vol. 34, no. 10, pages 2633-2646.

Mace, R.E., 2001, Aquifers of West Texas: An Overview, *in* Aquifers of West Texas: Texas Water Development Board Report 356, ed. R.E. Mace, W.F. Mullican III, and E.S. Angle, p. 1-16.

Machenberg, M.D., 1986, Eolian Deflation and Deposition, Texas Panhandle, *in* Geomorphology and Quaternary Stratigraphy of the Rolling Plains, Texas Panhandle, ed. T.C. Gustavson: University of Texas at Austin, Bureau of Economic Geology Guidebook No. 22, p. 41-44.

McGowen, J.H., and L.E. Garner, 1970, Physiographic Features and Stratification Features of Coarse-Grained Point Bars: Modern and Ancient Examples: Sedimentology, Volume 14, p. 77-111.

McGowen, J.H., G.E. Granata, and S.J. Seni, 1979, Depositional Framework of the Lower Dockum Group (Triassic) Texas Panhandle: The University of Texas at Austin, Bureau of Economic Geology Report of Investigations No. 97, 60 p.

Mullican, W.F., III, N.D. Johns, and A.E. Fryar, 1997, Playas and Recharge of the Ogallala Aquifer on the Southern High Plains of Texas – An Examination using Numerical Techniques: The University of Texas at Austin, Bureau of Economic Geology Report of Investigations No. 242, 72 p.

National Oceanic and Atmospheric Administration (NOAA), 1992, Earthquake database Search Within 250 KM of 32.433°N, 103.05°W, National Geophysical Data Center, Boulder, Colorado: Report to Terra Dynamics Incorporated, Austin, TX, 1 map, 1 table.

Nativ, R., 1988, Hydrogeology and Hydrochemistry of the Ogallala Aquifer, Southern High Plains, Texas Panhandle and Eastern New Mexico: The University of Texas at Austin, Bureau of Economic Geology Report of Investigations No. 177, 64 p.

Nativ, R. and G.N. Gutierrez, 1988, Hydrogeology and Hydrochemistry of Cretaceous Aquifers, Texas Panhandle and Eastern New Mexico: The University of Texas at Austin, Bureau of Economic Geology Geological Circular 88-3, 32 p.

Nicholson, A., Jr., and A. Clebsch, Jr., 1961, Geology and Ground-Water Conditions in Southern Lea County, New Mexico: New Mexico Bureau of Mines and Mineral Resources Ground-Water Report 6, Socorro, New Mexico, 123 p.

Nitao, J.J., 1991, "Theory of matrix and fracture flow regimes in unsaturated, fractured media," Proc., Second International High Level Radioactive Waste Management Conference, Las Vegas, NV, April 29-May 3, 1991.

Odessa American, 1998, Newspaper Article, Sinking Feeling, September 25, 1998.

Osterkamp, W.R., and W.W. Wood, 1984, Development and Escarpment Retreat of the Southern High Plains, *in* Whetstone, G.A. (ed.), Proceedings of the Ogallala Aquifer Symposium 2, Texas Tech Water Resources Center, Lubbock, Texas, p. 177-193.

Powers, D.W., and R.M. Holt, 1993, The Upper Cenozoic Gatuna Formation of Southeastern New Mexico: New Mexico Geological Society Guidebook, 44th Field Conference, p. 271-282.

Price, N.J., 1966, Fault and Joint Development in Brittle and Semi-Brittle Rock: Pergamon Press, New York, NY, 176 p.

Pruess, K., 1991, A General Purpose Numerical Simulator for Multiphase Fluid and Heat Flow, LBL-29400, Lawrence Berkeley National Laboratory, CA.Pruess, K. (editor), 1995, Proceedings, TOUGH Workshop 1995, Lawrence Berkeley National Laboratory, CA, May 11-13.

Pruess, K. (editor), 1998, Proceedings, TOUGH Workshop 1998, Lawrence Berkeley National Laboratory, CA, May 17-19.

Pruess, K. (editor), 2003, Proceedings, TOUGH Symposium 2003, Lawrence Berkeley National Laboratory, CA, May 12-14.

Reeves, C.C., Jr., 1966, Pluvial Lake Basins of West Texas: Journal of Geology, vol. 74, p. 269-291.

Reeves, C.C., Jr., 1970, Drainage Pattern Analysis, Southern High Plains, West Texas and Eastern New Mexico, *in* Mattox, R.B., and Miller, W.D., eds., The Ogallala Aquifer Symposium: Lubbock, Texas Tech University, International Center for Arid and Semiarid Land Studies, Special Report No. 39, p. 58-71.

Reeves, C.C., Jr., W.T. Parry, 1969, Age and Morphology of Small Lake Basins, Southern High Plains, Texas and Eastern New Mexico: Texas Journal of Science Volume 20, p. 349-354.

Sanford, A.R., R. Balch, L. Jaksha, and S. Delap, 1993, Location and Fault Mechanism of the 2 January 1992 Rattlesnake Canyon Earthquake in Southeastern New Mexico: New Mexico Institute of Mining and Technology, Geophysical Research Center and Geoscience Department, Geophysics Open-File Report 70, 10 p.

Sanford, A.R., K. Lin, I. Tsai, and L.H. Jaksha, 2002, Earthquake Catalogues for New Mexico and Bordering Areas: 1869-1998: New Mexico Bureau of Geology and Mineral Resources Circular 210, 9 p.

Seni, S.J., 1980, Sand-Body Geometry and Depositional Systems, Ogallala Formation, Texas: The University of Texas at Austin, Bureau of Economic Geology Report of Investigations No. 105, 36 p.

Simpkins, W.W., 1986, Rates of Hillslope Erosion at Six Study Areas on the High Plains and Rolling Plains of the Texas Panhandle, *in* Geomorphology and Quaternary Stratigraphy of the Rolling Plains, Texas Panhandle, ed. T.C. Gustavson: University of Texas at Austin, Bureau of Economic Geology Guidebook No. 22, p. 36-40.

Simpkins, W.W., and R.W. Baumgardner, Jr., 1982, Stream Incision and Scarp Retreat Rates Based on Volcanic Ash Date from the Seymour Formation, *in* Geology and Geohydrology of the Palo Duro Basin, Texas Panhandle, A Report on the Progress of Nuclear Waste Isolation Feasibility Studies (1981): The University of Texas at Austin, Bureau of Economic Geology Circular 82-7, p. 160-163.

Simpkins, W.W., T.C. Gustavson, and R.J. Finley, 1982, Erosion Process Studies in the Texas Panhandle—Analysis of a Two-Year Data Record, *in* Geology and Geohydrology of the Palo Duro Basin, Texas Panhandle, A Report on the Progress of Nuclear Waste Isolation Feasibility Studies (1981): The University of Texas at Austin, Bureau of Economic Geology Circular 82-7, p. 168-175.

Terra Dynamics, Incorporated, 1993, RCRA Permit Application for a Hazardous Waste Storage, Treatment and Disposal Facility Andrews County, Texas, Section VI. Geology Report: Terra Dynamics Incorporated, Austin, TX.

Texas Water Development Board, 1972, A Survey of the Subsurface Saline Water of Texas: TWDB Report 157,Volume 1, 113 p.

USAE, 1997, U.S. Army Corps of Engineers, The Hydrologic Evaluation of Landfill Performance (HELP) *Model*, Version 3.07, November 1997.

Van Genuchten, M.Th., 1980, "A closed-form equation for predicting the hydraulic conductivity of unsaturated soils," Soil Sci. Soc. Am. J., vol. 44, no. 5, pages 892-898.

West Texas Geological Society (WTGS), 1976, Lexicon of Permian Stratigraphic Names of West Texas and Southeastern New Mexico: West Texas Geological Society Publication 76-66, Correlation chart.

Wood, W.W., W.E. Sanford, and C.C. Reeves, Jr., 1992, Large Lake Basins of the Southern High Plains: Ground-Water Control of Their Origin?: Geology Volume 20, p. 535-538.

Wright, W.F., 1979, Petroleum Geology of the Permian Basin: West Texas Geological Society Publication 79-71, 98 p.

Wu, Y.S. C. Haukwa and G.S. Bodvarsson, 1999, "A site-scale model for fluid and heat flow in the unsaturated zone of Yucca Mountain, Nevada," J. Contaminant Hydrology, vol. 38, pages 185-215.

Zoback, M.D., and M.L. Zoback, 1991, Tectonic Stress Field of North America and Relative Plate Motions, *in* Neotectonics of North America, Decade Map Volume: Geological Society of America, ed. D.B. Slemmons, E.R. Engdahl, M.D. Zoback, and D.D. Blackwell, p. 339-366.

Zoback, M.L., M.D. Zoback, J. Adams, S. Bell, M. Suter, G. Suarez, K. Jacob, C. Estabrook, and M. Magee, 1991, Stress Map of North America, The Decade of North American Geology DNAG: The Geological Society of America, Boulder, Colorado, Continent-Scale Map-005, scale 1:5,000,000.

TABLE 6.4-1
HISTORICAL SEISMIC ACTIVITY WITHIN 25 km (155 MILE) RADIUS OF PROPOSED LANDFILL SITE (32.433N, 103.05W)

DATE	LOCATION		DISTANCE	DISTANCE	INTENSITY	MOMENT
	LATITUDE (N)	LONGITUDE (W)	(MILES)	(KM)		MAGNITUDE
08/16/31	30.6	104.1	140	225	VIII	
08/16/31	30.6	104.1	140	225		
08/16/31	30.6	104.1	140	225		
08/16/31	30.6	104.1	140	225		
08/16/31	30.6	104.1	140	225		
08/16/31	30.6	104.2	143	230	VIII	
08/16/31	30.7	104.6	150	241		
08/16/31	30.7	104.6	150	241		
08/18/31	30.6	104.1	140	225		
08/18/31	30.7	104.6	150	241	V	
08/18/31	30.7	104.6	150	241		
08/19/31	30.6	104.1	140	225	V	
08/19/31	30.6	104.1	140	225	VI	
08/19/31	30.7	104.6	150	241	III	
08/26/31	30.6	104.1	140	225	III	
08/26/31	30.7	104.6	150	241	III	
11/03/31	30.7	104.6	150	241	III	
12/20/35	34.4	103.2	136	219	V	
01/08/36	32.4	104.2	67	108	II	
01/08/36	32.4	104.2	67	108	II	
02/02/49	32.4	104.2	67	108	IV	
02/02/49	32.4	104.2	67	108		
05/22/52	33	105	120	193	IV	
01/27/55	30.6	104.5	152	245	IV	
01/27/55	30.6	104.5	152	245	IV	
01/27/55	30.6	104.5	152	245	IV	
12/10/61	32.24	103.86	49	79		
12/10/61	32.26	103.86	48	77		
12/10/61	32.263	103.865	48	77		
03/06/62	31.08	104.55	128	206		
02/11/64	34.35	103.73	138	222		
11/08/64	31.9	103	37	60		
11/08/64	31.93	102.98	35	56		
11/21/64	31.9	103	37	60		
11/21/64	31.92	102.98	35	56		
02/03/65	31.9	103	37	60		
02/03/65	31.92	102.96	35	56		
08/30/65	31.92	102.98	35	56		
08/30/65	32	102.3	53	85	IV	
08/30/65	32.08	102.42	44	71	IV	
08/30/65	32.1	102.3	49	79	IV	
08/30/65	32.1	102.3	49	79		
08/14/66	31.7	103.1	50	80	VI	
08/14/66	31.92	102.98	35	56		
08/14/66	32	102.6	40	64	VI	
08/14/66	32	102.6	40	64	VI	
08/14/66	32.12	102.34	47	76	VI	
05/02/68	33.02	105.27	135	217		

TABLE 6.4-1
HISTORICAL SEISMIC ACTIVITY WITHIN 25 km (155 MILE) RADIUS OF PROPOSED LANDFILL SITE (32.433N, 103.05W)

DATE	LOCATION		DISTANCE	DISTANCE	INTENSITY	MOMENT
	LATITUDE (N)	LONGITUDE (W)	(MILES)	(KM)		MAGNITUDE
05/02/68	33.02	105.27	135	217		
07/30/71	31.64	103.17	55	89	III	
07/30/71	31.7	103	50	80	III	
07/30/71	31.7	103.1	50	80	III	
07/30/71	31.72	102.996	49	79		
07/30/71	31.74	103.09	48	77		
07/31/71	31.59	103.12	58	93		
07/31/71	31.65	103.12	54	87	IV	
07/31/71	31.7	103.1	50	80	IV	
07/31/71	31.7	103.1	50	80	IV	
07/31/71	31.703	103.061	50	80		
09/24/71	31.6	103.2	58	93		
09/24/71	31.63	103.18	56	90		
07/26/72	32.68	103.98	56	90		
07/26/72	32.68	103.98	56	90		
10/02/74	31.98	100.71	140	225		
11/12/74	32.06	100.98	123	198		
11/28/74	32.3	104.1	61	98	IV	
11/28/74	32.31	104.14	63	102		4
11/28/74	32.31	104.14	64	103		
11/28/74	32.311	104.143	64	103		
11/28/74	32.63	104.01	57	92		
11/28/74	33.765	104.99	144	232		
12/30/74	30.92	103.11	104	167		
12/30/74	30.92	103.11	104	167		
08/01/75	30.57	104.49	154	248	II	
08/01/75	30.65	104.57	152	245		
08/01/75	31.42	104.01	89	144		5
08/01/75	31.425	104.012	89	143		
01/19/76	30.9	103.1	37	60		
01/19/76	31.9	103.077	37	60		
01/19/76	31.9	103.08	37	60		4
01/19/76	31.9	103.09	37	60	IV	
01/22/76	31.9	103.07	37	60	III	
01/22/76	31.9	103.07	37	60		3
01/22/76	31.9	103.07	37	60		
01/22/76	31.9	103.071	37	60		
01/25/76	31.9	103.08	37	59		4
01/25/76	31.9	103.09	37	60	V	
01/25/76	31.902	103.08	37	60	V	
01/25/76	31.93	103.09	35	56		
04/03/76	31.3	103.17	78	126		
04/21/76	32.21	103.1	16	26		
04/21/76	32.21	103.1	16	26		
05/01/76	32.27	103.14	12	19		
05/01/76	32.4	103.1	3	5		
08/05/76	31.57	103.02	60	97		
08/05/76	31.57	103.02	60	97		

TABLE 6.4-1
HISTORICAL SEISMIC ACTIVITY WITHIN 25 km (155 MILE) RADIUS OF PROPOSED LANDFILL SITE (32.433N, 103.05W)

DATE	LOCATION		DISTANCE	DISTANCE	INTENSITY	MOMENT
	LATITUDE (N)	LONGITUDE (W)	(MILES)	(KM)		MAGNITUDE
09/17/76	31.4	102.5	78	126		
09/17/76	32.21	103.1	16	26		
09/17/76	32.21	103.1	16	26		
09/19/76	30.69	104.43	144	232		
12/19/76	32.259	103.08	12	19		
12/19/76	32.26	103.08	12	19		
04/07/77	32.23	103.07	14	23	IV	
04/07/77	32.23	103.07	14	23		
04/26/77	31.9	103.08	37	59		3
04/26/77	31.9	103.08	37	60		
04/26/77	31.902	103.083	37	60		
04/26/77	32	103.1	30	48		
06/07/77	32.85	100.9	128	206		
06/07/77	32.858	100.77	135	217		
06/07/77	33.058	100.749	140	225		
06/07/77	33.06	100.75	141	227		4
06/07/77	33.13	100.94	131	211		
06/08/77	32.7	100.72	136	219		
06/08/77	32.8	100.9	127	204		
06/08/77	32.858	100.77	135	217		
06/08/77	32.89	100.95	126	203		
06/17/77	32.346	100.4	154	248		
06/17/77	32.35	100.4	154	248		
07/22/77	31.8	102.7	48	77		
11/27/77	32.862	100.68	140	225		
11/27/77	33.03	101.08	121	195		
11/28/77	32.95	100.84	134	216		4
11/28/77	32.954	100.837	133	214		
11/28/77	32.96	100.88	131	211		
11/28/77	33.022	100.84	134	216		
02/18/78	31.35	104.56	115	185		
03/02/78	31.52	102.41	73	117		
03/02/78	31.55	102.5	69	111	V	
03/02/78	31.56	102.51	68	110		4
03/02/78	31.562	102.512	68	109	III	
06/16/78	32.87	100.99	123	198		
06/16/78	32.961	100.79	136	219		
06/16/78	32.99	100.88	131	211		
06/16/78	33.03	100.766	138	222		
06/16/78	33.03	100.77	138	222	V	
06/16/78	33.03	100.77	139	224		5
06/16/78	33.067	101.19	116	187		
06/16/78	33.1	101.2	117	188		
06/29/78	31.05	101.94	115	185		
07/05/79	32.9	101.31	105	169		
07/05/79	32.949	100.895	130	209		
07/05/79	32.95	100.89	130	210		3
07/05/79	33	100.92	130	209		

TABLE 6.4-1
HISTORICAL SEISMIC ACTIVITY WITHIN 25 km (155 MILE) RADIUS OF PROPOSED LANDFILL SITE (32.433N, 103.05W)

DATE	LOCATION		DISTANCE	DISTANCE	INTENSITY	MOMENT
	LATITUDE (N)	LONGITUDE (W)	(MILES)	(KM)		MAGNITUDE
08/03/79	32.85	100.94	125	201		
08/03/79	32.851	100.74	137	220		
05/08/81	32.212	101.51	91	146		
11/10/81	32	100.67	142	229	III	
01/04/82	31.18	102.49	93	149		4
01/04/82	31.18	102.49	92	148		
01/04/82	31.182	102.492	92	148		
04/26/82	33.02	100.84	135	217		3
04/26/82	33.02	100.84	134	216		
04/26/82	33.021	100.844	134	216		
11/09/82	31.99	100.7	142	228		3
11/28/82	33	100.8	136	219		
11/28/82	33	100.84	135	217		3
11/28/82	33.003	100.842	134	216	IV	
09/11/84	31.991	100.697	140	225		
09/11/84	32	100.7	140	225		
09/19/84	32.027	100.688	140	225		
09/19/84	32.027	100.688	140	225		
09/19/84	32.03	100.69	142	228		3
12/04/84	32.26	103.56	31	50		3
12/04/84	32.266	103.556	32	51		
12/04/84	32.266	103.556	32	51		
01/25/86	32.06	100.73	139	223		3
01/25/86	32.064	100.733	137	220		
01/30/86	32.066	100.693	140	225	IV	
01/30/86	32.07	100.69	140	226		3
01/02/92	32.33	103.1	7/11*	11/18		5
01/02/92	32.336	103.101	7/11*	11/18	V	
08/26/92	32.17	102.71	27	44		3
06/23/93	31.35	102.51	82	132		3
04/14/95	30.28	103.35	149	240		6
04/14/95	30.3	103.35	148	238		3
04/14/95	30.3	103.35	148	238		3
04/14/95	30.3	103.35	148	238		3
04/14/95	30.3	103.35	148	238		3
04/14/95	30.3	103.35	148	238		2
04/14/95	30.3	103.35	148	238		3
04/14/95	30.3	103.35	148	238		2
04/14/95	30.3	103.35	148	238		3
04/14/95	30.3	103.35	148	238		3
04/14/95	30.3	103.35	148	238		2
04/15/95	30.27	103.32	150	241		4
04/15/95	30.3	103.35	148	238		2
04/16/95	30.3	103.35	148	238		2
04/16/95	30.3	103.35	148	238		3
04/16/95	30.3	103.35	148	238		2
04/17/95	30.3	103.35	148	238		3
04/21/95	30.3	103.35	148	238		3

TABLE 6.4-1
HISTORICAL SEISMIC ACTIVITY WITHIN 25 km (155 MILE) RADIUS OF PROPOSED LANDFILL SITE (32.433N, 103.05W)

DATE	LOCATION		DISTANCE	DISTANCE	INTENSITY	MOMENT
	LATITUDE (N)	LONGITUDE (W)	(MILES)	(KM)		MAGNITUDE
06/01/95	30.3	103.35	148	238		4
07/06/95	30.3	103.35	148	238		3
07/06/95	30.3	103.35	148	238		3
11/12/95	30.3	103.35	148	238		4
04/15/98	30.19	103.3	Unknown	Unknown		4
03/01/99	32.57	104.66	93	150		3
03/14/99	32.59	104.63	92	148		4
03/17/99	32.58	104.67	94	151		4
05/30/99	32.58	104.66	94	151		4
08/09/99	32.57	104.59	89	144		3
02/02/00	32.58	104.63	91	147		3
02/26/00	30.24	103.61	155	249		3
06/02/01	32.33	103.14	9	14		3
11/22/01	31.79	102.63	52	83		3
09/17/02	32.58	104.63	92	148		4
09/17/02	32.58	104.63	92	148		3
06/21/03	32.67	104.5	85	137		4

Sources: National Oceanographic and Atmospheric Administration (1992)
United States Geological Survey (2004) http://neic.usgs.gov/

Definition of I Tremor not felt, or rarely felt only under especially favorable conditions
- II Tremor felt indoors by few people; may cause slight movement of liquids and suspended or delicate objects
- III Tremor felt indoors by several people; may cause swinging of suspended objects; movement may be appreciable on upper levels of tall buildings
- IV Tremor felt indoors by many people; causing dishes and windows to rattle; noticeable movement of delicate objects
- V Tremor felt by nearly all people; causes breakage of many delicate objects (dishes, glassware, etc); trees and bushes shaken slightly
- VI Tremor felt by all people, both indoors and outdoors; causes considerable breakage of delicate objects, movement of furnishings, slight cracking of chimneys and plaster wall material.
- VIII Fright, general alarm approaches panic; twisting fall of chimneys, columns, monuments and partial collapse of buildings, homes, etc.; moved, overturned very heavy furniture; sand and mud ejected in small amounts

Moment Magnitude: Moment Magnitude is the measure of total energy released by an earthquake, and is based on the area of the fault that ruptured in the earthquake.

* USGS location is at 7 miles: New Mexico Tech location is at 11 miles

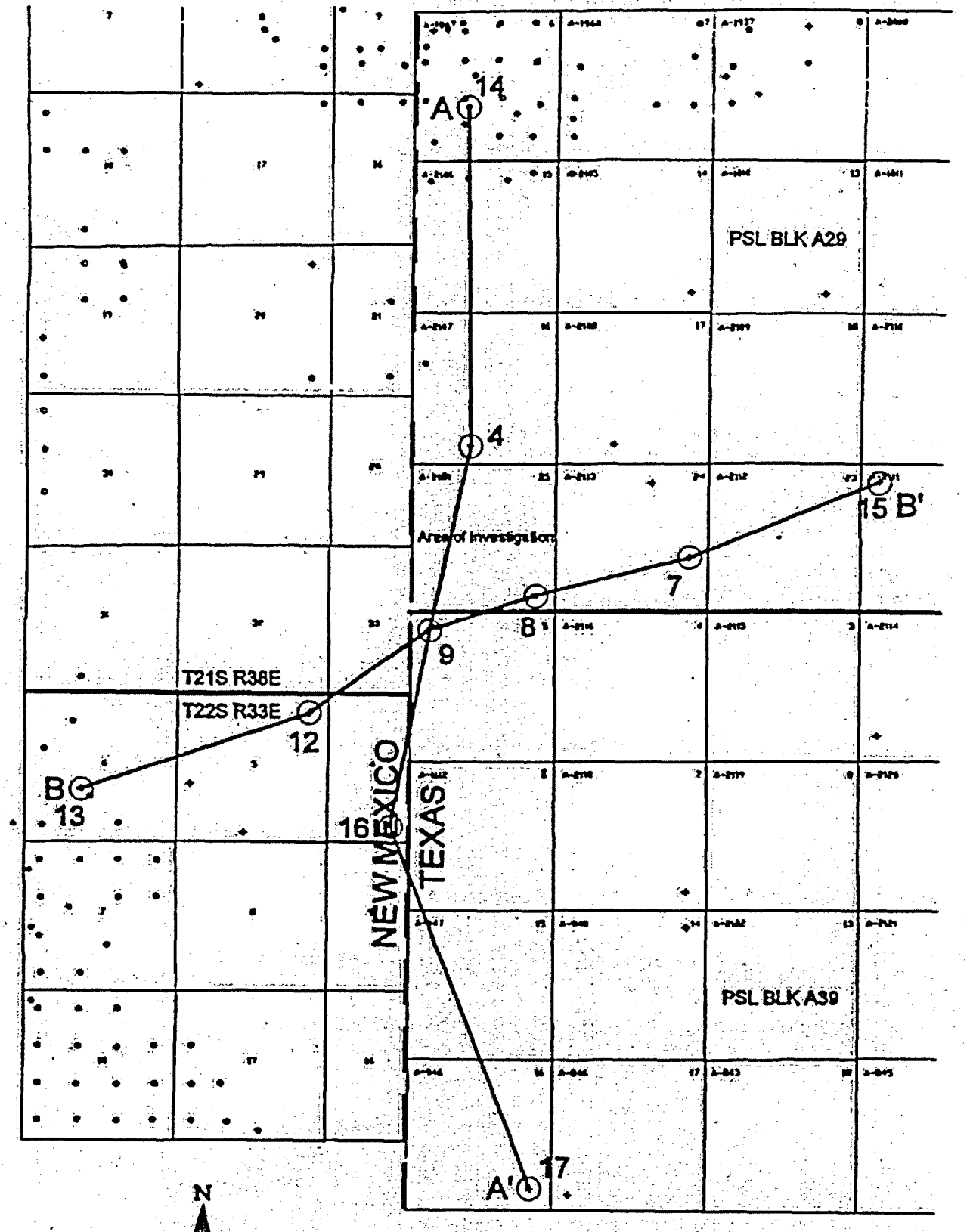

N

0 4000 8000
FEET

Source: Terra Dynamics, 1993

Date: 02/05/04
File: WCS_Fig6.2-1.fh11

INTERA INCORPORATED
9111A Research Blvd.
Austin, TX 78758

COOK-JOYCE INC.
ENGINEERING AND CONSULTING
312 WEST ELEVENTH
AUSTIN, TEXAS 78701-2000
(512) 474-9097 FAX (512) 474-8483

Location of Stratigraphic Cross Sections

Figure 6.2-1

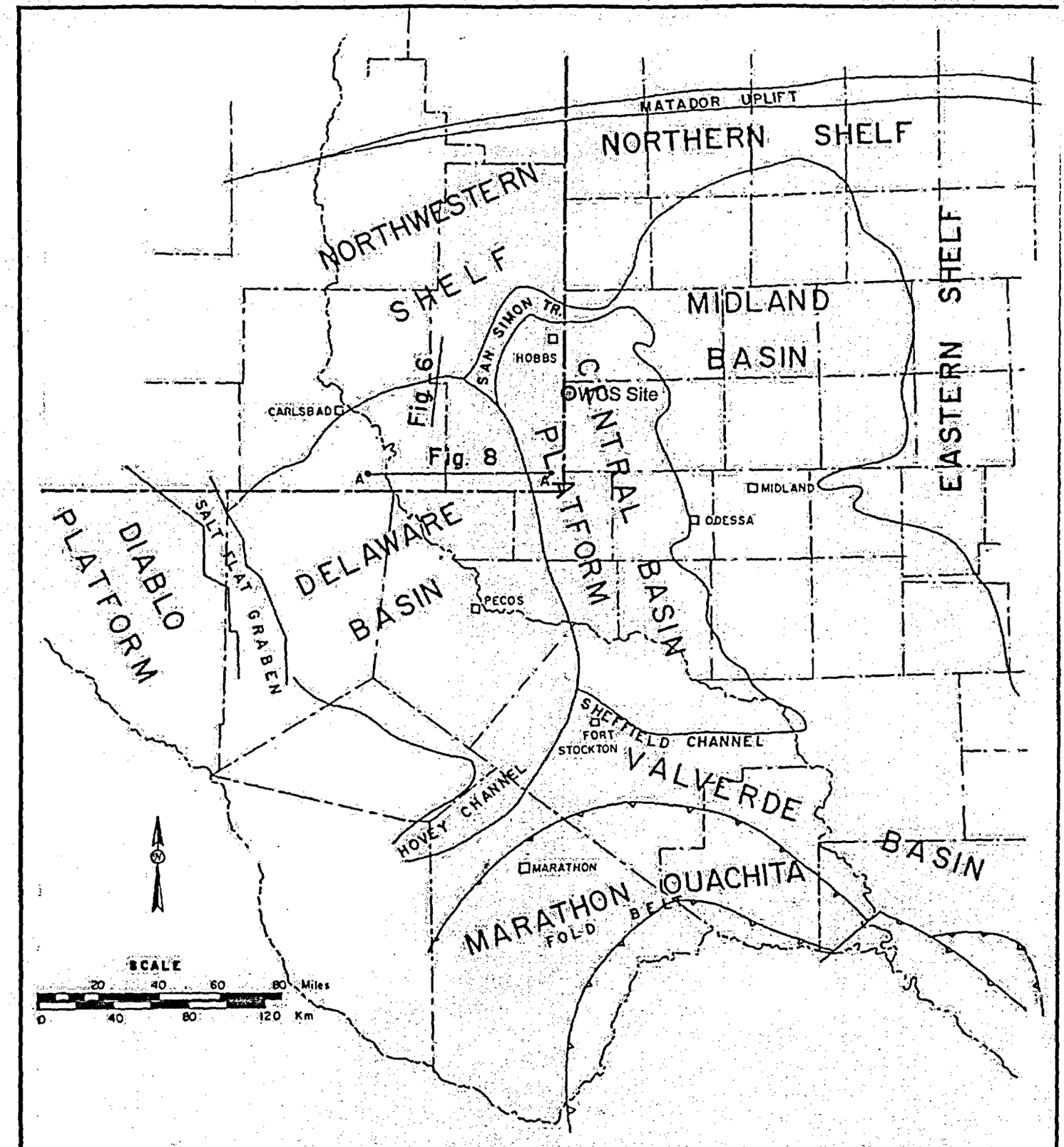

Source: Hills, 1985

Date: 02/04/04 File: WCS_Fig6.4-1.fh11	Major Structural Provinces of West Texas and Southeastern New Mexico
INTERA INCORPORATED 9111A Research Blvd. Austin, TX 78758 COOK-JOYCE INC. ENGINEERING AND CONSULTING 612 WEST ELEVENTH AUSTIN, TEXAS 78701-2000 (512) 474-9097 FAX (512) 474-8483	Figure 6.4-1

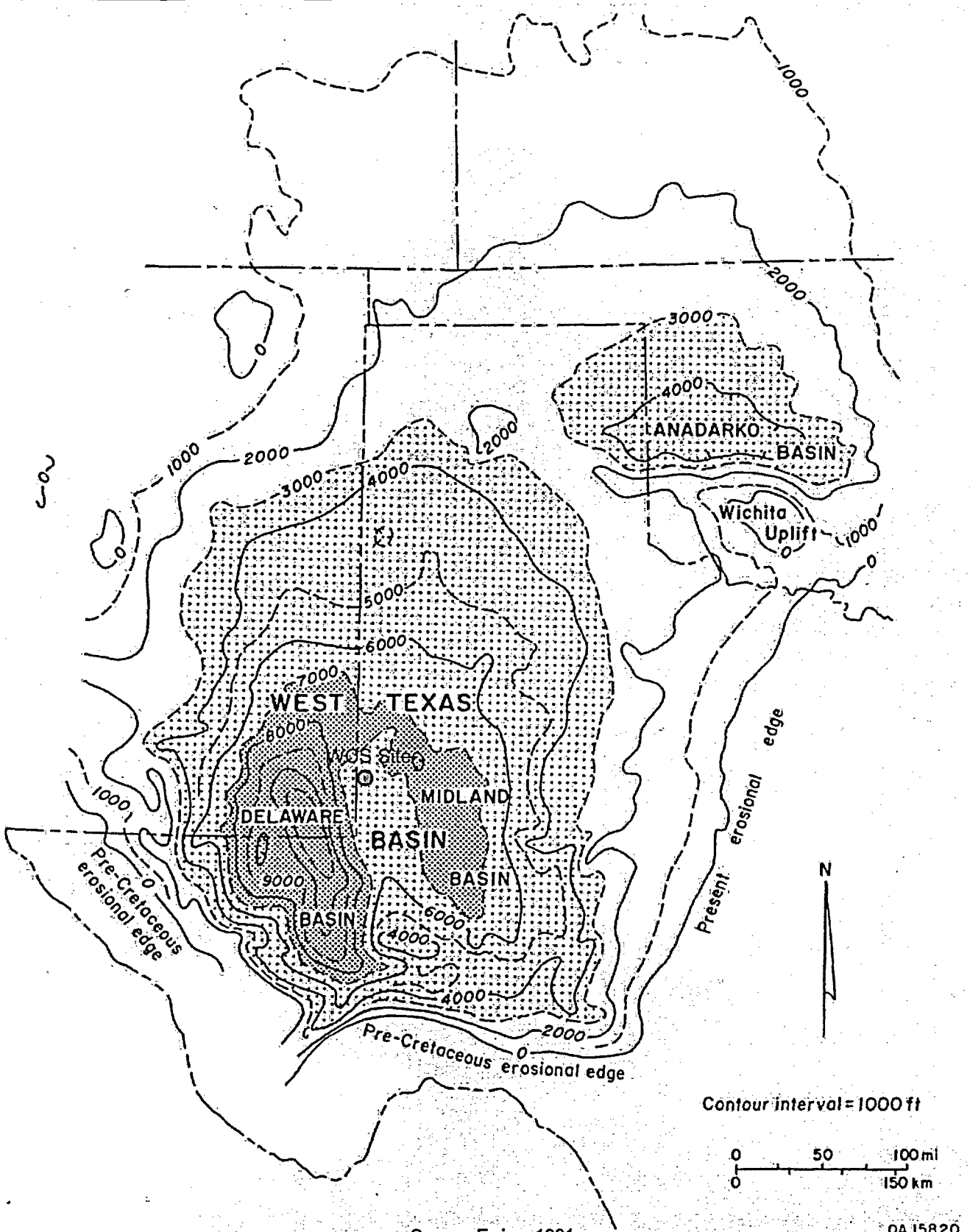

Source: Ewing, 1991

QA 15820

Date: 02/04/04
File: WCS_Fig6.4-2.fh11

INTERA INCORPORATED
9111A Research Blvd.
Austin, TX 78758

COOK-JOYCE INC.
ENGINEERING AND CONSULTING
812 WEST ELEVENTH
AUSTIN, TEXAS 78701-2000
(512) 474-9097 FAX (512) 474-8483

Isopach Map of post-Wolfcampian Permian Strata in the West Texas and Andarko Basins

Figure 6.4-2

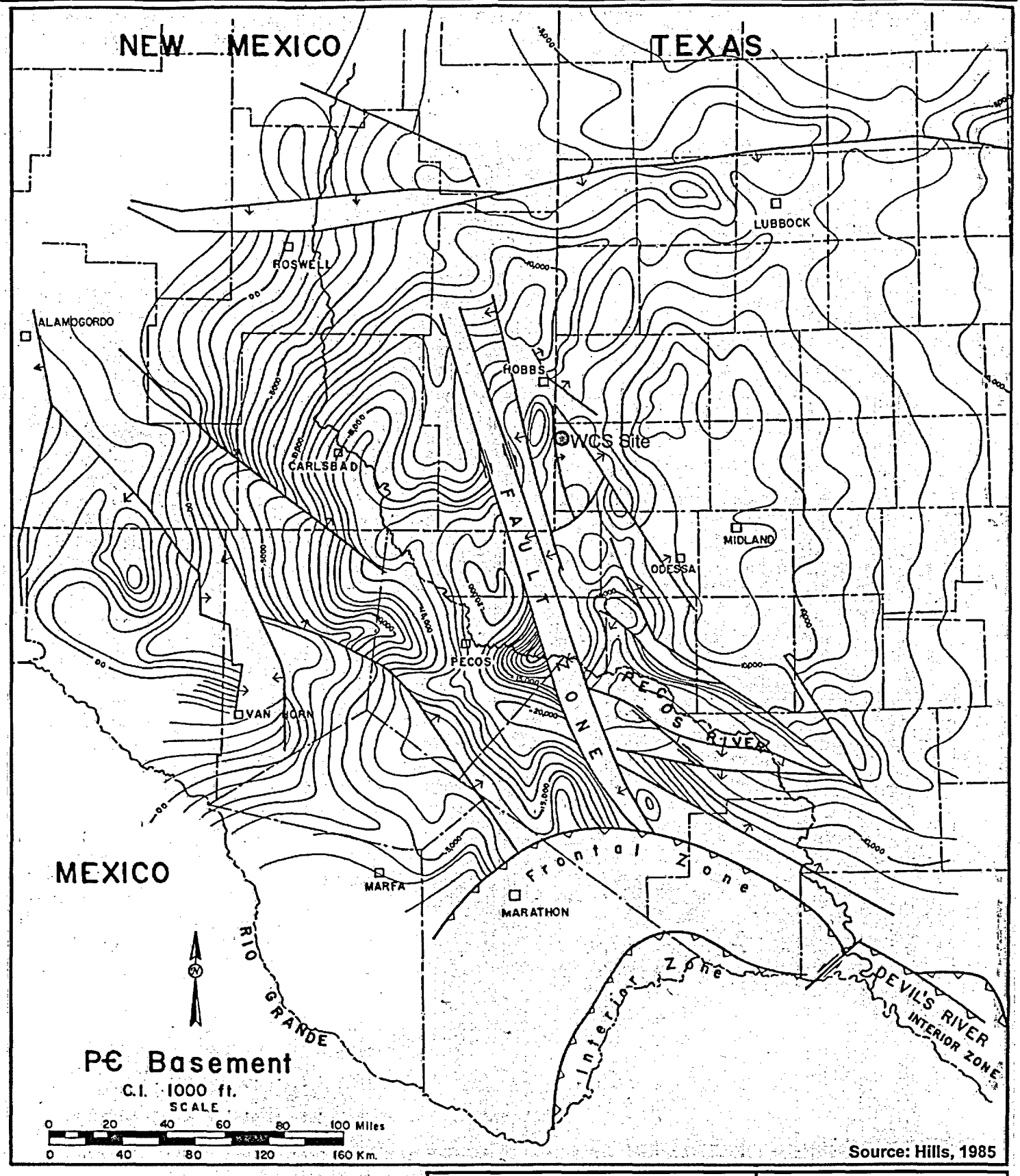

Date: 02/04/04
File: WCS_Fig6.4-1.fh11

INTERA INCORPORATED
9111A Research Blvd.
Austin, TX 78758

COOK-JOYCE INC.
ENGINEERING AND CONSULTING
612 WEST ELEVENTH
AUSTIN, TEXAS 78701-2000
(512) 474-9097 FAX (512) 474-8463

Regional Structure Contour Map of the Precambrian Basement

Figure 6.4-3

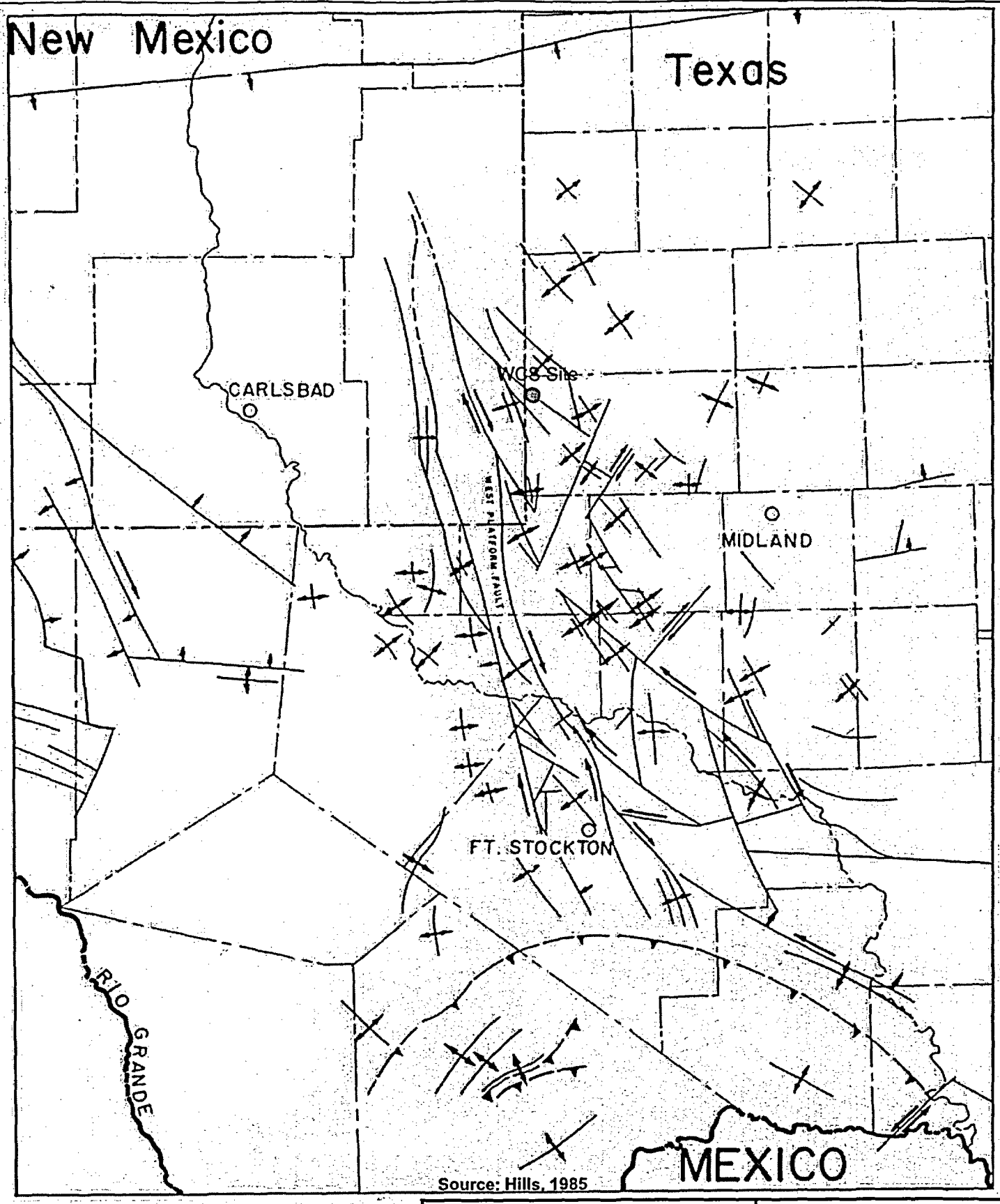

Source: Hills, 1985

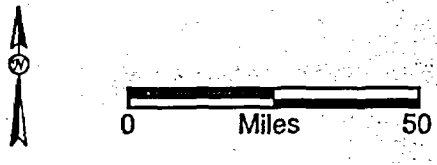

Date: 02/04/04
File: WCS_Fig6.4-4.fh11

INTERA INCORPORATED
9111A Research Blvd.
Austin, TX 78758

COOK-JOYCE INC.
ENGINEERING AND CONSULTING
812 WEST ELEVENTH
AUSTIN, TEXAS 78701-2000
(512) 474-8097 FAX (512) 474-8463

Major Tectonic Features of the Permian Basin - Late Mississippian to Early Permain

Figure 6.4-4

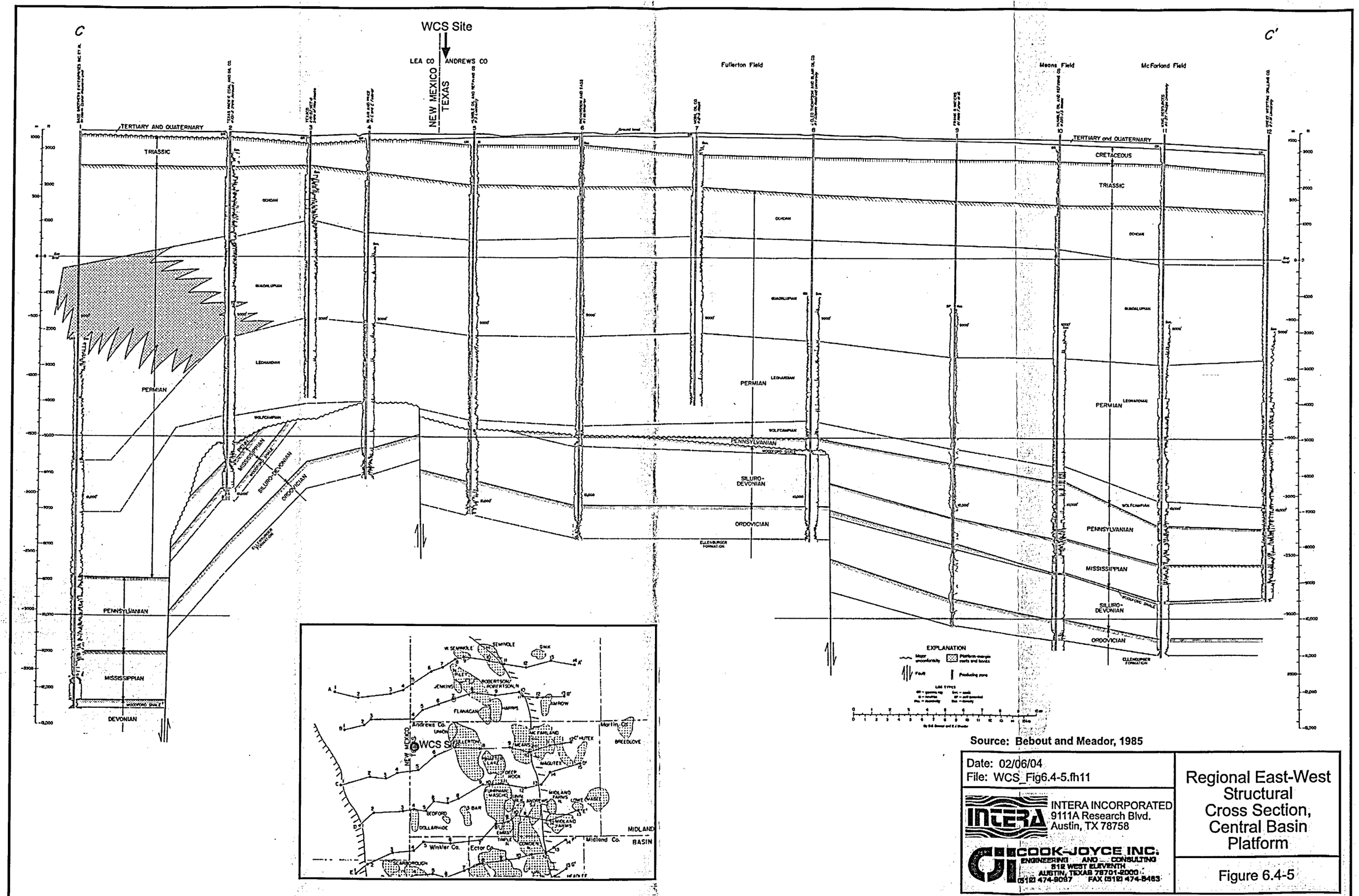

Date: 02/06/04
File: WCS_Fig6.4-5.fh11

INTERA INCORPORATED
9111A Research Blvd.
Austin, TX 78758

COOK-JOYCE INC.
ENGINEERING AND CONSULTING
512 WEST ELEVENTH
AUSTIN, TEXAS 78701-2000
(512) 474-9097 FAX (512) 474-5483

Regional East-West Structural Cross Section, Central Basin Platform

Figure 6.4-5

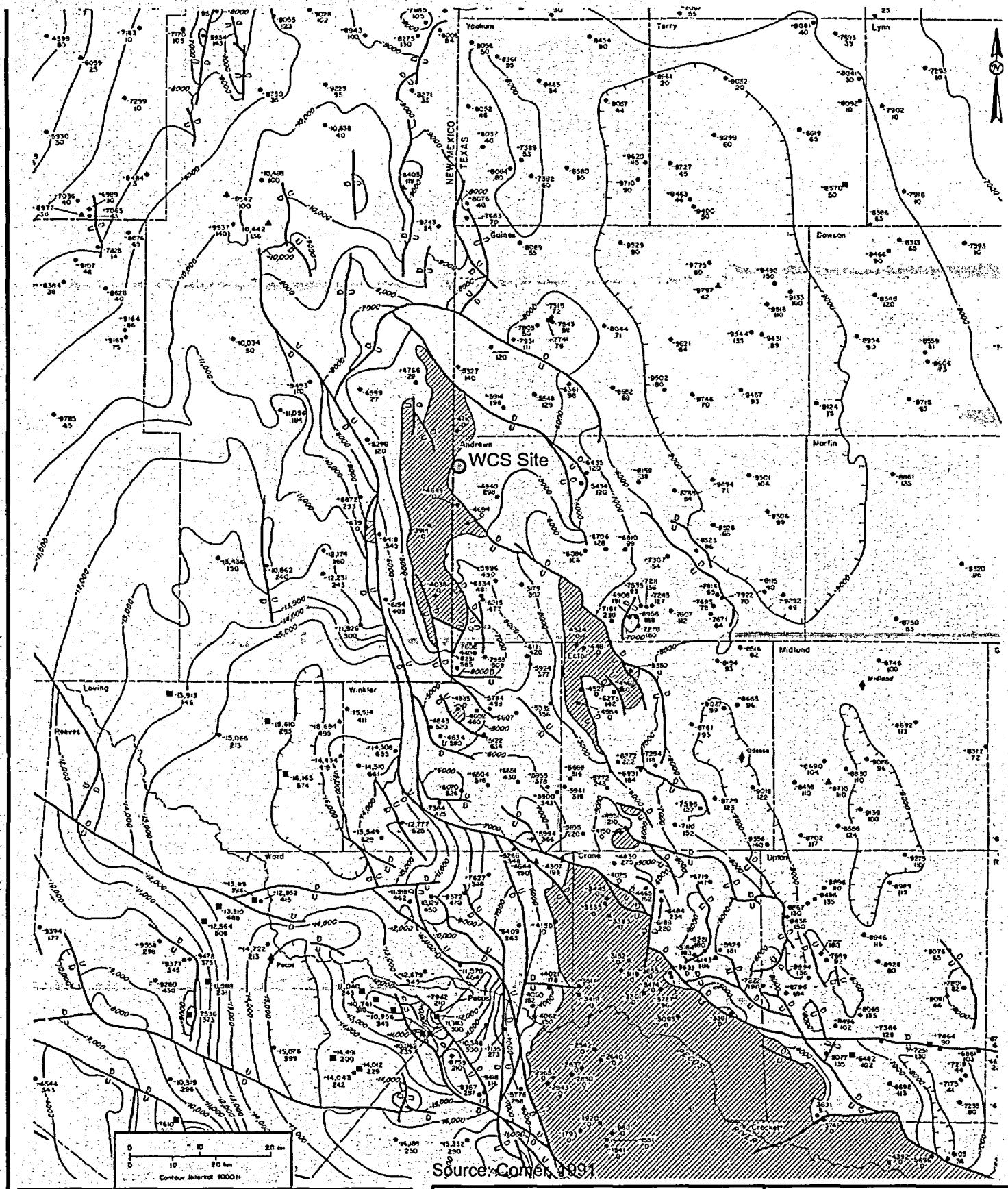

Source: Comer, 1991

EXPLANATION

Wireline log	-4307	Subsea elevation, top of Woodford (ft)
Scout ticket	193	Thickness of Woodford (ft)
Core	-7000	Structure contour in feet below sea level, drawn on top of Woodford Formation; extrapolated where control is sparse on the basis of elevation of top of Ellenburger (SE) or top of Devonian (NW)
Woodford absent		

Date: 02/04/04
File: WCS_Fig6.4-7.fh11

INTERA INCORPORATED
9111A Research Blvd.
Austin, TX 78758

COOK-JOYCE INC.
ENGINEERING AND CONSULTING
812 WEST ELEVENTH
AUSTIN, TEXAS 78701-2000
(512) 474-9097 FAX (512) 474-8463

Regional Structure Contour Map of the Woodford Formation

Figure 6.4-7

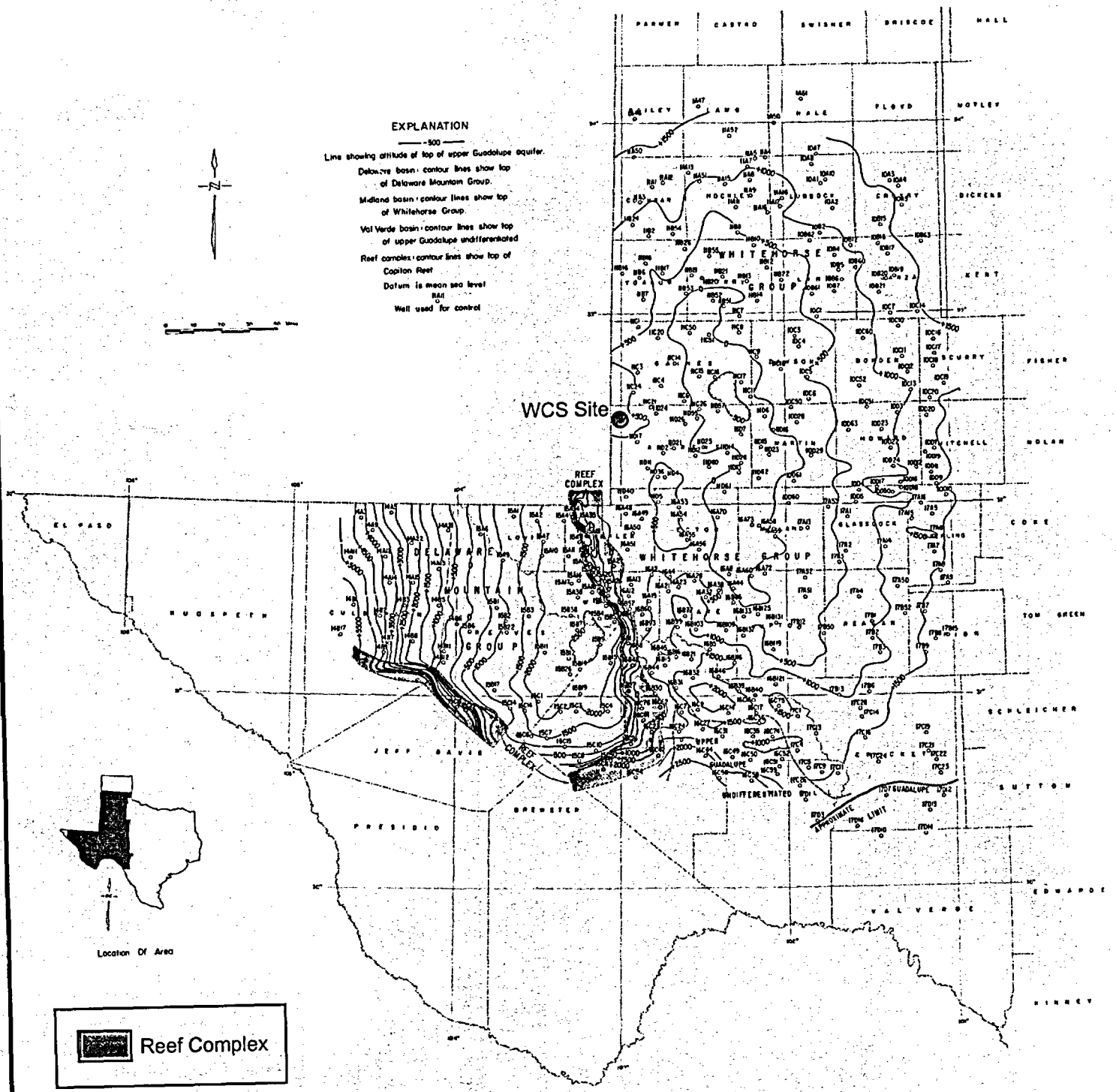

Source: Texas Water Development Board, 1972

Date: 02/04/04 File: WCS_Fig6.4-8.fh11	Regional Structure Contour Map of the Upper Guadalupe (Whitehorse Group)
INTERA INCORPORATED 9111A Research Blvd. Austin, TX 78758 COOK-JOYCE INC. ENGINEERING AND CONSULTING 812 WEST ELEVENTH AUSTIN, TEXAS 78701-2000 (512) 474-9097 FAX (512) 474-8483	Figure 6.4-8

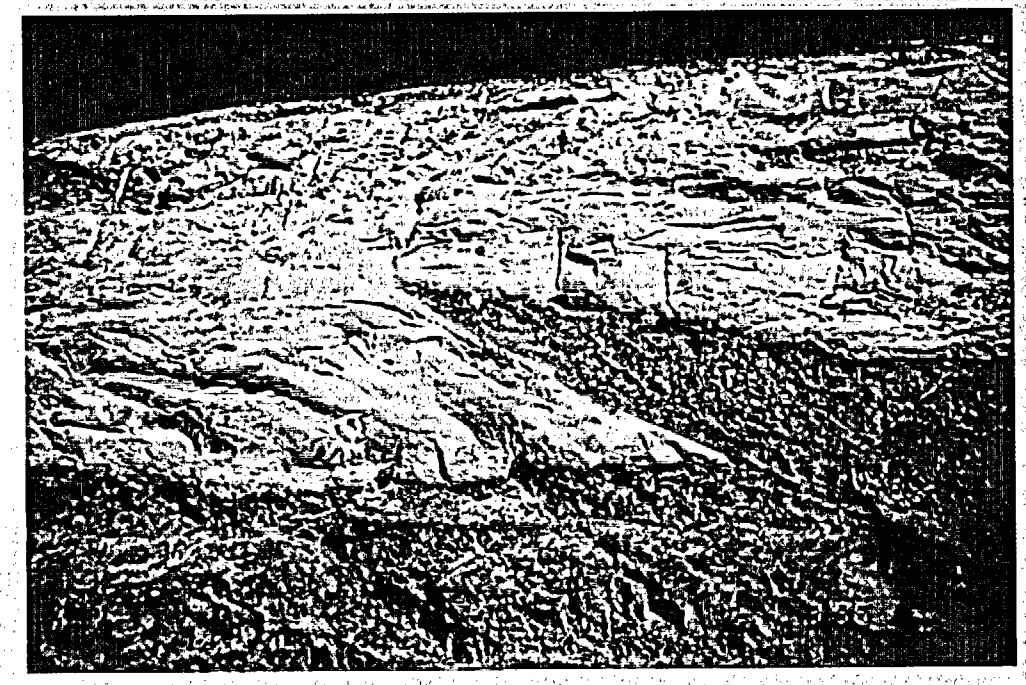

Date: 06/15/04
File: WCS_Fig6.4-9.fh11

INTERA INCORPORATED
9111A Research Blvd.
Austin, TX 78758

COOK-JOYCE INC.
ENGINEERING AND CONSULTING
512 WEST ELEVENTH
AUSTIN, TEXAS 78701-2000
(512) 474-9097 FAX (512) 474-8463

1996 Photographs of Reverse Fault in Red Beds

Figure 6.4-9

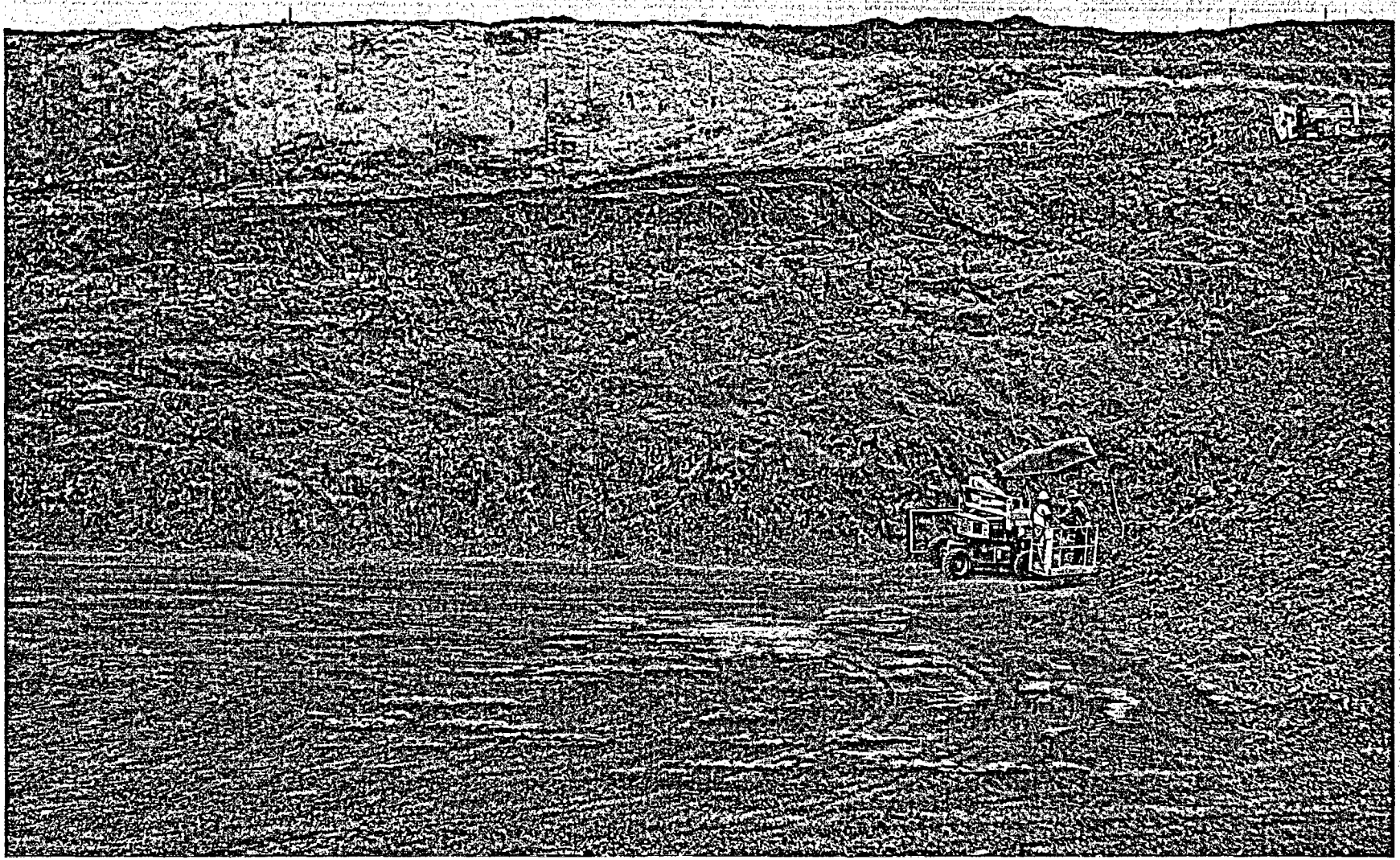

Date: 06/15/04
File: WCS_Fig6.4-10.fh11

INTERA INCORPORATED
9111A Research Blvd.
Austin, TX 78758

COOK-JOYCE INC.
ENGINEERING AND CONSULTING
512 WEST ELEVENTH
AUSTIN, TEXAS 78701-2000
(512) 474-9097 FAX (512) 474-8483

2004 Photograph of Excavation Showing Lower and Upper Walls and Offset Sandstone Layer in Lower Wall

Figure 6.4-10

THIS PAGE IS AN OVERSIZED DRAWING OR FIGURE,

THAT CAN BE VIEWED AT THE RECORD TITLED:

FIGURE 6.4-11
"EAST WALL CROSS-SECTION"

WITHIN THIS PACKAGE

D-01

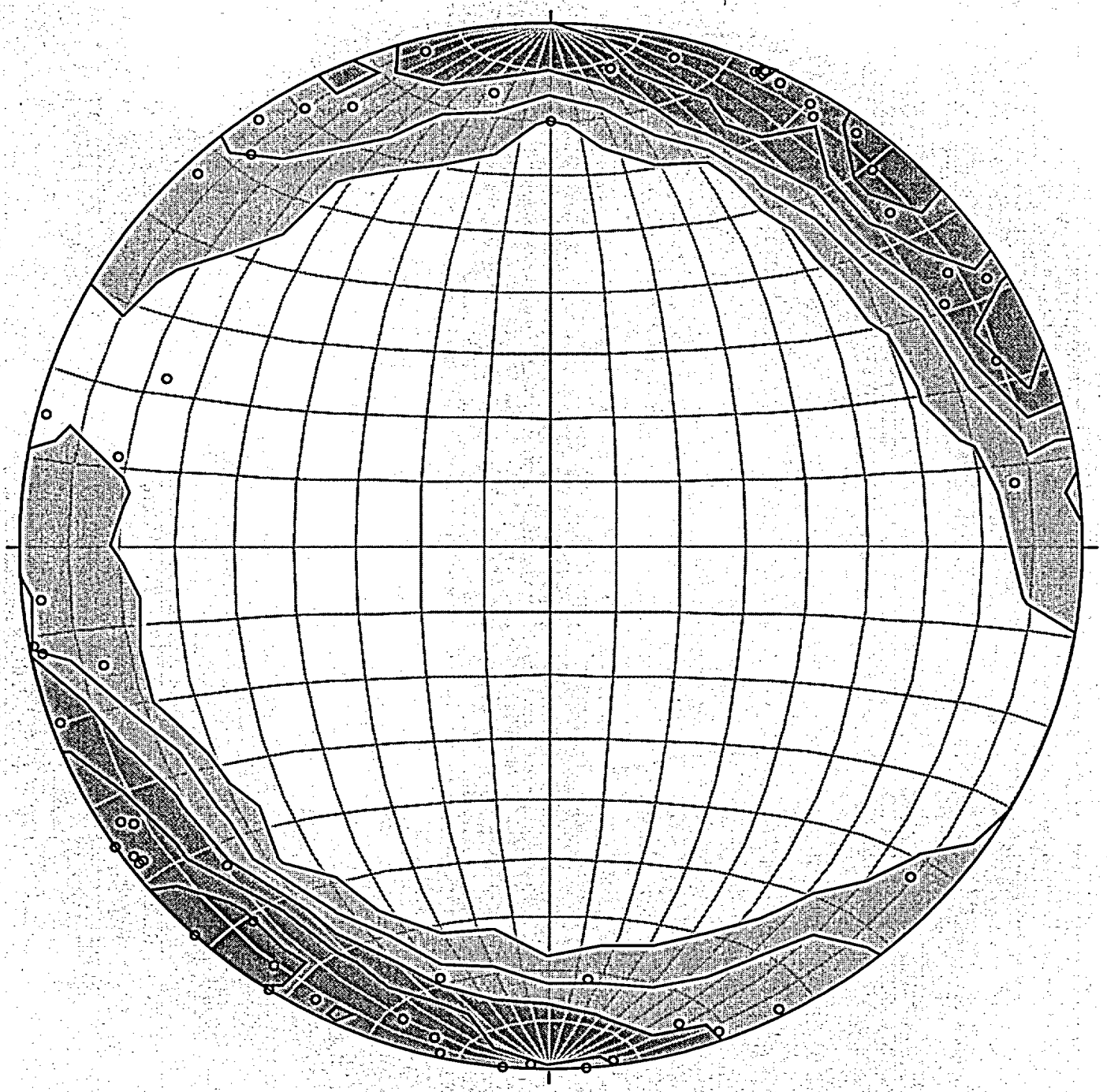

o Plane Pole

—— Kamb Contour

KAMB CONTOUR OF P-AXES (n = 0):

Contour Int = 2.0; Counting Circle Area = 0.067

Expected Number = 3.73;

Significance Level = 2.0 sigma

Date: 06/14/2004

File: WCS_Fig6.4-12.fh11

INTERA INCORPORATED
9111A Research Blvd.
Austin, TX 78758

COOK-JOYCE INC.
ENGINEERING AND CONSULTING
512 WEST ELEVENTH
AUSTIN, TEXAS 78701-2000
(512) 474-9097 FAX (512) 474-8483

Poles of Subvertical Joint Planes and Kamb Contours, Lower Wall

Figure 6.4-12

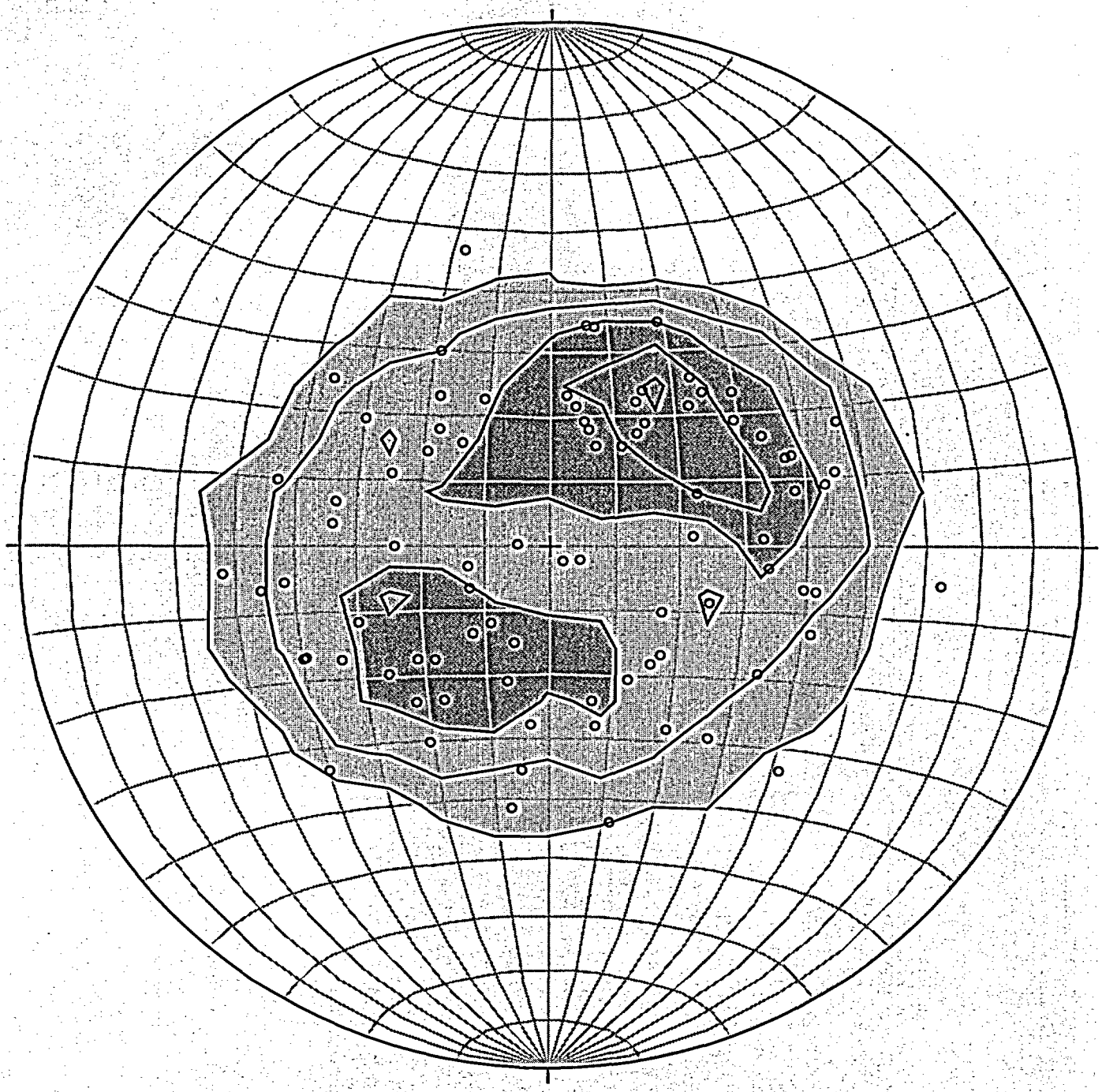

o Plane Pole

—— Kamb Contour

LINES SCATTER PLOT (n = 85):

Contour Int = 2.0; Counting Circle Area = 0.045

Expected Number = 3.82;

Significance Level = 2.0 sigma

Date: 06/14/2004
File: WCS_Fig6.4-13.fh11

INTERA INCORPORATED
9111A Research Blvd.
Austin, TX 78758

COOK-JOYCE INC.
ENGINEERING AND CONSULTING
812 WEST ELEVENTH
AUSTIN, TEXAS 78701-2000
(512) 474-9097 FAX (512) 474-8483

Poles of Irregular Joint Planes and Kamb Contours, Lower Wall

Figure 6.4-13

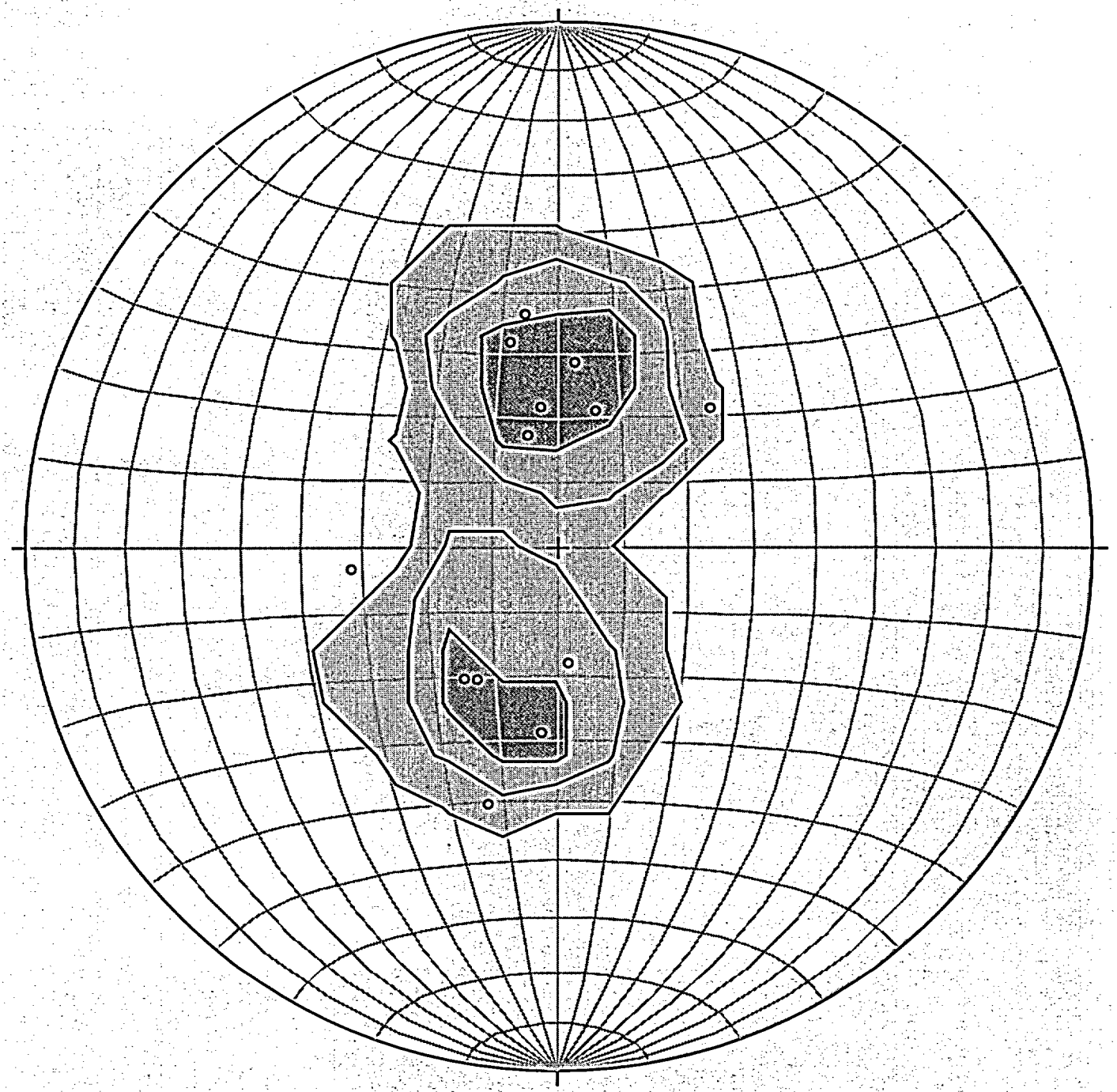

o Plane Pole

—— Kamb Contour

KAMB CONTOUR OF P-AXES (n = 14):

Contour Int = 2.0; Counting Circle Area = 0.067

Expected Number = 0.93;

Significance Level = 1.0 sigma

Date: 06/14/2004

File: WCS_Fig6.4-14.fh11

INTERA INCORPORATED
9111A Research Blvd.
Austin, TX 78758

COOK-JOYCE INC.
ENGINEERING AND CONSULTING
812 WEST ELEVENTH
AUSTIN, TEXAS 78701-2000
(512) 474-9097 FAX (512) 474-8483

Poles of Fault Planes and Kamb Contours, Lower Wall

Figure 6.4-14

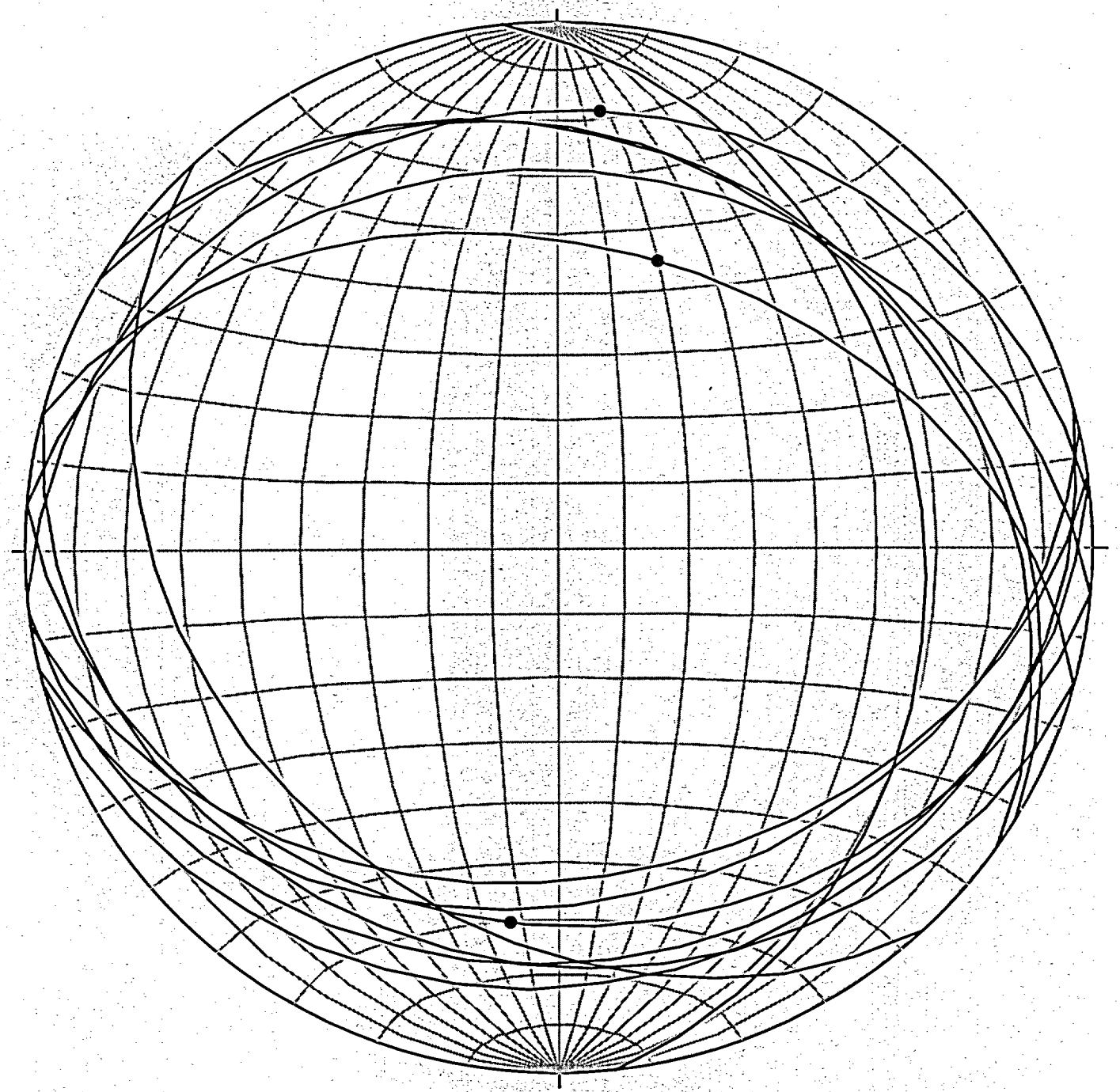

● Slickenside Direction

—— Great Circle

LINES SCATTER PLOT (n = 3):

Planes (n = 14):

Date: 06/14/2004
File: WCS_Fig6.4-15.fh11

INTERA INCORPORATED
9111A Research Blvd.
Austin, TX 78758

COOK-JOYCE INC.
ENGINEERING AND CONSULTING
612 WEST ELEVENTH
AUSTIN, TEXAS 78701-2000
(512) 474-9097 FAX (512) 474-8483

Great Circles for Fault Planes with Slickenside Directions, Lower Wall

Figure 6.4-15

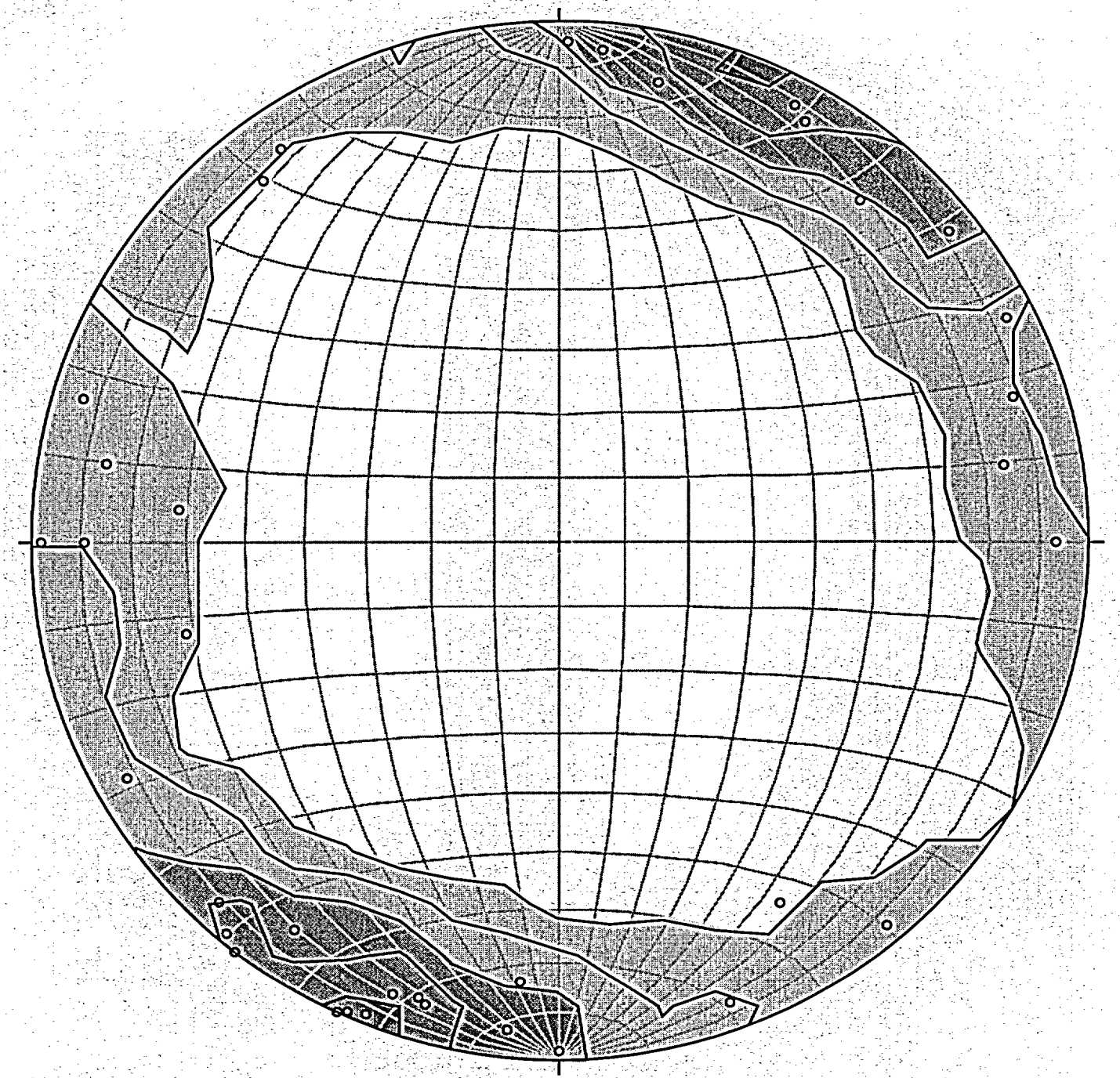

o Plane Pole

—— Kamb Contour

KAMB CONTOUR OF P-AXES (n = 36):

Contour Int = 2.0; Counting Circle Area = 0.100

Expected Number = 3.60;

Significance Level = 2.0 sigma

Date: 06/14/2004

File: WCS_Fig6.4-16.fh11

INTERA INCORPORATED
9111A Research Blvd.
Austin, TX 78758

COOK-JOYCE INC.
ENGINEERING AND CONSULTING
812 WEST ELEVENTH
AUSTIN, TEXAS 78701-2000
(512) 474-9097 FAX (512) 474-8483

Poles of Subvertical Joint Planes and Kamb Contours, Upper Wall

Figure 6.4-16

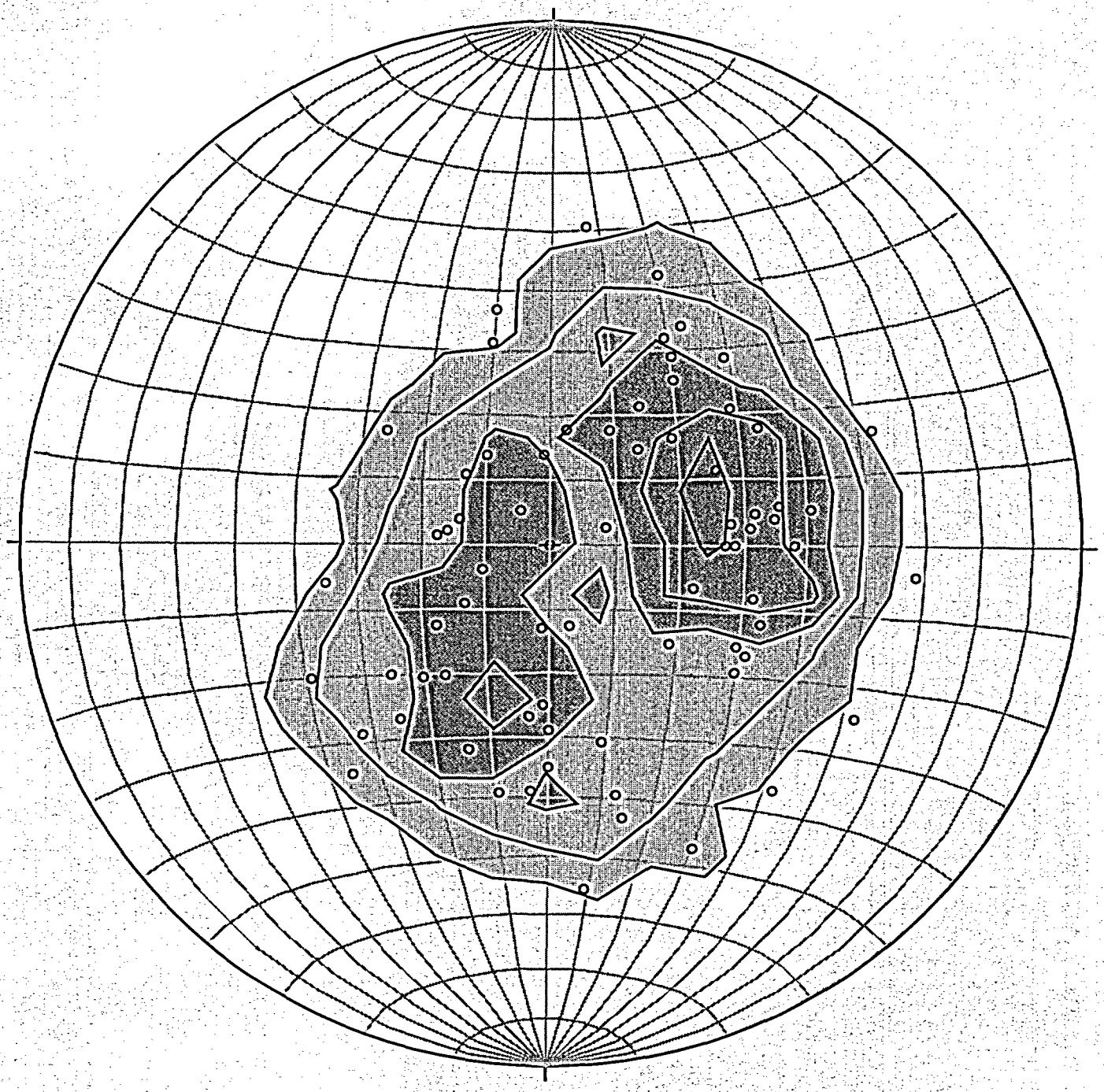

o Plane Pole

—— Kamb Contour

LINES SCATTER PLOT (n = 75):

Contour Int = 2.0; Counting Circle Area = 0.051

Expected Number = 3.80;

Significance Level = 2.0 sigma

Date: 06/14/2004 File: WCS_Fig6.4-17.fh11	Poles of Irregular Joint Planes and Kamb Contours, Upper Wall
INTERA INCORPORATED 9111A Research Blvd. Austin, TX 78758 COOK-JOYCE INC. ENGINEERING AND CONSULTING 812 WEST ELEVENTH AUSTIN, TEXAS 78701-2000 (512) 474-2097 FAX (512) 474-8483	Figure 6.4-17

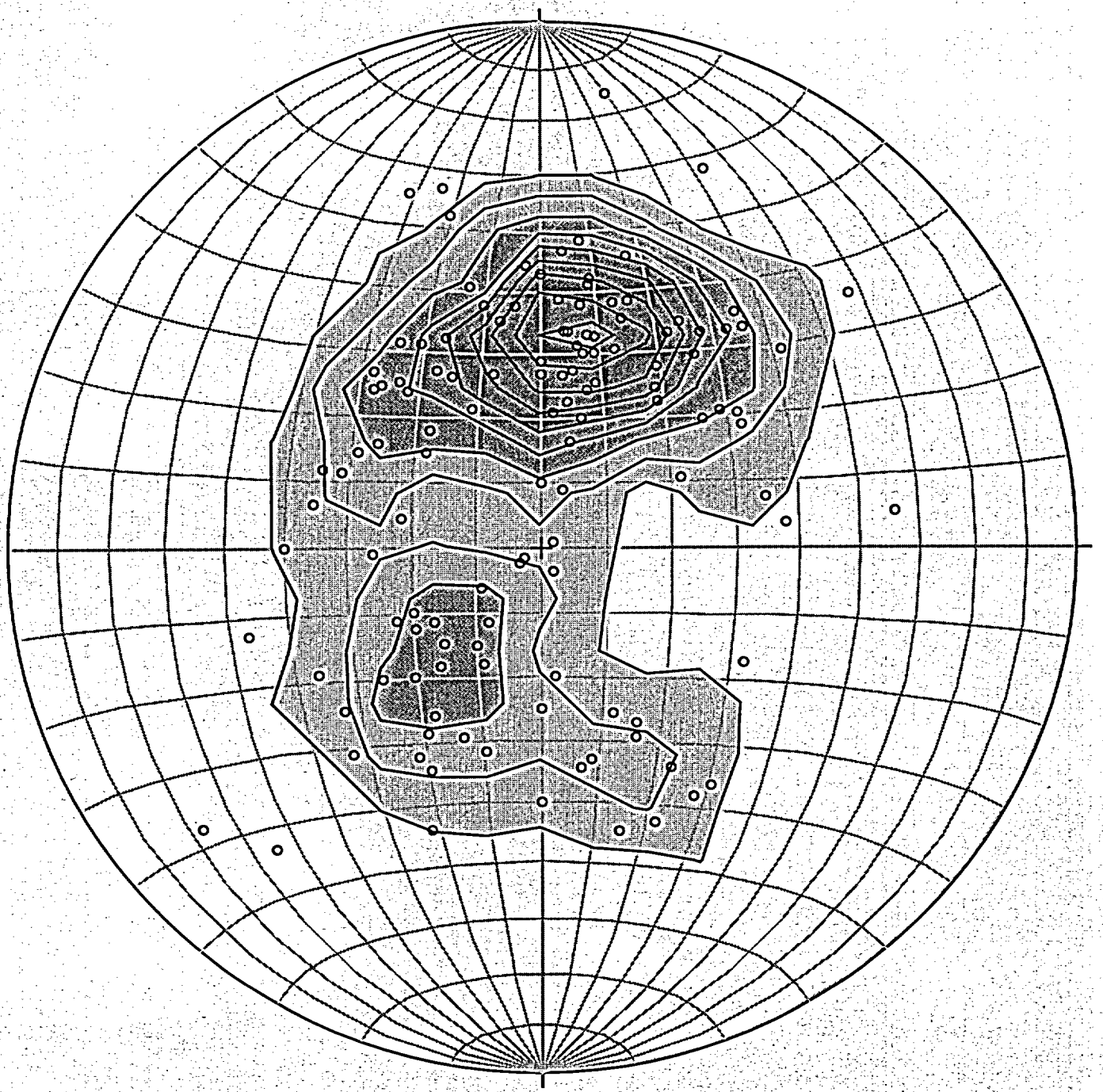

o Plane Pole

—— Kamb Contour

KAMB CONTOUR OF P-AXES (n = 138):

Contour Int = 2.0; Counting Circle Area = 0.028

Expected Number = 3.89;

Significance Level = 2.0 sigma

Date: 06/14/2004

File: WCS_Fig6.4-18.fh11

INTERA INCORPORATED
9111A Research Blvd.
Austin, TX 78758

COOK-JOYCE INC.
ENGINEERING AND CONSULTING
612 WEST ELEVENTH
AUSTIN, TEXAS 78701-2000
(512) 474-9097 FAX (512) 474-8483

Poles of Fault Planes and Kamb Contours, Upper Wall

Figure 6.4-18

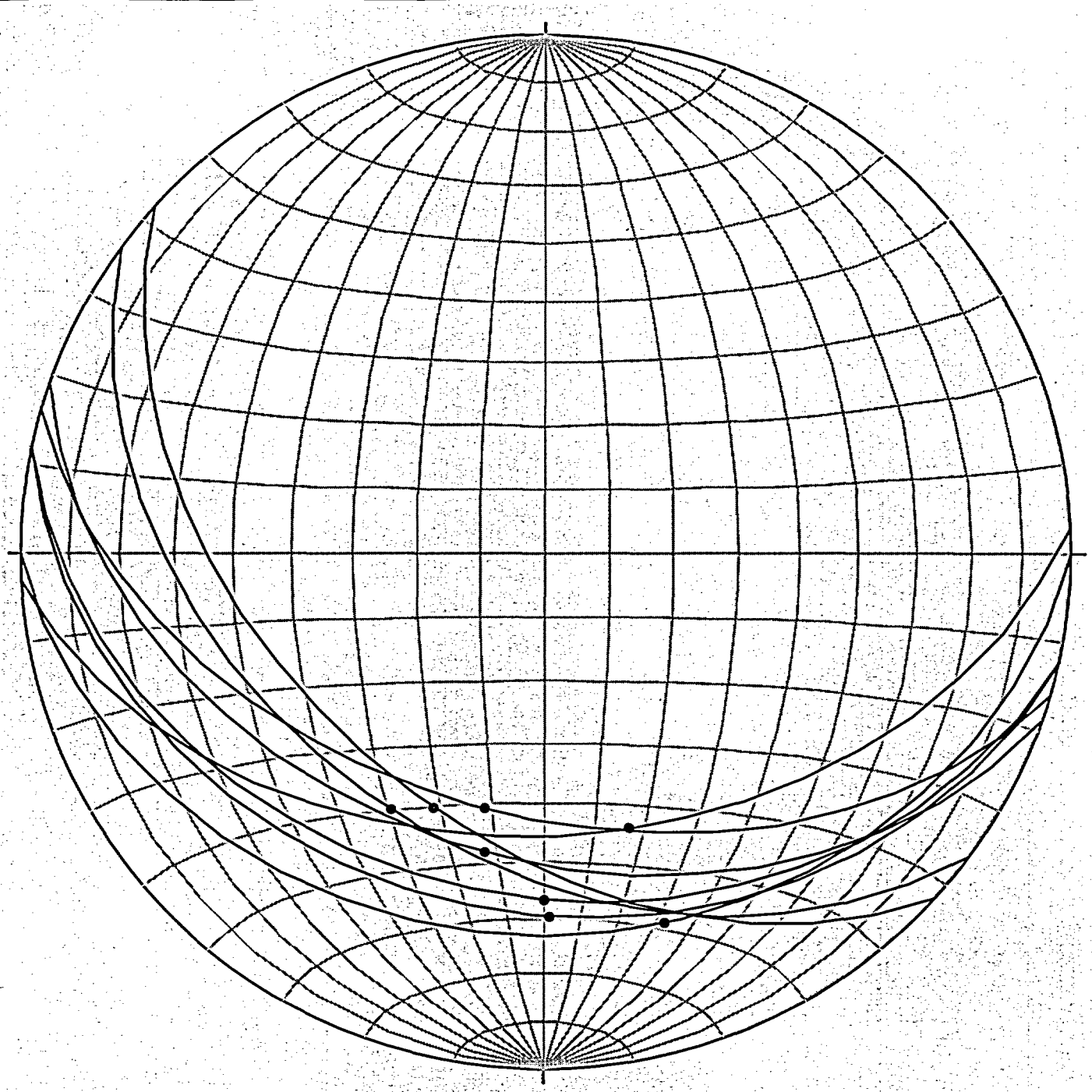

● Slickenside Direction

—— Kamb Contour

LINES SCATTER PLOT (n = 8):

Planes (n = 8):

Date: 06/14/2004 File: WCS_Fig6.4-19.fh11	Great Circles for Fault Planes with Slickenside Directions, Upper Wall
INTERA INCORPORATED 9111A Research Blvd. Austin, TX 78758 COOK-JOYCE INC. ENGINEERING AND CONSULTING 512 WEST ELEVENTH AUSTIN, TEXAS 78701-2000 (512) 474-9097 FAX (512) 474-8463	Figure 6.4-19

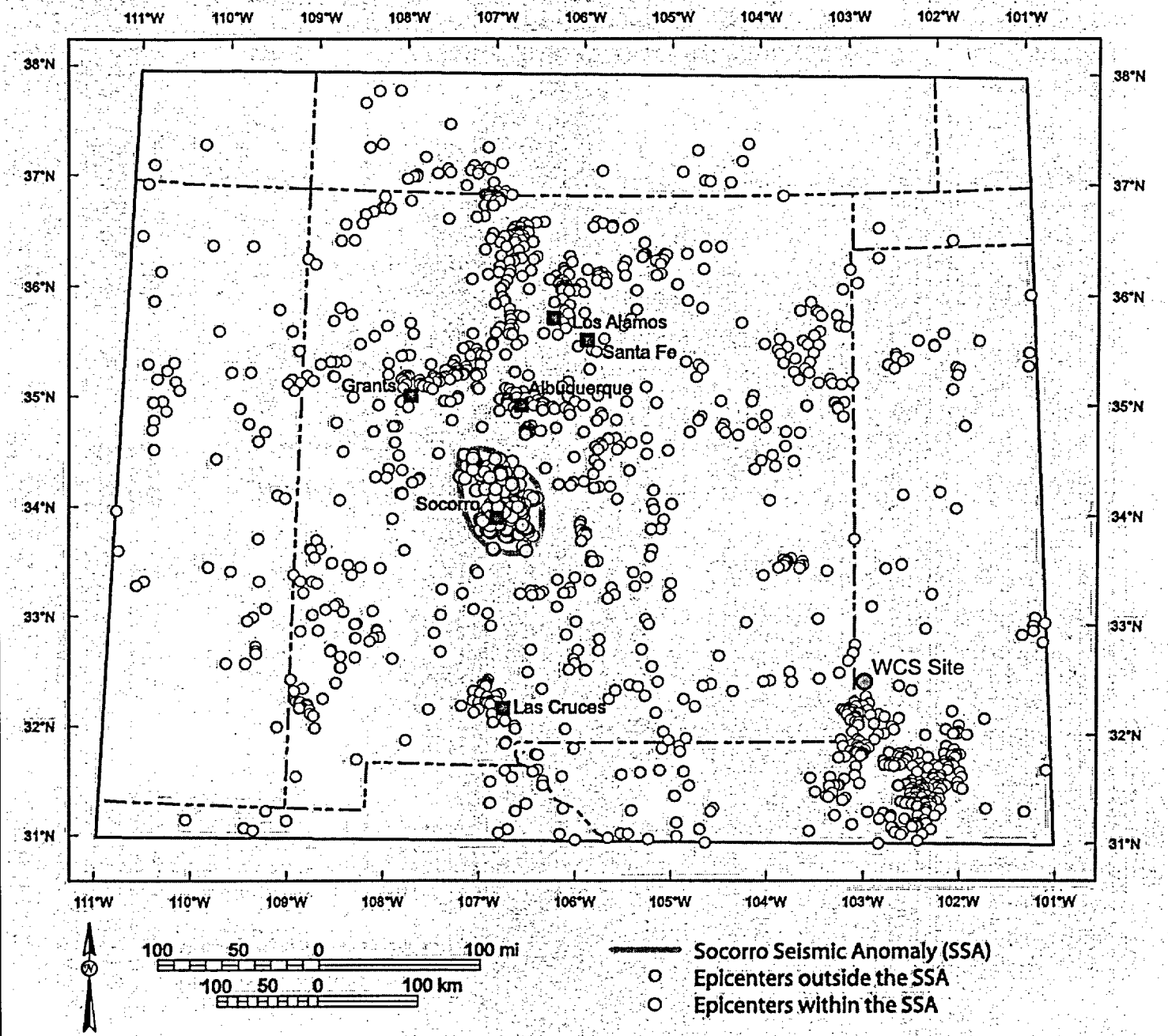

Source: Sanford et al., 2002

Date: 06/14/04 File: WCS_Fig6.4-20.fh11	Seismicity of New Mexico and Bordering Areas (1962 - 1995; Moment Magnitudes > 1.3)
INTERA INCORPORATED 9111A Research Blvd. Austin, TX 78758 COOK-JOYCE INC. ENGINEERING AND CONSULTING 812 WEST ELEVENTH AUSTIN, TEXAS 78701-2000 (512) 474-9097 FAX (512) 474-8483	Figure 6.4-20

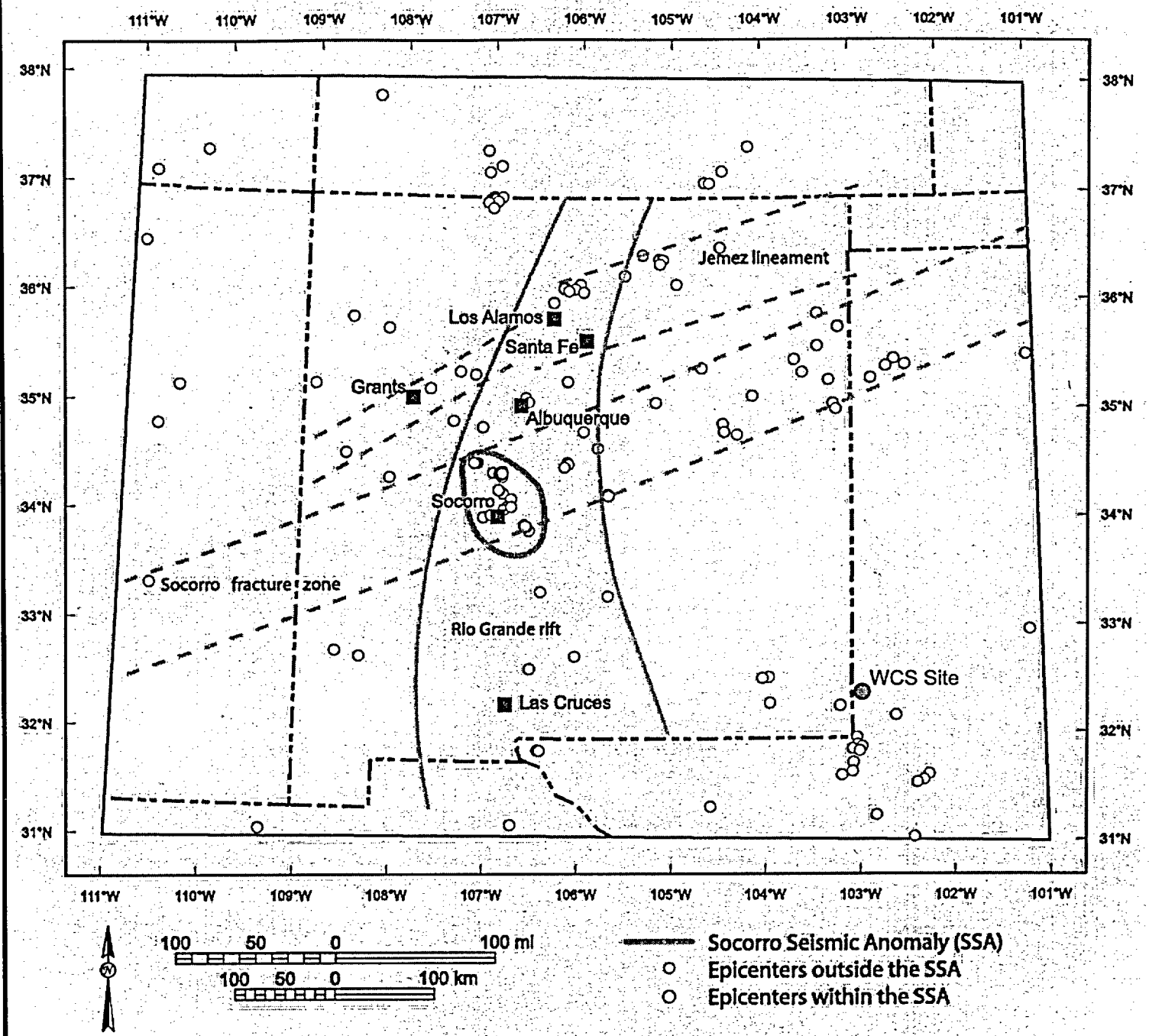

Source: Sanford et al., 2002

Date: 06/14/04 File: WCS_Fig6.4-21.fh11	Seismicity of New Mexico and Bordering Areas (1962 - 1995; Moment Magnitudes > 3)
INTERA INCORPORATED 9111A Research Blvd. Austin, TX 78758 COOK-JOYCE INC. ENGINEERING AND CONSULTING 812 WEST ELEVENTH AUSTIN, TEXAS 78701-2000 (512) 474-9087 FAX (512) 474-8463	Figure 6.4-21

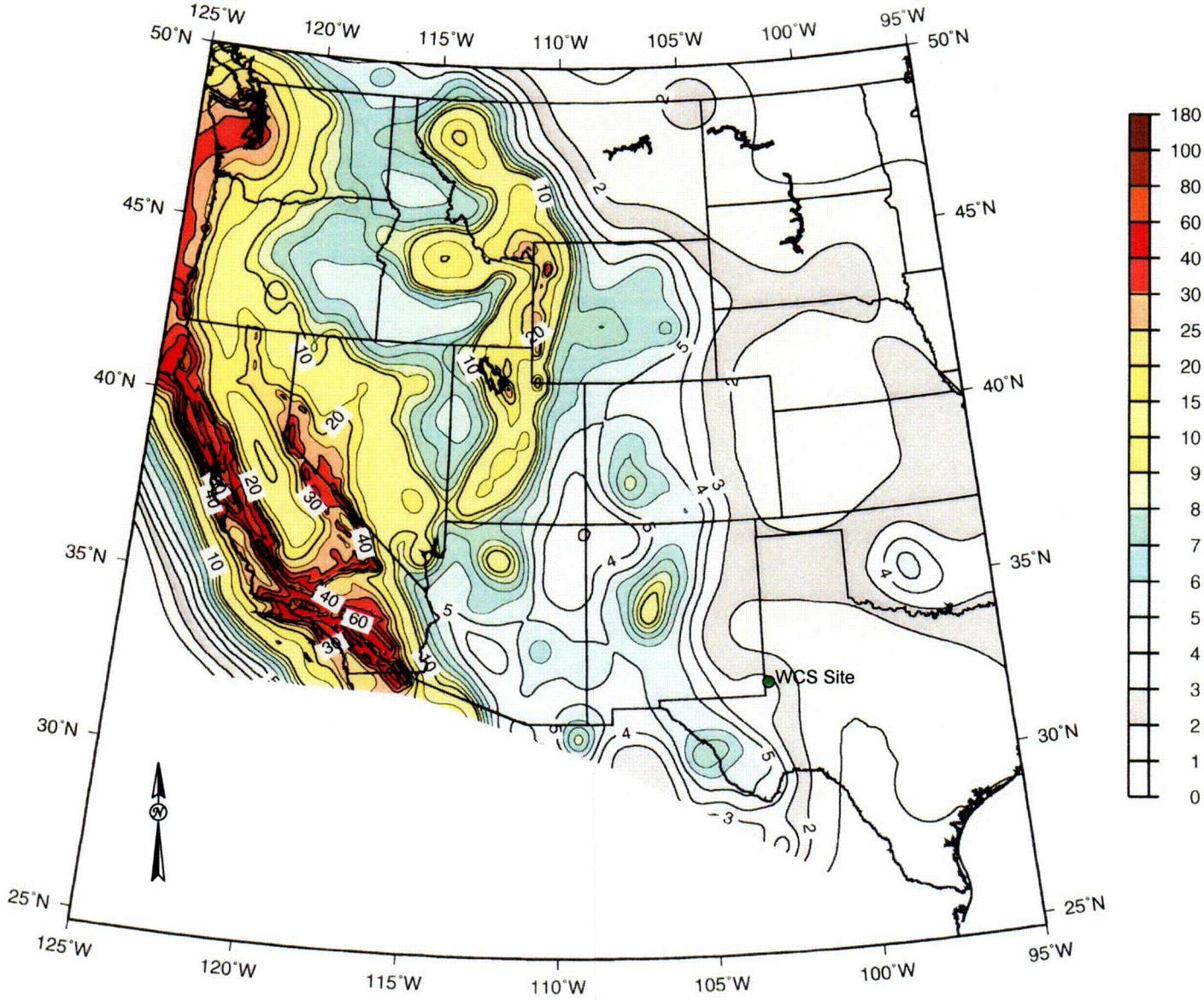

Source: http://geohazards.cr.usgs.gov/eg

Date: 06/14/04 File: WCS_Fig6.4-22.fh11	Peak Ground Acceleration (%g) with 10% Probability of Exceedance in 50 Years
INTERA INCORPORATED 9111A Research Blvd. Austin, TX 78758 COOK-JOYCE INC. ENGINEERING AND CONSULTING 812 WEST ELEVENTH AUSTIN, TEXAS 78701-2000 (512) 474-9097 FAX (512) 474-8463	Figure 6.4-22

C01

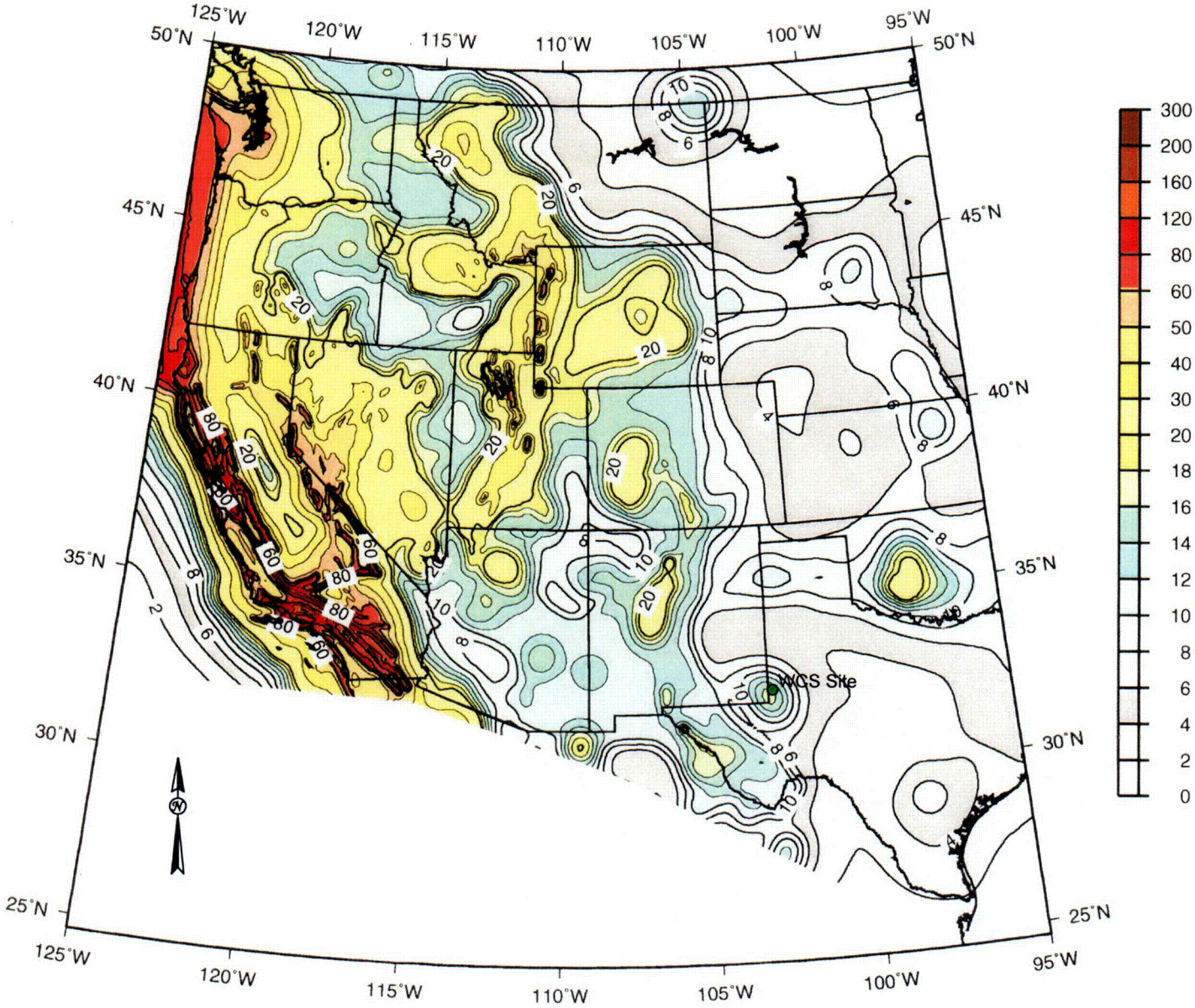

Source: http://geohazards.cr.usgs.gov/eg

Date: 06/14/04 File: WCS_Fig6.4-23.fh11	Peak Ground Acceleration (%g) with 2% Probability of Exceedance in 50 Years
INTERA INCORPORATED 9111A Research Blvd. Austin, TX 78758 COOK-JOYCE INC. ENGINEERING AND CONSULTING 812 WEST ELEVENTH AUSTIN, TEXAS 78701-2000 (512) 474-9097 FAX (512) 474-8463	Figure 6.4-23

C02

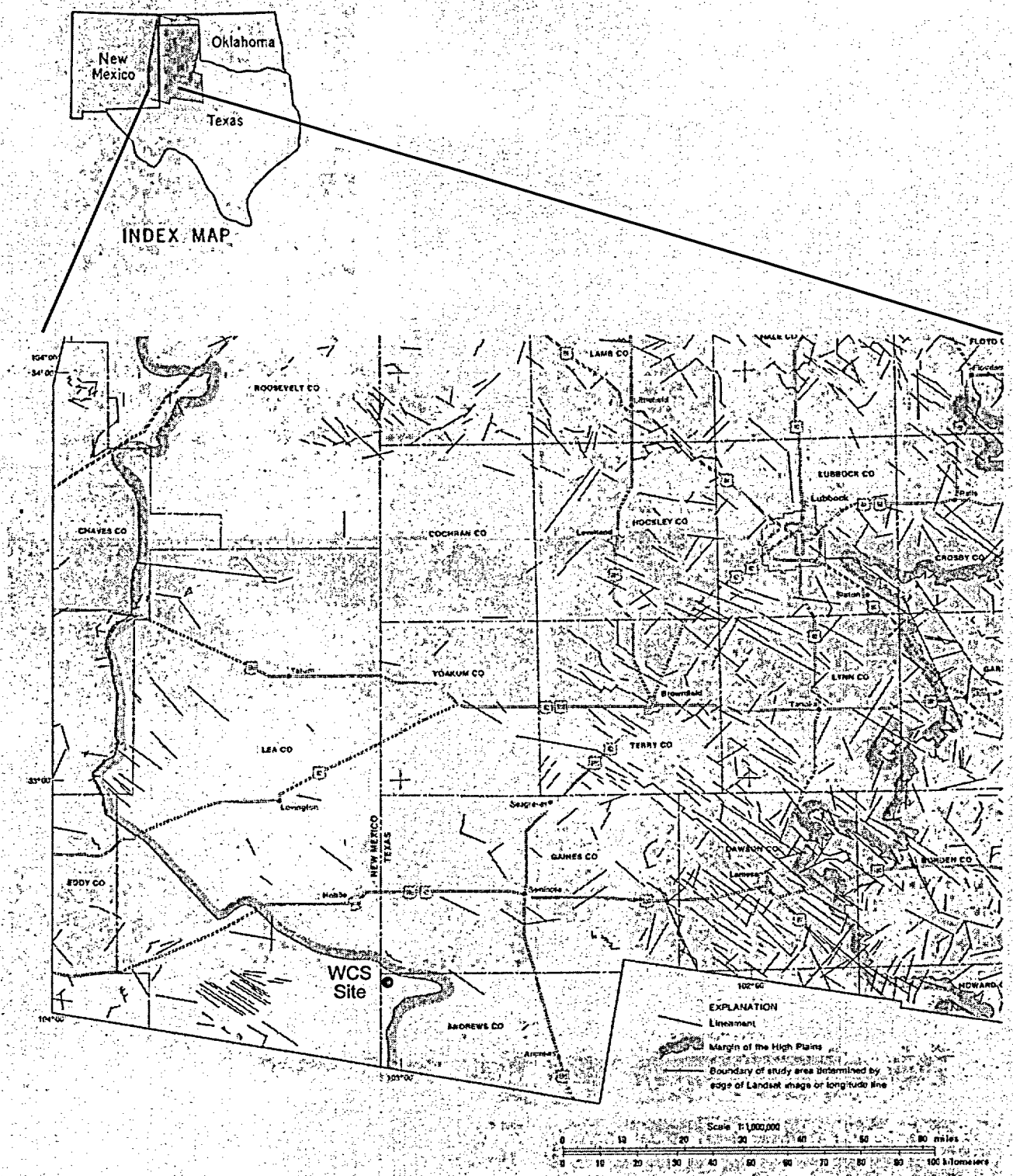

Source: Finley and Gustavson, 1981

Date: 06/14/04
File: WCS_Fig6.4-24.fh11

INTERA INCORPORATED
9111A Research Blvd.
Austin, TX 78758

COOK-JOYCE INC.
ENGINEERING AND CONSULTING
812 WEST ELEVENTH
AUSTIN, TEXAS 78701-2000
(512) 474-2097 FAX (512) 474-8463

Lineament Map of the Texas Panhandle and Parts of Oklahoma and New Mexico

Figure 6.4-24

THIS PAGE IS AN OVERSIZED DRAWING OR FIGURE,

THAT CAN BE VIEWED AT THE RECORD TITLED:

PLATE 6.2-2 "DIP-ORENTED STRATIGRAPHIC CROSS SECTION A-A'"

WITHIN THIS PACKAGE..

D-02

THIS PAGE IS AN OVERSIZED DRAWING OR FIGURE,

THAT CAN BE VIEWED AT THE RECORD TITLED:

PLATE 6.2-3 "STRIKE-ORIENTED STRATIGRAPHIC CROSS SECTION B-B"

WITHIN THIS PACKAGE..

D-03

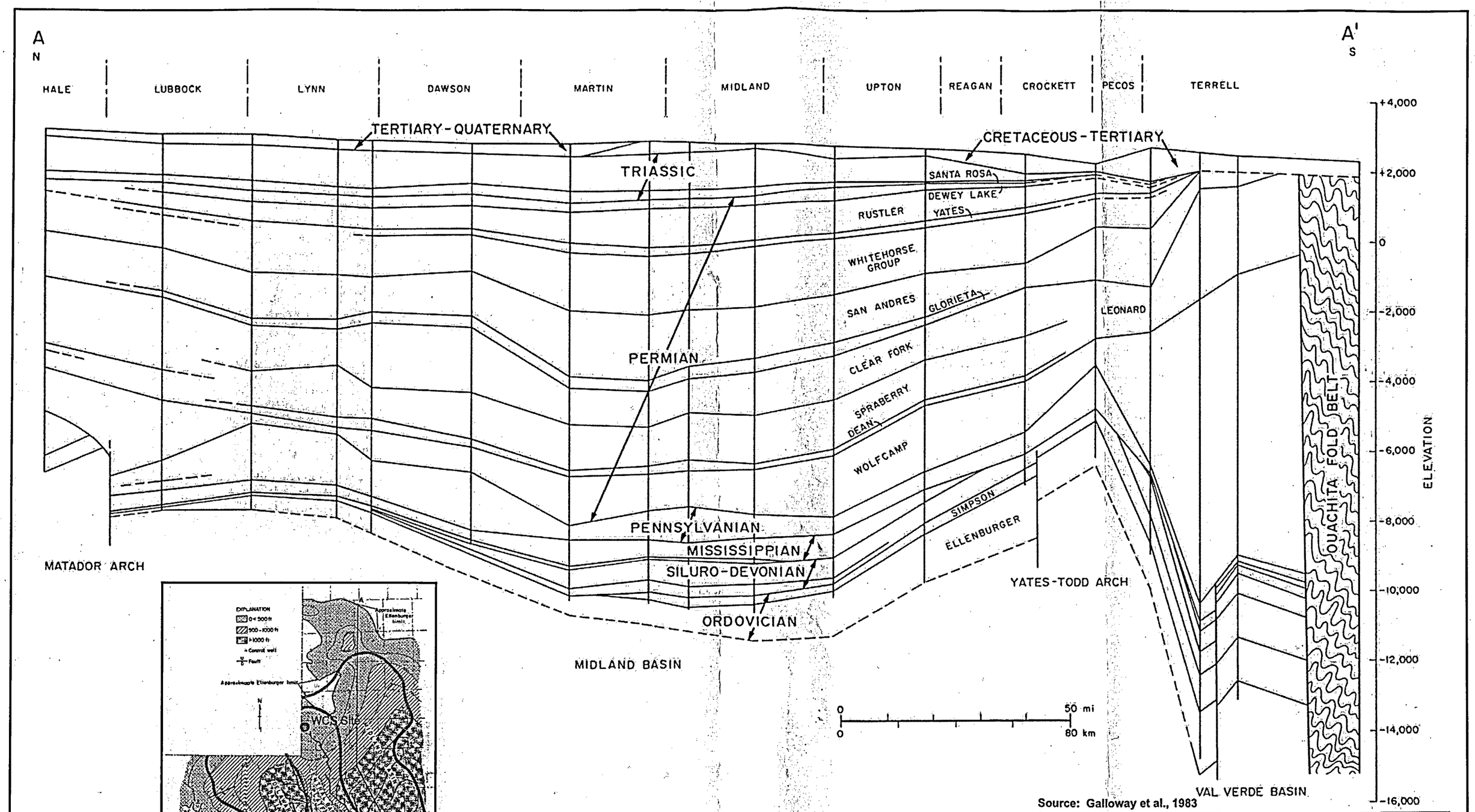

Source: Galloway et al., 1983

Date: 02/04/04
File: WCS_Fig6.2-3.fh11

INTERA INCORPORATED
9111A Research Blvd.
Austin, TX 78758

COOK-JOYCE INC.
ENGINEERING AND CONSULTING
612 WEST ELEVENTH
AUSTIN, TEXAS 78701-2000
(512) 474-9097 FAX (512) 474-8463

Regional North-South Structural Cross Section, Matador Arch to Val Verde Basin

Figure 6.4-6

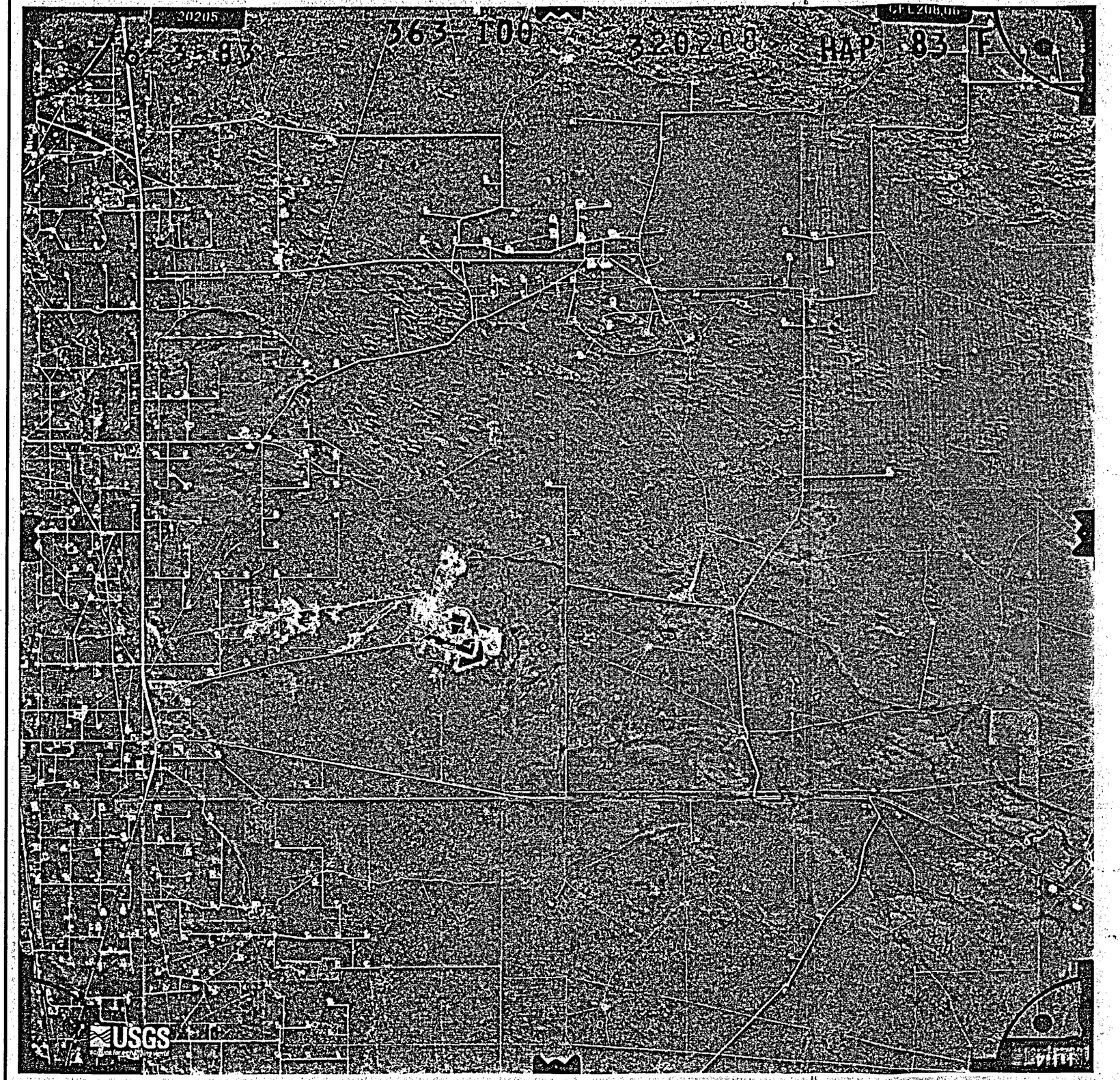

Date: 06/14/04
File:. WCS_Fig6.4-25.fh11

INTERA INCORPORATED
9111A Research Blvd.
Austin, TX 78758

COOK-JOYCE INC.
ENGINEERING AND CONSULTING
812 WEST ELEVENTH
AUSTIN, TEXAS 78701-2000
(512) 474-9097 FAX (512) 474-5483

1983 Color Infrared Photograph - WCS Area

Figure 6.4-25

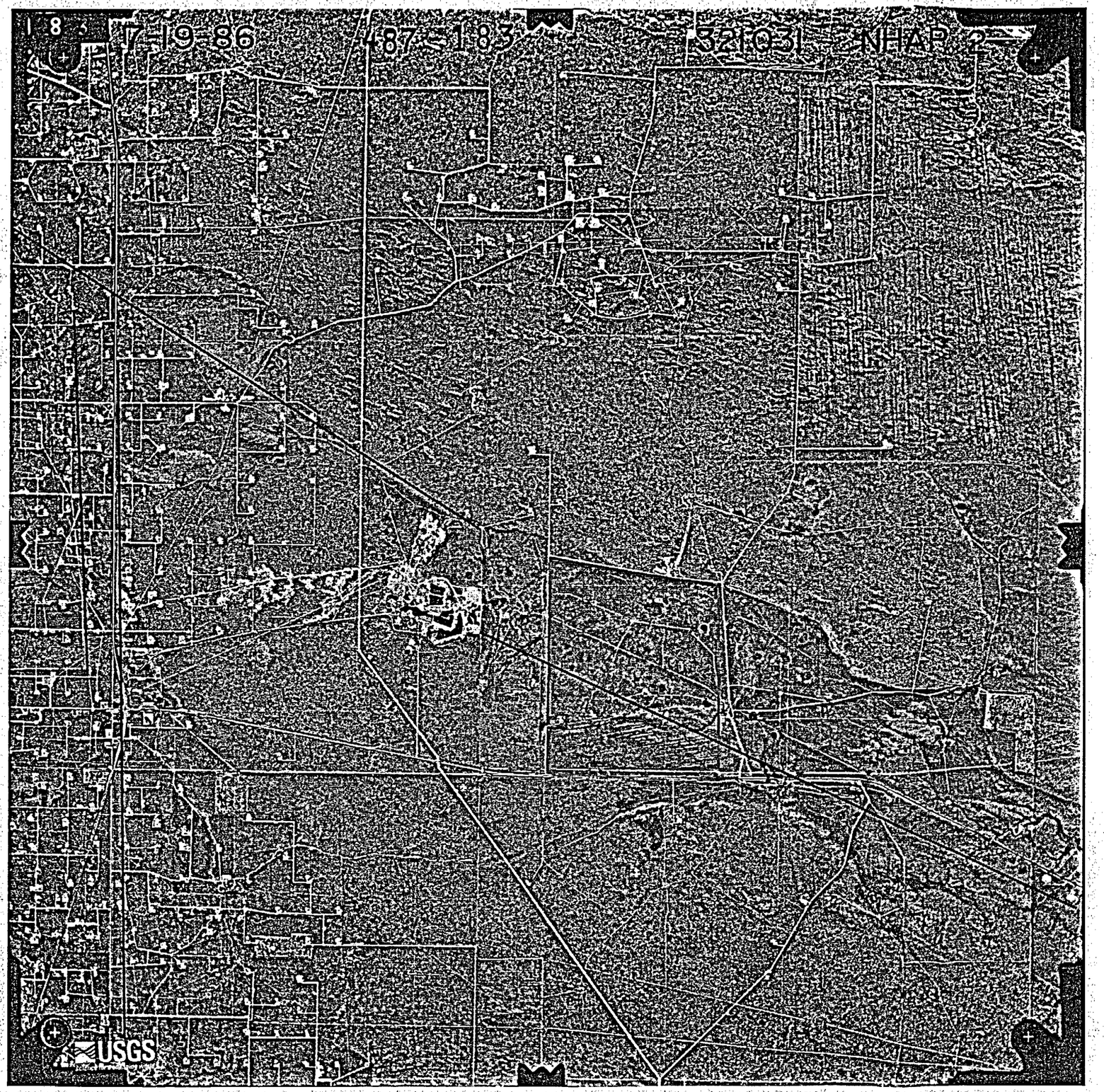

N

0 1 2

Approximate Scale in Miles

Lineaments

RCRA Permitted Area

Date: 06/14/04
File: WCS_Fig6.4-26.fh11

INTERA INCORPORATED
9111A Research Blvd.
Austin, TX 78758

COOK-JOYCE INC.
ENGINEERING AND CONSULTING
812 WEST ELEVENTH
AUSTIN, TEXAS 78701-2000
(512) 474-9097 FAX (512) 474-8483

1986 Color Infrared Photograph - WCS Area

Figure 6.4-26